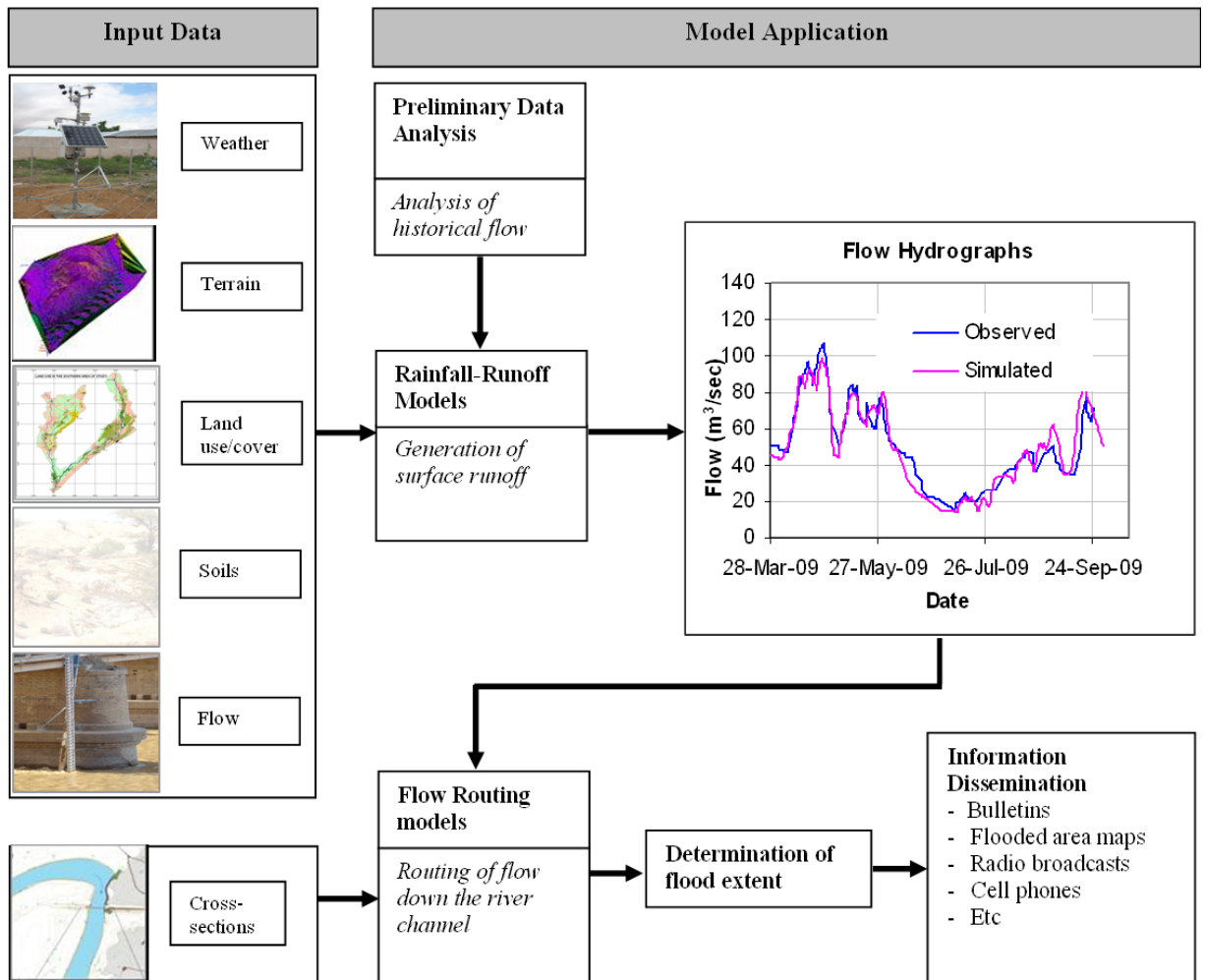


Somalia Flood Forecasting System



Technical Report No. W-16
December 2009

Somalia Water and Land Information Management
Ngecha Road, Lake View. P.O Box 30470-00100, Nairobi, Kenya.
Tel +254 020 4000300 - Fax +254 020 4000333,
Email: swalim@fao.org Website: <http://www.faoswalim.org>.



Disclaimer

The designations employed and the presentation of material in this information product do not imply the expression of any opinion whatsoever on the part of the Food and Agriculture Organization of the United Nations and the SWALIM project concerning the legal status of any country, territory, city or area of its authorities, or concerning the delimitation of its frontiers or boundaries.

This document should be cited as follows:

Muthusi F. M. and Gadain H. M. (2009), Somalia Flood Forecasting System. Technical Report N° W-16, FAO-SWALIM, Nairobi, Kenya

List of Abbreviations

ANN	Artificial Neural Network
AR	Auto Regression
AWS	Automatic Weather Station
CHARM	Collaborative Historical African Rainfall Model
DEM	Digital Elevation Model
DTM	Digital Terrain Model
ECMWF	European Centre for Medium Range Weather Forecast
ERA	ECMWF Re-Analysis
EROS	Earth Resources Observation and Science of USGS
EU	European Union
FEWS NET	Famine Early Warning Systems Network
FWG	Flood Working Group
GeoSFM	Geospatial Stream Flow Model
GFMFS	Galway River Flow Modelling and Forecasting System
GIS	Geographic Information System
GUI	Graphical User Interface
HEC-RAS	Hydrologic Engineering Centre - River Analysis System
JRC	Joint Research Centre
LPM	Linear Perturbation Model
LVGFM	Linearly Varying Gain Factor Model
NGO	Non Governmental Organization
NOAA-CPC	National Oceanic and Atmospheric Administration – Climate Prediction Centre
NWP	Numerical Weather Prediction
OF	Objective Function
OLS	Ordinary Least Squares
RFE	Rainfall Estimates
SCE-UA	Shuffle Complex Evolution Metropolis, University of Arizona
SCS	Soil Conservation Service
SLM	Simple Linear Model
SRTM	Shuttle Radar Topography Mission
SWALIM	Somalia Water and Land Information Management
USAID	United States Agency for International Development
USGS	United States Geological Survey

Somali Climate Seasons

<i>Gu</i>	April to June main rainy season
<i>Hagaa</i>	July to September hot and windy season
<i>Deyr</i>	October to November short rainy season
<i>Jilaal</i>	December to March very dry and cool season

Table of Contents

List of Abbreviations	iii
Somali Climate Seasons.....	iv
List of Figures	vii
List of Tables	ix
Acknowledgement	x
Chapter 1	1
Introduction.....	1
1.0 Background.....	1
1.1 Objectives of the Report.....	2
1.2 Juba and Shabelle River Basins	2
1.2.1 Juba Basin.....	2
1.2.2 Shabelle Basin.....	3
1.3 Flood Forecasting Model Components	4
1.3.1 Rainfall-Runoff Model.....	4
1.3.2 Flow Routing Model	4
1.4 Layout of the Report	4
Chapter 2	7
Data Availability and Analysis.....	7
2.0 Introduction.....	7
2.1 Data Availability	7
2.1.1 Flow Data.....	7
2.1.2 Rainfall Data	12
2.1.3 Channel Characteristics Data	12
2.1.4 Spatial Data	12
2.2 Preliminary Data Analysis	16
2.2.1 Flow Data.....	16
2.2.1.1 Seasonal Flows.....	16
2.2.1.2 Shifts in Data Series.....	19
2.2.1.3 Preliminary Routing Analysis.....	24
2.2.2 Rainfall Data	28
Chapter 3	29
Description of Hydrological Models.....	29
3.1 General Overview	29
3.1 Rainfall Runoff Models	30
3.1.1 LISFLOOD Model.....	30
3.1.2 Geospatial Stream flow Model – GeoSFM.....	32
3.2 Inflow and Flood Routing Models.....	34
3.2.1 Hydrodynamic Routing Models.....	35
3.2.1.1 HEC River Analysis System (RAS) Model	35
3.2.2 Galway Flow Modelling and Forecasting System (GFMFS)	36
3.2.3 Regression Models.....	38
3.3 Real-Time Flow Forecasting.....	39
3.4 Model Calibration and Verification	40

Chapter 4	41
Models Application and Results	41
4.0 Model Evaluation Criteria.....	41
4.1 Application of LISFLOOD Model.....	41
4.1.1 Data Used to Configure LISFLOOD Model.....	41
4.1.2 Model Calibration	41
4.1.3 Calibration Results.....	42
4.2 Application of the USGS Model.....	44
4.2.1 Data Used to Configure the USGS Model.....	44
4.2.2 Model Calibration	44
4.2.3 Model Results	45
4.3 Application of HECRAS Model	46
4.3.1 HECRAS Data Requirements	46
4.3.2 Model Calibration	48
4.3.3 Model Results	49
4.4 Application of GFMFS	52
4.4.1 GFMFS Data Requirements.....	52
4.4.2 Model Calibration	52
4.4.3 Model Results	52
4.5 Regression Models.....	54
4.5.1 Data Used.....	55
4.5.2 Model Results	55
4.6 Model’s Summary Results	62
Chapter 5	64
Challenges and Limitations.....	64
5.1 Data Limitations.....	64
5.2 Model Limitations.....	65
Chapter 6	66
Conclusions and Recommendations.....	66
6.1 Conclusions.....	66
6.2 Recommendations.....	66
Bibliography and Literature Consulted.....	68
Annexes	69
Annex A: List of Rainfall Monitoring Stations	70
Annex B: Results of Models Calibration	75

List of Figures

Figure 1.1: Juba and Shabelle River Basins.....	3
Figure 1.2: Structure of the Somalia Flood Forecasting System	6
Figure 2.1: Location of Pre-war Gauging Stations along Juba and Shabelle Rivers ...	8
Figure 2.2: Rating Curves for Selected Stations in Juba.....	10
Figure 2.3: Rating Curves for Selected Stations in Shabelle	11
Figure 2.4: Locations of Rainfall Stations in Southern Somalia.....	13
Figure 2.5: Cross Sections for Selected Stations along Juba River	14
Figure 2.6: Cross Sections for Selected Stations along Shabelle River	15
Figure 2.7: Seasonal Mean Flows for Stations along Shabelle River	17
Figure 2.8: Seasonal Mean Flows for Stations along Juba River	17
Figure 2.9: Correlation of Flow between Belet Weyne and Afgoi Stations	18
Figure 2.10: Correlation of Flow between Luuq and Jamame Stations.....	18
Figure 2.11: Double Mass Curve for Belet Weyne and Bulu Burti Flows	20
Figure 2.12: Double Mass Curve for Luuq and Bardere Flows.....	20
Figure 2.13: Long Term Mean Flow at Luuq	22
Figure 2.14: Long Term Mean Flow at Bardere	22
Figure 2.15: Double Mass Curve for Luuq and Corrected Bardere Flows	23
Figure 2.16: Long Term Mean Flow at Bardere after Data Correction	23
Figure 2.17: Correlation between Luuq and Bardere Flow at no Lag-time	25
Figure 2.18: Correlation between Luuq and Bardere Flows at 2-Days Lag-time.....	25
Figure 2.19: Correlation between Belet Weyne and Bulu Burti Flows at Lag zero ..	26
Figure 2.20: Correlation between Belet Weyne and Bulu Burti Flows at 2-Days Lag- time.....	26
Figure 2.21: Scatter Plot of Rising Hydrograph Phase for Belet Weyne and Bulu Burti Flows with 2 Day Lag.....	27
Figure 2.22: Scatter Plot of Falling Hydrograph Phase for Belet Weyne and Bulu Burti Flows with 2 Day Lag.....	28
Figure 3.1: Overview of the LISFLOOD Model Internal Structure	31
Figure 3.2: Overview of the GeoSFM Model Internal Structure	33
Figure 3.3: Representation of Terms in the Energy Equation for HEC-RAS.....	36
Figure 3.4: Schematic Diagram of Linear Perturbation Model (LPM).....	37
Figure 4.1: Observed and Simulated Flow at Belet Weyne using LISFLOOD.....	43
Figure 4.2: Observed and Simulated Flow at Luuq using LISFLOOD	43
Figure 4.3: Simulated and Observed Flow at Luuq using ECMWF Data	45
Figure 4.4: Simulated and Observed Flow at Luuq using RFE Data.....	45
Figure 4.5: HECRAS River Network	47
Figure 4.6: HECRAS Channel Geometry	47
Figure 4.7: Scatter Graphs for Observed and Simulated Flow at Bulu Burti and Bardere using HECRAS.....	50
Figure 4.8: Observed and Forecast Flow at Bulu Burti using HECRAS	51
Figure 4.9: Observed and Forecast Flow at Bardere using HECRAS	51
Figure 4.10: Scatter Graphs for Observed and Simulated Flows at Bulu Burti and Bardere using GFMFS	53
Figure 4.11: Hydrograph of Observed and GFMFS Forecast Flows at Bulu Burti ..	54

Figure 4.12: Hydrograph of Observed and GFMFS Forecast Flows at Bardere	54
Figure 4.13: Bardere, 2 Day Forecast Based on Observed Levels at Luuq	56
Figure 4.14: Bulu Burti, 2 Day Forecast Based on Observed Levels at Belet Weyne	56
Figure 4.15: Observed and Forecast River Levels at Bardere Based on Observed Levels at Luuq.....	57
Figure 4.16: Observed and Forecast River Levels at Bulu Burti Based on Observed Levels at Belet Weyne	57
Figure 4.17: Belet Weyne - Bulu Burti with a 2 Day Lag during High Flows	58
Figure 4.18: Luuq - Bardere with a 2 Day Lag During High Flows.....	58
Figure 4.19: Observed and Forecast Flows at Bulu Burti.....	59
Figure 4.20: Observed and Forecast Flows at Bardera	59
Figure 4.21: Luuq - Bardera Peaks	60
Figure 4.22: Forecast Peaks at Bardera.....	61
Figure 4.23: Belet Weyne - Bulu Burti Peaks.....	61
Figure 4.24: Forecast Peaks at Bulu Burti	62

List of Tables

Table 2.1: Gauging Stations in Juba and Shabelle River	9
Table 2.2: Details of the Pre-war Daily Rainfall Stations in South Somalia	12
Table 2.3: Summary of Spatial Weather Data	16
Table 2.4: Data Adjustments for Selected Stations in Juba and Shabelle.....	19
Table 2.5: Lag Times between Upstream and Downstream Stations along Juba and Shabelle Rivers	24
Table 2.6: Lag Times at Rising and Falling Hydrograph Phases for Belet Weyne and Bulo Burti.....	27
Table 3.1: GeoSFM Model Parameters.....	34
Table 4.1: Correlation Coefficients for Different Models used in the Study.....	63

Acknowledgement

The authors would like to acknowledge with gratitude Dr. Zoltan Balint, SWALIM Chief Technical Advisor for his technical input and guidance during this study and review of this document.

Many thanks to all SWALIM staff who contributed in data preparation and analysis. The roles of Peris Muchiri, SWALIM Hydro-Meteorologist in the analysis of historical data; and Gabriel Oduori, SWALIM GIS Expert in preparation of GIS datasets are highly appreciated.

Chapter 1

Introduction

1.0 Background

Floods are a common phenomenon in the riverine areas of the Juba and Shabelle River basin. The two rivers exhibit seasonal characteristics in their hydrological regime with high tendency of flooding especially during the Deyr (October to November) rain season. Some of the major flood events in the two basins in the past few decades occurred in the years 1961, 1977, 1981, 1997 and 2006. The floods are mainly caused by high rains experienced on the upper catchments of the two rivers in the Ethiopian highlands. However, the contribution of human activities to the floods is also significant, with the riparian farmers cutting the river banks to allow water flow into their fields during low flows. These illegal activities have increased after collapse of the central government in 1991 and exacerbated by El Nino 1997/98 rains that contributed to further destruction of the irrigation and flood control infrastructure.

The flood recurrence at the Juba and Shabelle Rivers pose a lot of flooding risks along the two rivers, mainly in the middle and lower reaches. This has necessitated the need for development of a hydrological forecasting system that could warn people in advance of impending floods to save life and property. Such a forecasting system would reduce human suffering caused by the frequent flooding while preserving the environmental benefits of floods.

In Somalia, SWALIM and UN-OCHA are leading efforts in flood management under the Flood Working Group (FWG); an interagency forum for information sharing, flood preparedness and response management. SWALIM has been mandated under the FWG to develop the flood forecasting system for Juba and Shabelle Rivers to advance early warning for better preparedness and response.

The success of such a system depends much on availability of quality hydrometeorological data in real time which has been a great challenge to Somalia and the neighbouring countries that share the basin with Somalia (Ethiopia and Kenya). However, since its inception, SWALIM has done a lot to overcome the data challenges by re-establishing data collection networks which existed before the collapse of the former government. New stations have also been set up, including state of the art telemetric Automatic Weather Stations (AWS) to monitor weather and river flow parameters. Negotiations with Ethiopia on transboundary data sharing were initiated. The AWS installation is still on-going, and once complete it will provide a good coverage of real time data collection which will enhance flood forecasting in the rivers as well as flash floods resulting from overland runoff in the northern part of the country.

To come up with the most appropriate flood forecasting system for the Juba and Shabelle Rivers, different types of models were applied. A short description of the

models and the results obtained for each model applied are presented in proceeding chapters of this report.

1.1 Objectives of the Report

The objective of this report is to document results of different models tested in the development of a flood forecasting system for the Juba and Shabelle River basins in Somalia, and recommend the way forward.

1.2 Juba and Shabelle River Basins

Somalia has only two perennial rivers, Juba and Shabelle, both of which originate from the Ethiopian highlands and flow across southern Somalia to the Indian Ocean. About two-thirds of the two river basins lie outside Somalia, mostly in Ethiopia. Figure 1.1 shows the Juba and Shabelle River basins and the key river gauging stations used in this study. Technically, the Shabelle is a tributary of the Juba, and as such constitutes a single basin, but since flows from the Shabelle join the Juba only very rarely, and even then result from localised rainfall, the rivers are effectively separate.

1.2.1 Juba Basin

The Juba Basin lies roughly between $38^{\circ} 1'$ and $46^{\circ} 0'$ east of the Prime Meridian and between $0^{\circ} 15'$ and $7^{\circ} 28'$ north of the Equator. The altitude of the Juba Basin ranges from few meters above sea level at Indian Ocean to over 3,000 metres above sea level (a.s.l.) in the Ethiopian highlands. The total catchment area of the Juba Basin at the mouth of the river near Kismayo is about 221,000 km² (based on catchment delineation using SRTM 30m DEM from USGS), 65% of which is in Ethiopia, 30% in Somalia and 5% in Kenya.

The Juba River has three main tributaries: Weyb, Genale and Dawa in its upper catchment all of which flow south-eastwards. Tributaries of Genale River originate from the southern flanks of the Bale Mountains, and from the Sidamo Mountains in the north-west. Dawa originates in the Sidamo Mountains while Weyb River originates from the northern parts of the Bale Mountains.

The total length of the Juba River is about 1,808 km (measured on the longest tributary), of which 804 km lies in Ethiopia and 1,004 km lies in Somalia (based on SRTM 30m derived streams from USGS). Rivers Genale and Dawa flow in deep valleys until they reach flatter and broader areas along their respective flood plains at elevations below 400m a.s.l. However, Weyb River flows mostly in a wide valley with intermitted deeply incised reaches along its course. The Weyb converges with Genale near the Somalia border at Doolow, before joining Dawa shortly downstream. The joint channel downstream of this point is the main Juba River. After entering Somalia, the river continues to flow south-easterly until it reaches the town of Luuq, from which point it flows gently towards south and into the Indian Ocean.

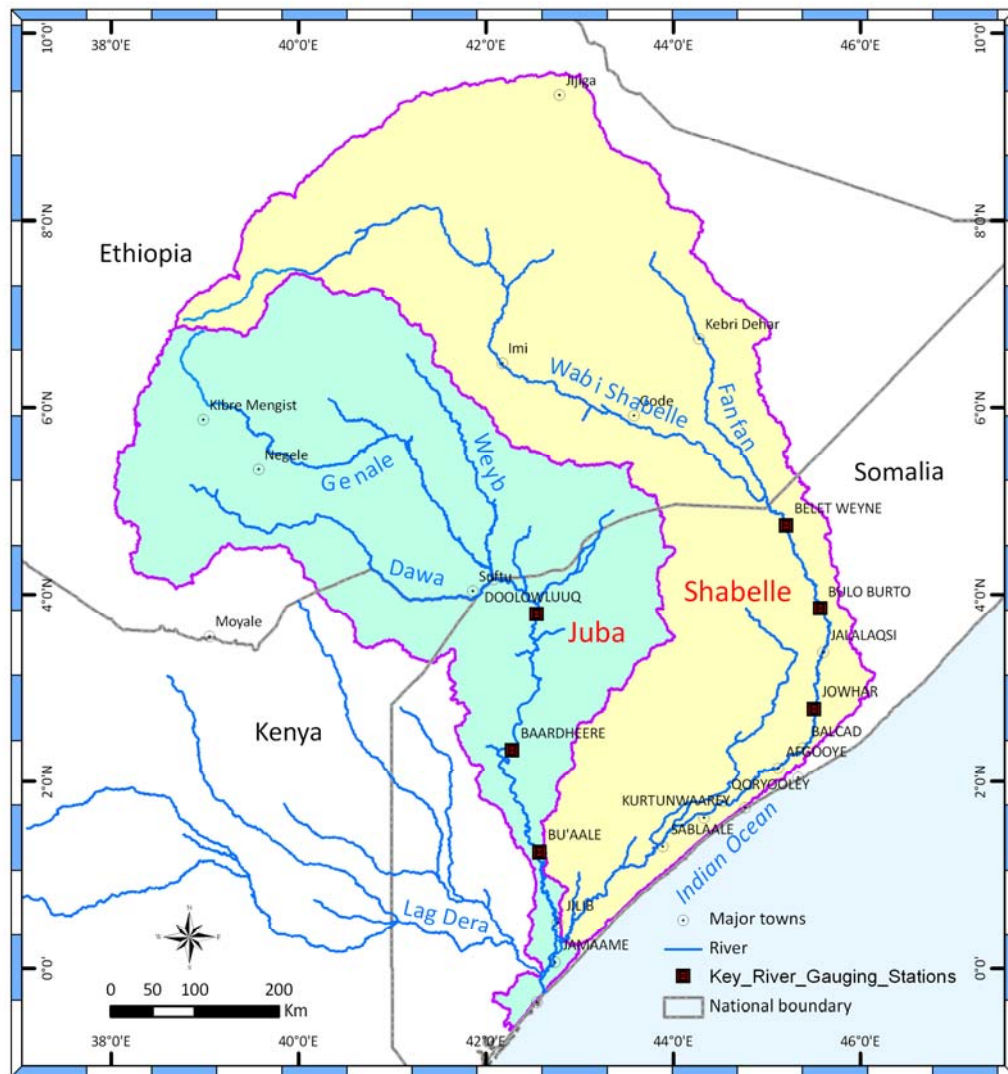


Figure 1.1: Juba and Shabelle River Basins

1.2.2 Shabelle Basin

The Shabelle Basin lies roughly between 38° 40' and 46° 9' east of the Prime Meridian and between 0° 15' and 9° 38' north of the Equator. The river rises from the Bale mountain ranges of the eastern Ethiopian highlands at an altitude of about 4,230m a.s.l. The total catchment area of the Shabelle River at its confluence with the Juba River is about 297,000km², based on catchment delineation using SRTM 30m from USGS. Two-thirds of the catchment (188,700km²) lies in Ethiopia and the rest (108,300km²) in Somalia.

The basin within Ethiopia can be divided into three valleys: the upper valley where the river is intermixed between steep slopes, plain lands and meanders in deep

valleys; the middle valley where the river is suddenly deeply embedded in limestone plateaus; and a lower valley where the river flows in a vast alluvial plain with very gentle slope of 0.25 to 0.35m/km. The total length of the main course of the river from the source to the Somalia border is about 1,290km.

Inside Somalia, Shabelle River traverses an additional distance of 1,236km of gently sloping terrain. Near the outlet along the coastal stretch of Indian Ocean, the river runs into a series of swamps. Downstream of the swamps the river resumes a defined channel, but the flows are very much reduced and the Shabelle discharges into the Juba only in times of exceptional floods.

1.3 Flood Forecasting Model Components

The flood forecasting system is composed of two main model components which are: rainfall runoff and channel flow routing models. The two components are briefly discussed below, with a general structure of the system presented in Figure 1.2.

1.3.1 Rainfall-Runoff Model

Rainfall-Runoff models are used to calculate the water balance across the catchment, hence determine the amount of runoff which finds its way into the river channel for a given storm. The rainfall runoff models tested in this study were LISFLOOD and US Geological Survey Geospatial Stream flow Model (USGS GeoSFM). The lack of rainfall and other weather related data for the upper catchments (within Ethiopia) limited the use of these models to satellite based rainfall data. The poor coverage of rainfall stations within the basin also limited the application of the rainfall-runoff models within Somalia catchments.

1.3.2 Flow Routing Model

Flow routing models are used to translate generated runoff from rainfall-runoff models, or observed river flow from upstream to downstream stations. The routing models used in the study were regression models, system models (Galway Flow Modelling and Forecasting System – GFMFS) and a hydrodynamic model (HEC River Analysis System RAS). These models are discussed in details in chapter three of this report.

1.4 Layout of the Report

This report contains six chapters arranged as follows:

Chapter one discusses the background and purpose of this report and gives an overview of the flood forecasting system. Chapter two gives a description of the data used in the modelling and preliminary analysis done on the data. Chapter three provides a detailed description of the rainfall-runoff and flow routing models used.

Chapter four describes the application of the models and results obtained. Chapter five outlines the challenges and major limitations to the development of a flood forecasting system for Somalia. Chapter six gives the conclusion, and recommendations for further development of a flood forecasting system for Somalia.

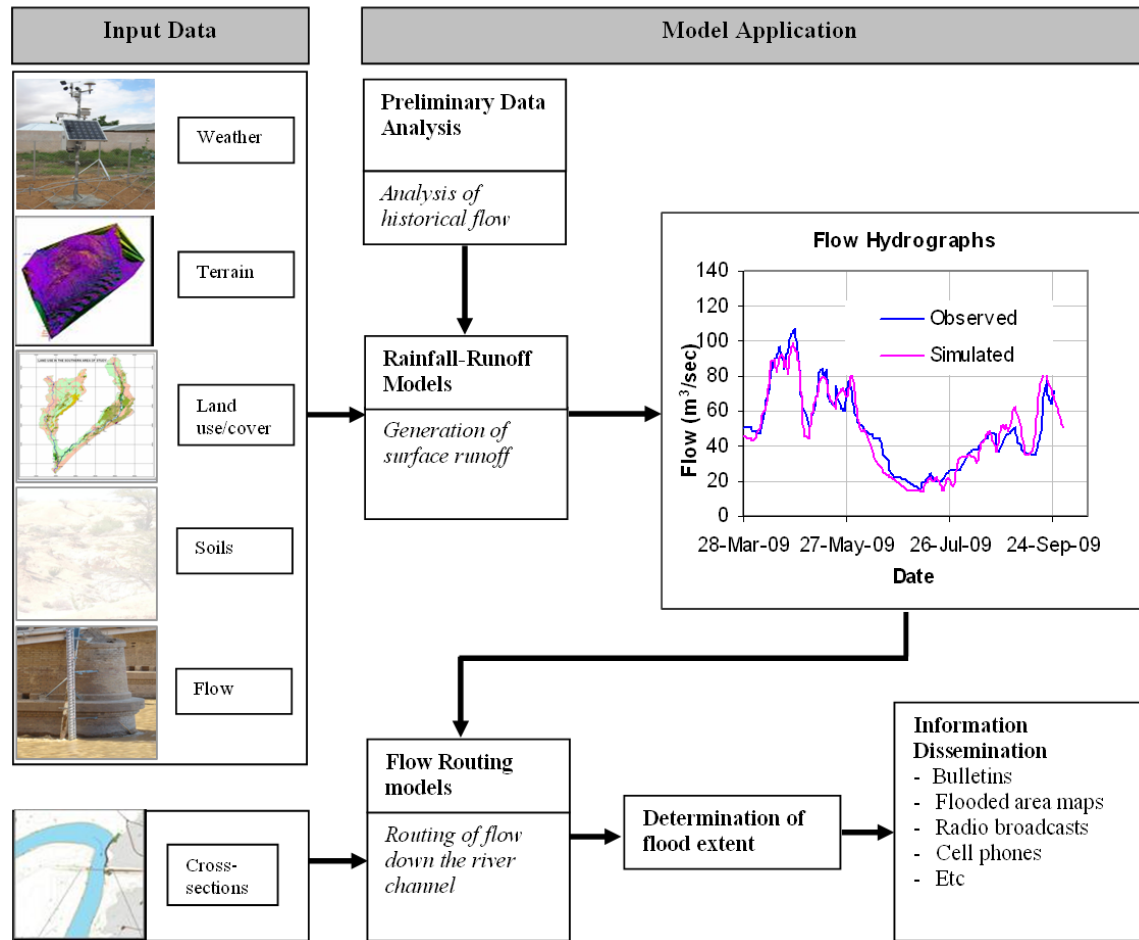


Figure 1.2: Structure of the Somalia Flood Forecasting System

Chapter 2

Data Availability and Analysis

2.0 Introduction

This chapter discusses data availability, pre-processing and analysis. The data available for the study comprises of flow data for key gauging stations, channel geometric data, and available archived rainfall, evaporation and spatial data – soils, digital elevation model (DEM), satellite based Rainfall Estimates (RFE), land use and land cover.

2.1 Data Availability

The historical hydro meteorological data for Somalia dates back to 1950s, but has many gaps. The period between 1990 and 2002/3, when SWALIM started re-establishing data collection networks has no data at all. The post war data is of good quality, but runs for only a couple of years and may not be sufficient for model calibration and validation.

2.1.1 Flow Data

The former Somali government through the ministry of agriculture used to collect flow data for key stations along the Juba and Shabelle Rivers. During the period of civil strife, all the river gauging stations were destroyed, and data collection only resumed after SWALIM rehabilitated the river gauges between 2002 and 2008. Table 2.1 gives a summary of the gauging stations and Figure 2.1 shows the location of these stations.

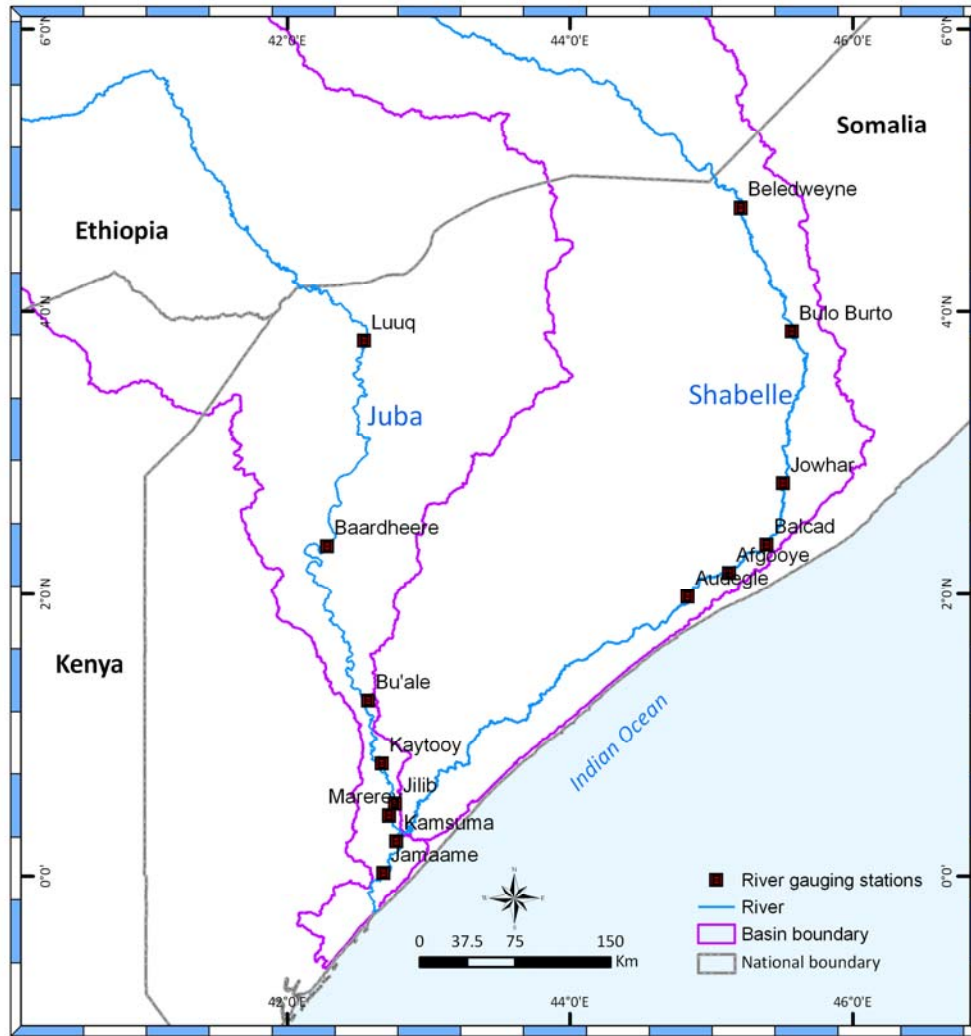


Figure 2.1: Location of Pre-war Gauging Stations along Juba and Shabelle Rivers

Table 2.1: Gauging Stations in Juba and Shabelle River

Station Name	Time Series	Area (sq km)	Lat	Long	Record Pre-war	% Fill	Record Post-war	% Fill
Juba River								
Luuq	Daily Flow	166,000	3.788	42.538	1951-1990	74.7	2002 to date	98.7
Bardheere	Daily Flow	216,730	2.338	42.283	1963-1990	55.6	2002 to date	99.1
Jamame	Daily Flow	268,800	0.018	42.683	1963-1990	39.8	-	
Kaitoi	Daily Flow	240,000	0.788	42.667	1963-1990	48.3	-	
Mareere	Daily Flow	240,000	0.450	42.700	1977-1990	83.9	-	
Buale	Daily Level		1.245	42.573	-	-	2008 to date	100.0
Shabelle River								
Belet Weyne	Daily Flow	207,000	4.733	45.203	1951-1990	87.4	2002 to date	99.5
Bulo Burti	Daily Flow	231,000	3.853	45.570	1963-1990	61.7	2002 to date	99.0
Mahadey Weyne	Daily Flow	255,300	2.970	45.525	1963-1990	69.1	2008 to date	
Jowhar	Daily Level	264,000	2.767	45.500	-		1999 to date	97.7
Afgoi	Daily Flow	278,000	2.140	45.122	1963-1990	87.8	-	
Audegle	Daily Flow	280,000	1.985	44.833	1963-1990	50.3	-	

There were rating curves developed in all the pre-war river gauging stations. The historical rating curves for some of the gauging stations are presented in Figures 2.2 and 2.3. These rating curves are still currently in use, more than twenty years since they were last updated. It is evident that a lot of land degradation has occurred for the last few decades, mainly due to erosion. The eroded soil may have found its way to the rivers, causing deposition. The river banks are also likely to have been eroded, therefore changing the channel cross section, which affects the rating curve.

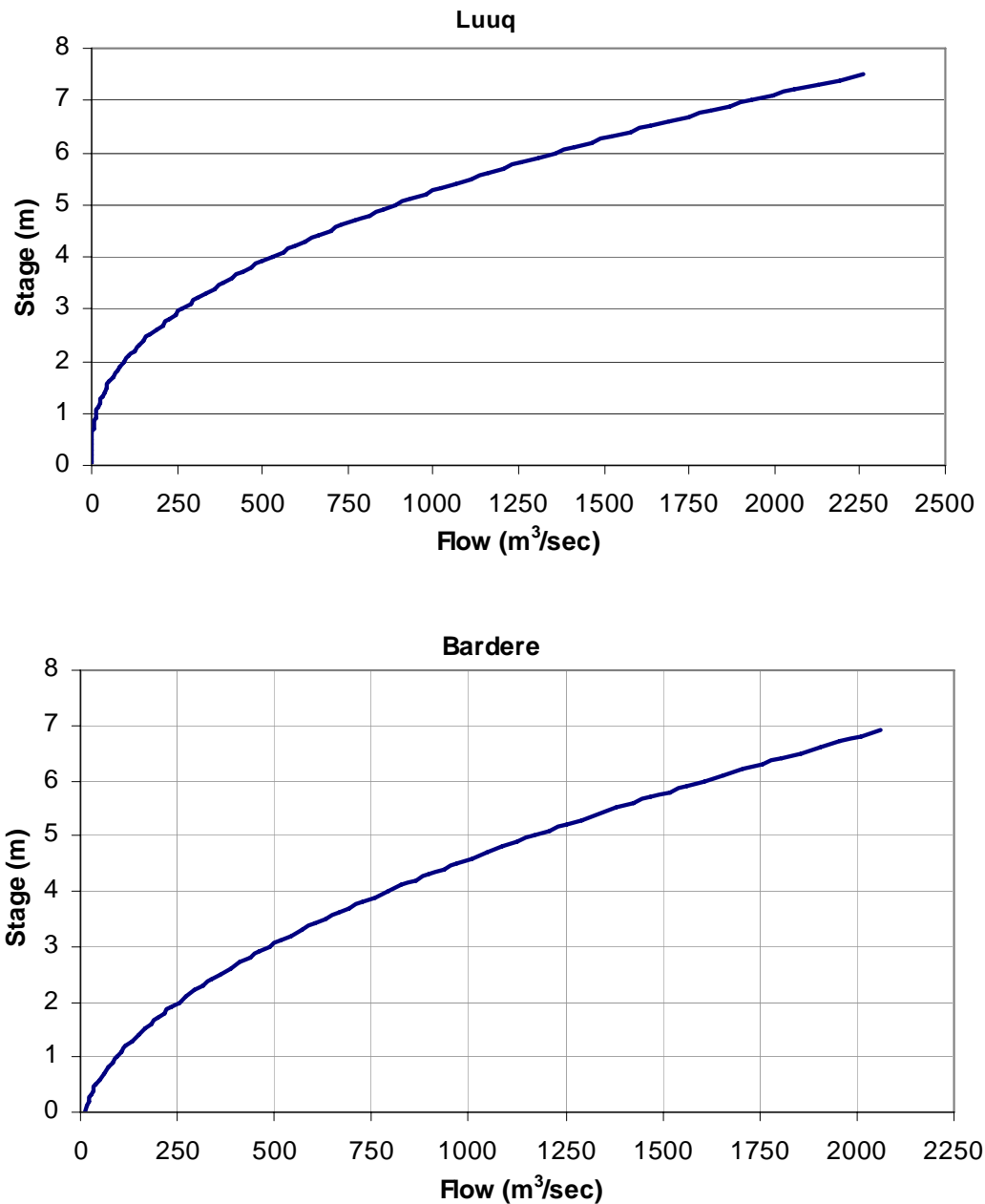


Figure 2.2: Rating Curves for Selected Stations in Juba

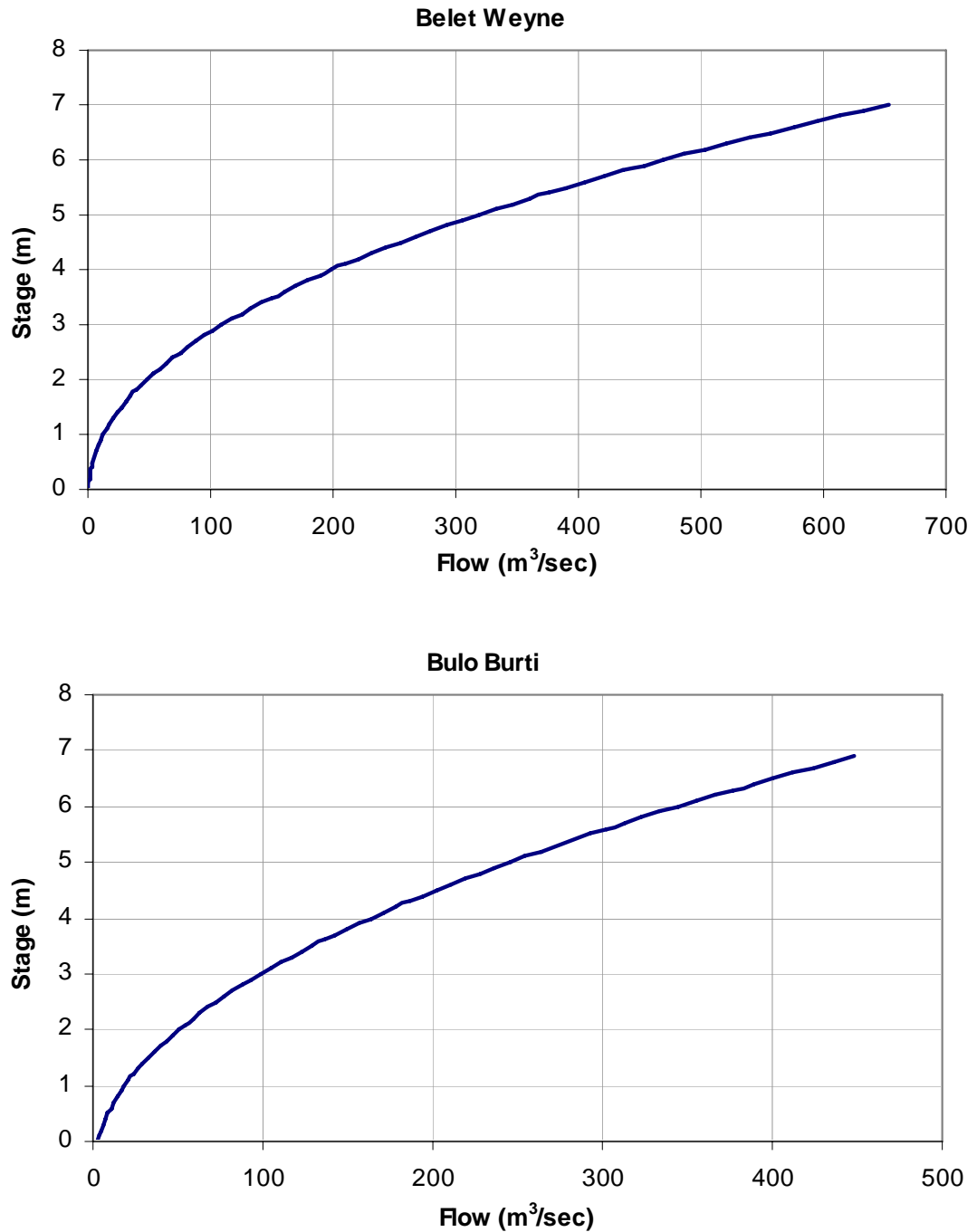


Figure 2.3: Rating Curves for Selected Stations in Shabelle

The rating curves have however not been updated since late 1980's. It is only recently that SWALIM started collecting discharge measurement in six locations (3 in Juba and 3 in Shabelle), to update the old rating curves and establish new ones for the new stations at Jowhar and Buale.

2.1.2 Rainfall Data

Rainfall data play a central role in developing rainfall-runoff models. Most runoff in Juba and Shabelle comes from the Ethiopian highlands. However, in extremely wet years the contribution of the Somali portion of the catchments may be significant. The rainfall data discussed in this section are mainly from within Somalia, as data from Ethiopia were not available.

There were a total of thirteen daily rainfall stations in Somalia before the break of war, eight of which were located in the south. More than forty other stations recorded monthly rainfall. Currently, there are over thirty daily recording stations in south Somalia. Figure 2.4 shows the location of the rainfall stations. The pre-war stations are summarized in Table 2.2 and a summary of post-war stations is attached in Table A.1 in the Annex A.

Table 2.2: Details of the Pre-war Daily Rainfall Stations in South Somalia

Station Name	Station ID	Lat	Long	Period	MAR ¹	% Fill
Afgoi	SO25FG00	2.133	45.133	1955-1986	584	69
Bardera	SO22BRDR	2.350	42.300	1924-1986	473	85
Belet Weyne	SO45BLTN	4.700	45.217	1943-1986	330	92
Jowhar	SO25GHR0	2.767	45.500	1922-1986	492	51
Baidoa	SO33SCBD	3.133	43.667	1922-1986	577	80
Jilib	SO02JLB0	0.433	42.800	1930-1986	663	45
Kismayo	SO02CHSM	-0.367	42.433	1894-1986	419	94
Luuq	SO32LGGN	3.583	42.450	1922-1986	271	77
Mogadishu	SO25MGDS	2.033	45.350	1911-1985		99

2.1.3 Channel Characteristics Data

The channel characteristics used in the study were generated from the aerial survey done on the riverine areas of the two rivers. The extent of the survey is on average 2.5km on either side of the river channel. The channel characteristics needed for this study were mainly the cross sections and embankments, which were extracted from the Digital Terrain Model (DTM), processed from the aerial photography data. Figures 2.5 and 2.6 present cross sections for selected stations along the Juba and Shabelle Rivers.

2.1.4 Spatial Data

There were different types of spatial data used in this study. They include a digital terrain model (DTM) data generated from the aerial photography; soils and land use /

¹ MAR is the Mean Annual Rainfall

land cover data from SWALIM archives. Different weather related satellite based data were also used to run the rainfall-runoff models (LISFLOOD and USGS GeoSFM). Table 2.3 gives a summary of the satellite based weather data.

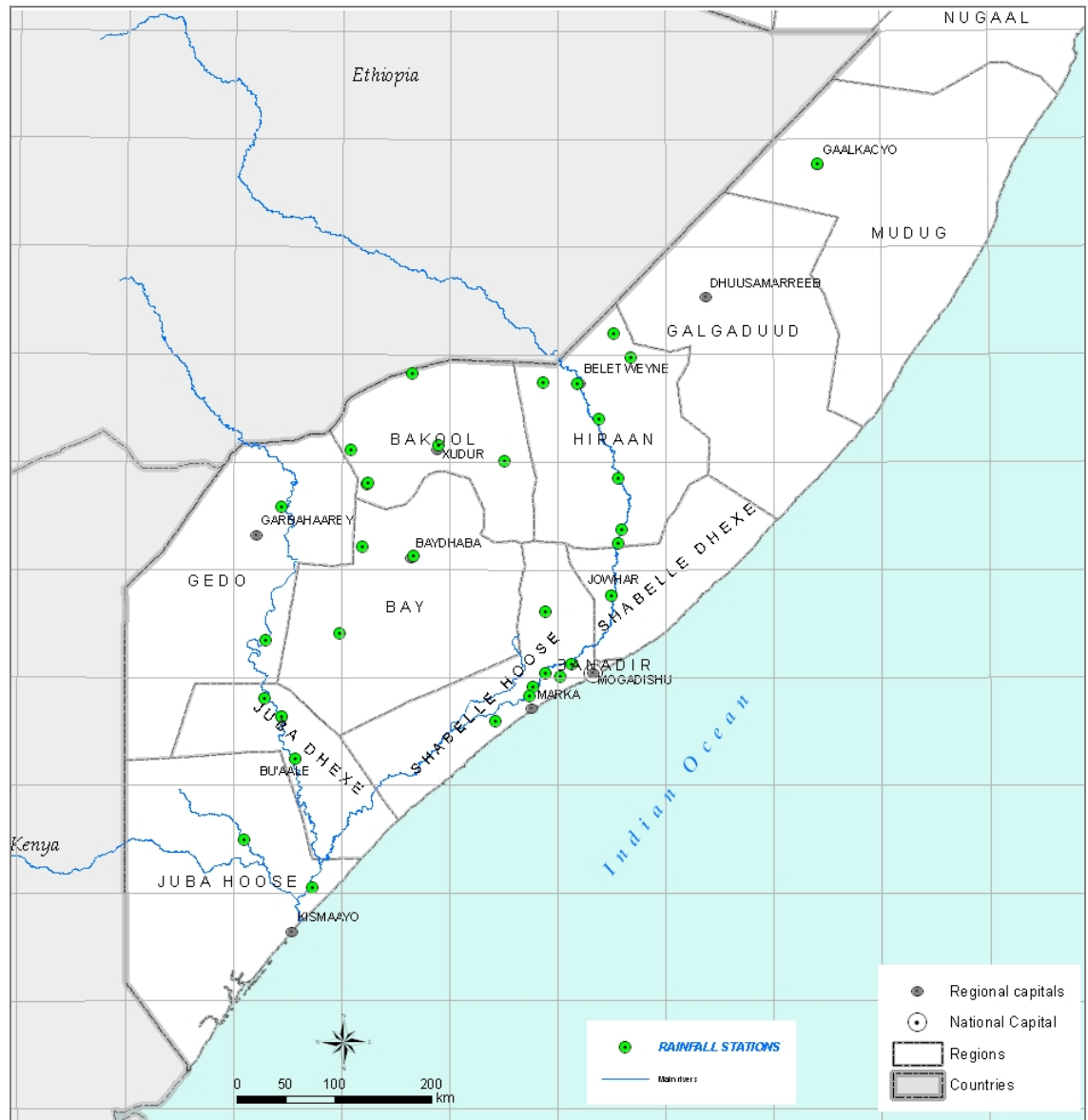


Figure 2.4: Locations of Rainfall Stations in Southern Somalia

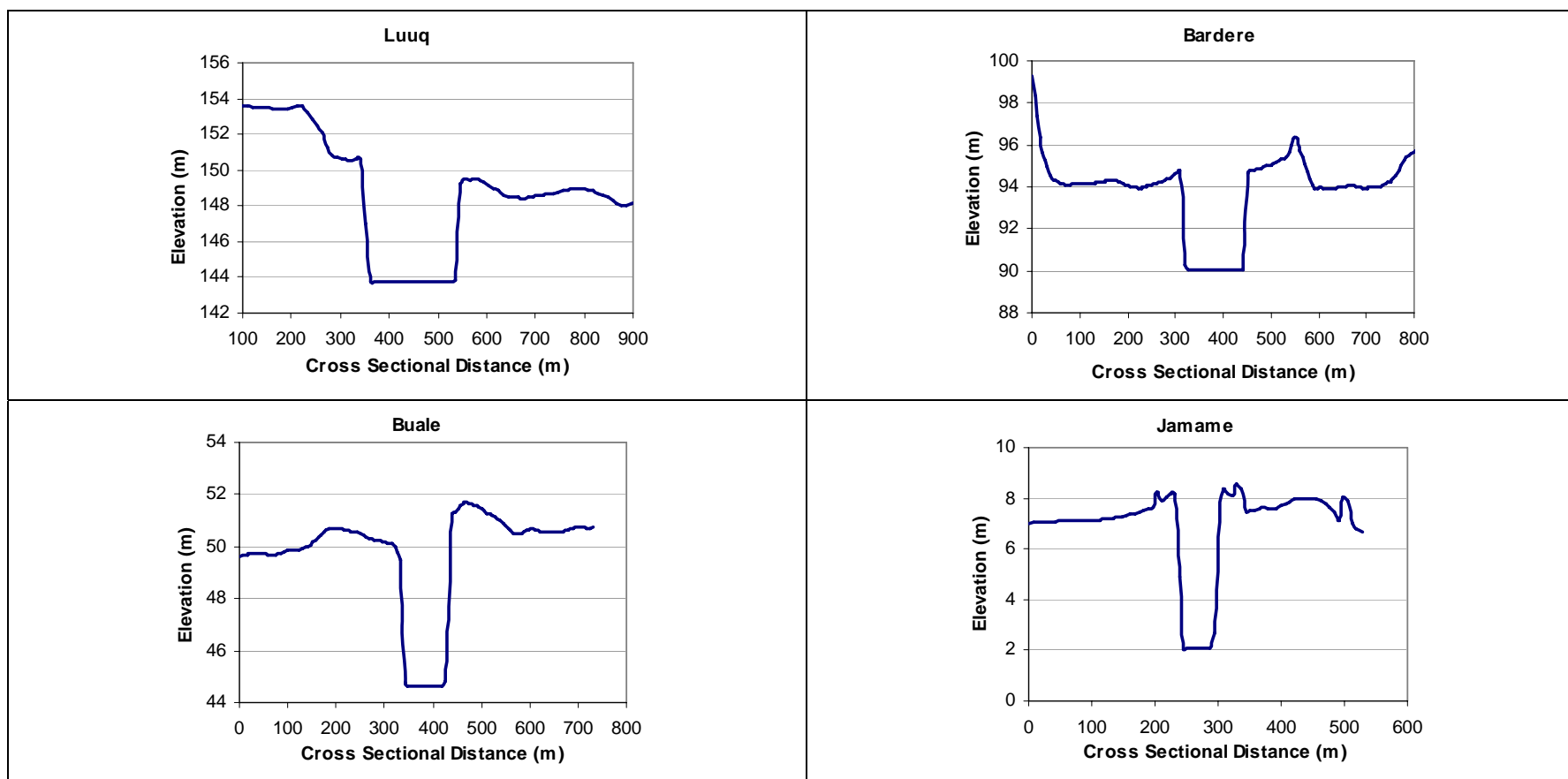


Figure 2.5: Cross Sections for Selected Stations along Juba River

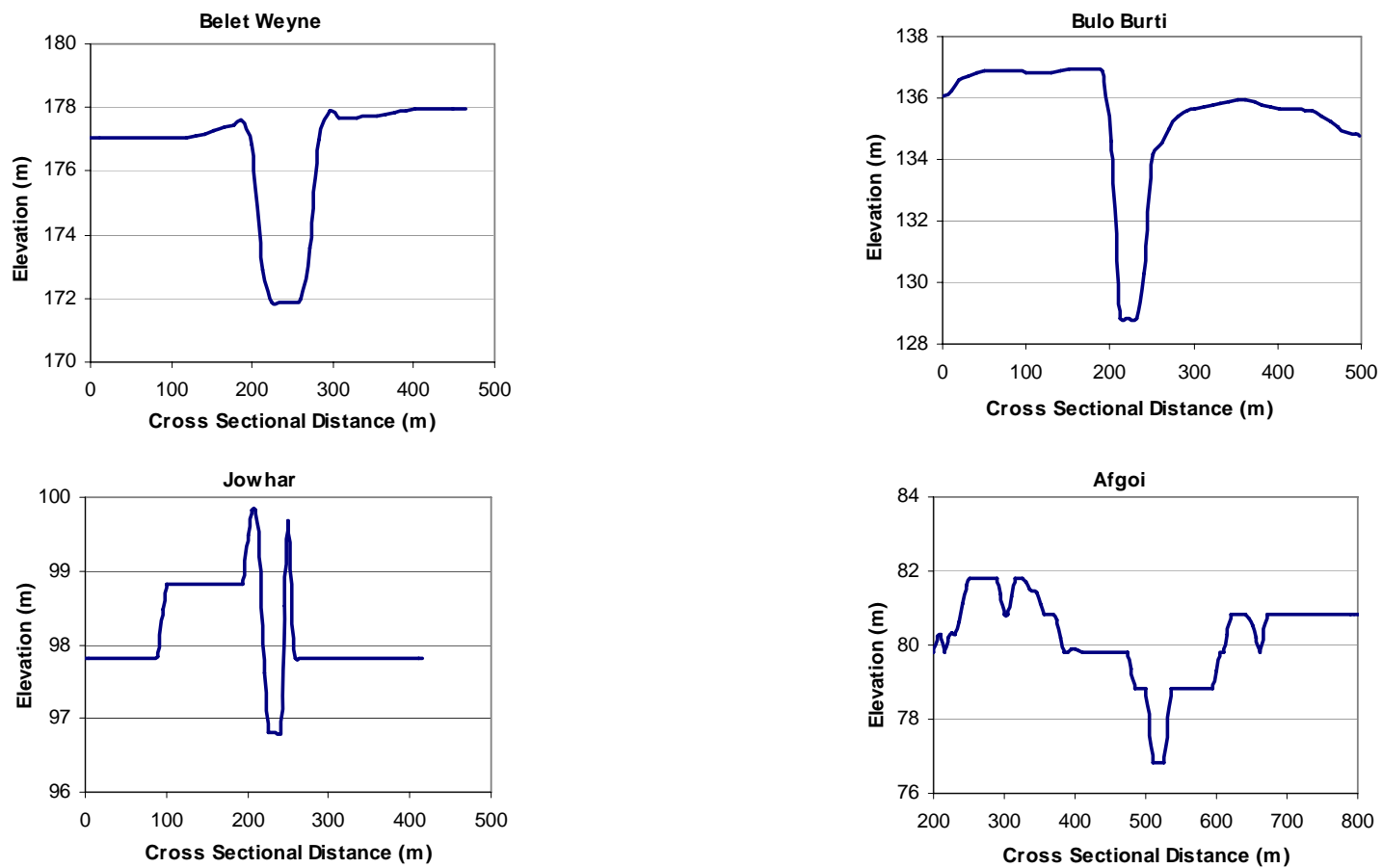


Figure 2.6: Cross Sections for Selected Stations along Shabelle River

Table 2.3: Summary of Spatial Weather Data

	ERA-40	CHARM	ERA-interim	RFE	VAREPS
Released by	European Centre for Medium-Range Weather Forecasts (ECMWF)	United States Geologic Survey and Geography Department (USGS Geography)	European Centre for Medium-Range Weather Forecasts (ECMWF)	National Oceanic and Atmospheric Administration, Climate Prediction Centre (NOAA-CPC)	European Centre for Medium-Range Weather Forecasts (ECMWF)
Data type	Reanalysis of past observations using NWP models	Blended gauge-satellite product	Reanalysis of past observations using NWP models	Blended gauge-satellite product	Probabilistic re-forecasts using Ensemble Prediction Systems
Temporal resolution	6 h	24 h	6 h	24 h	Staggered, 3 h (day 1-4) and 6 h (day 5-15)
Spatial resolution	120 km	0.1-degree	80 km	0.1-degree	Staggered, 50 km (day 1-5) and 80 km (day 5-15)
Time periods provided	01.01.1959 – 31.08.2002	01.01.1961 – 31.12.1996	01.09.2002 – 31.12.2007	01.01.2001 – 31.12.2008	01.10.1977 – 25.11.1977, 16.03.1981 – 03.05.1981

2.2 Preliminary Data Analysis

2.2.1 Flow Data

2.2.1.1 Seasonal Flows

Flow in the Juba and Shabelle Rivers depend on the *Gu* and *Deyr* rainy seasons which occur in April to June and October to November respectively. Light rains are also experienced in July to September especially in the Shabelle catchment.

During the two rainy seasons, flow in Juba and Shabelle Rivers is very high, occasionally resulting to floods. However, flow decreases to low levels during dry seasons, as can be seen in the Figures 2.7 and 2.8.

Flow in the two rivers is high in upstream stations, and continues to decrease as the rivers progress downstream. The decrease in flow is caused by, among other factors:

- i) Little or no contribution at all from the catchments within Somalia
- ii) Over bank spillage during high river flows
- iii) Water extraction for irrigation purposes
- iv) Losses due to evaporation and ground water recharge.

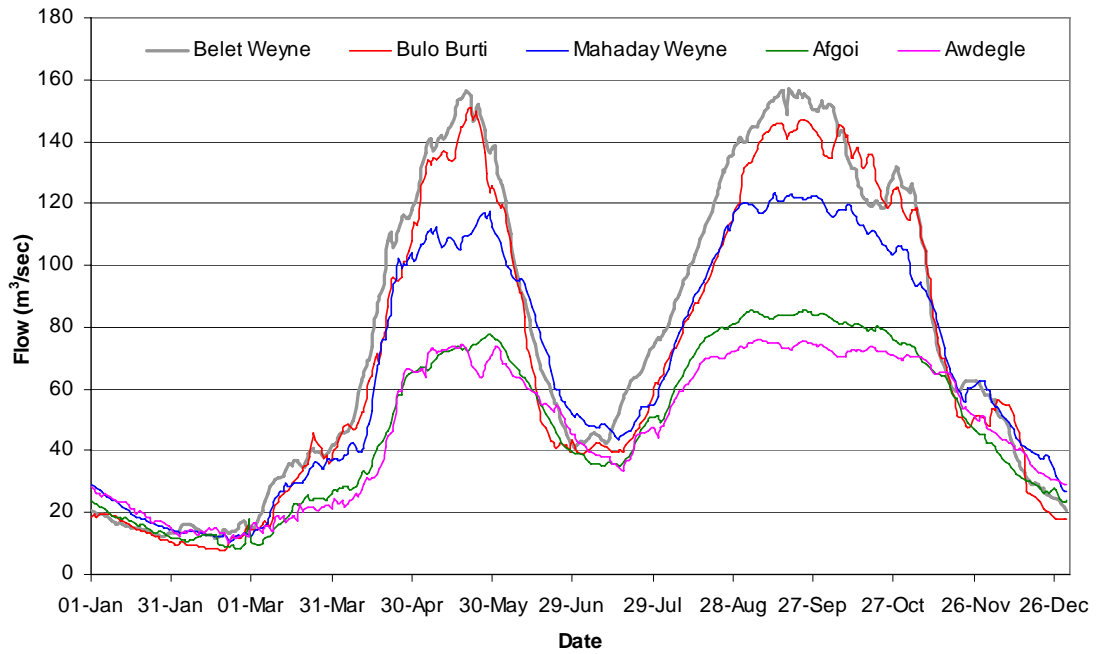


Figure 2.7: Seasonal Mean Flows for Stations along Shabelle River

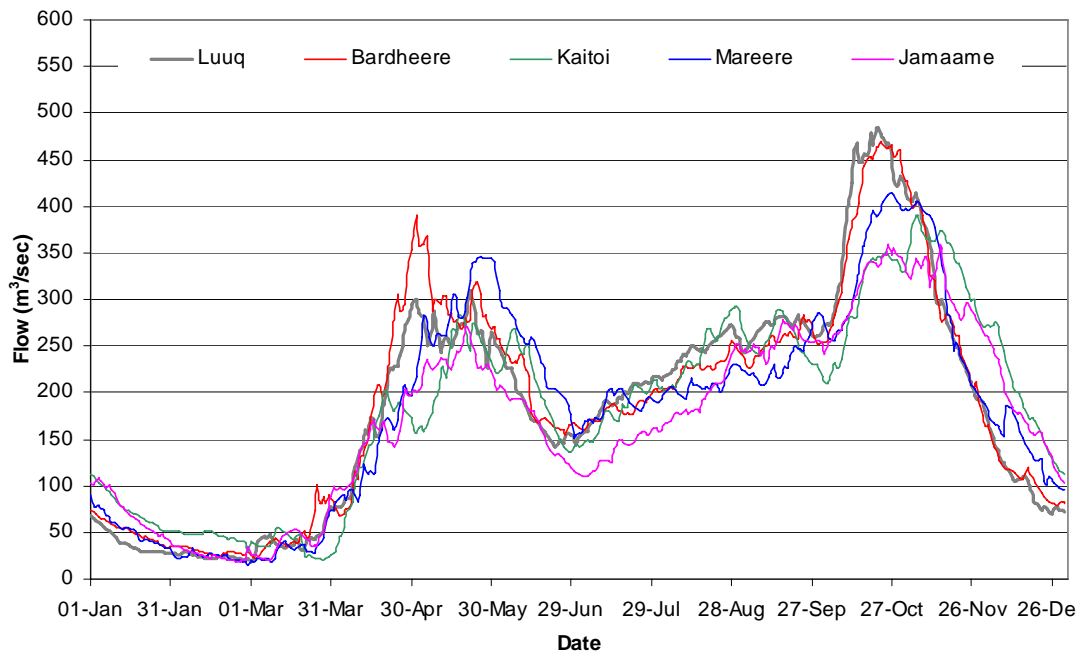


Figure 2.8: Seasonal Mean Flows for Stations along Juba River

The change in flow from the upstream to the downstream stations is more pronounced in Shabelle than in Juba. The peak flow in Belet Weyne is about double the peak flow at Afgoi (Figure 2.9), while in Juba the ratio of high peaks between the extreme upstream and downstream stations is within 25%, Figure 2.10.

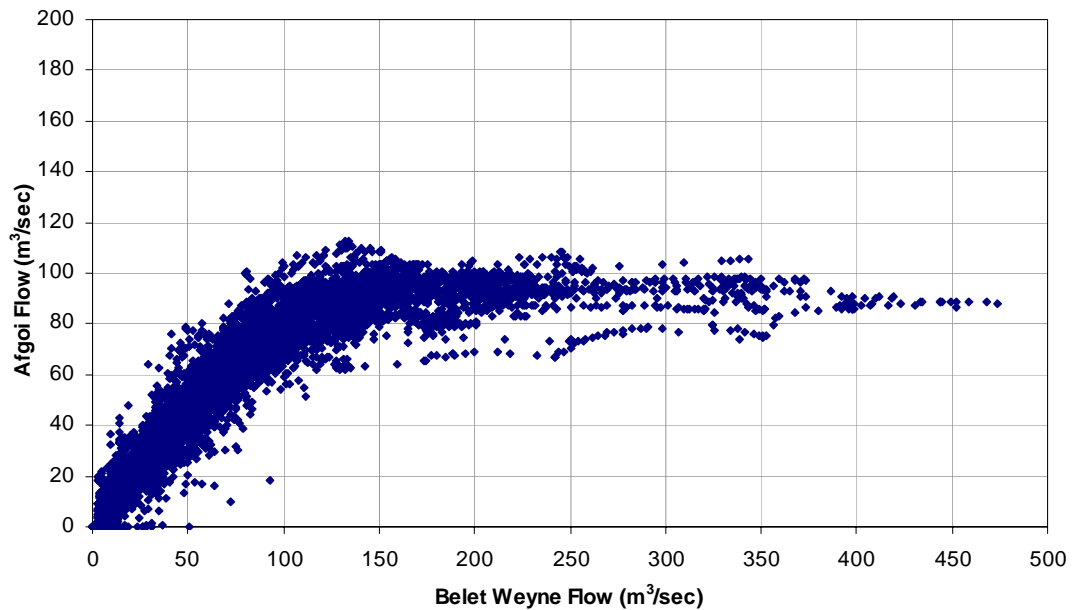


Figure 2.9: Correlation of Flow between Belet Weyne and Afgoi Stations

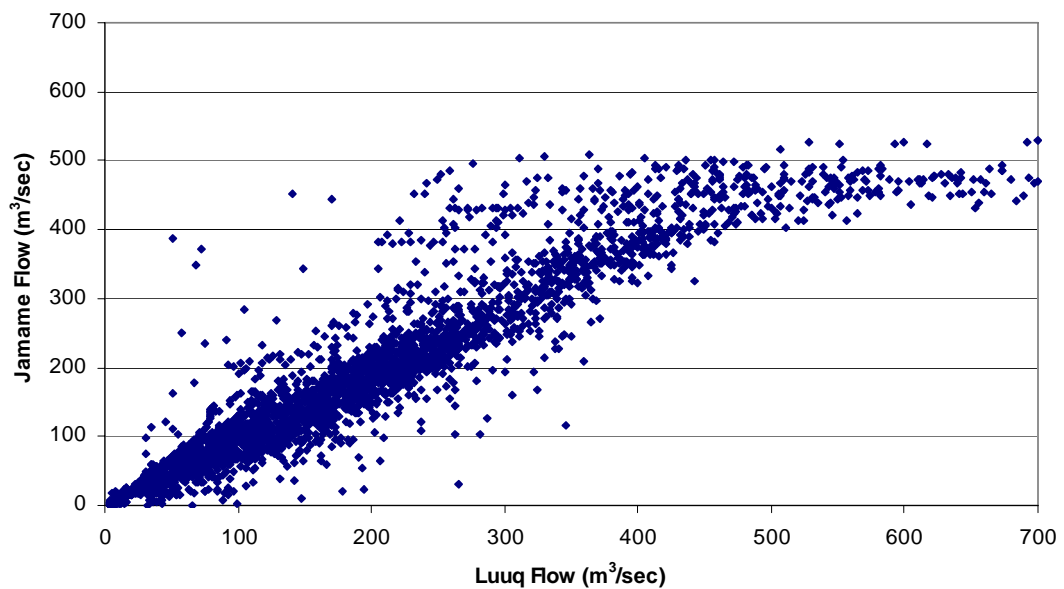


Figure 2.10: Correlation of Flow between Luuq and Jamame Stations

The high discrepancies in the upstream and downstream reaches of Shabelle River can be attributed to the channel characteristics. In Belet Weyne, the river channel is wide, deep and well defined, as can be seen from the river cross sections presented in Figure 2.6. Downstream, the river becomes shallow, and eventually becomes a swamp near the junction with Juba. This means that downstream the river reaches bank full at almost half the bank full flow in upstream stations. Most of the excess flow spills over-bank, and is responsible for the frequent flooding in the lower reaches of Shabelle. Juba has a better defined channel for most of the reach, though at the downstream sections near the outlet the channel gets shallow as well.

2.2.1.2 Shifts in Data Series

For the key gauging stations used in this study, further data analysis were done to establish the consistency of pre-war and post-war data sets. As mentioned elsewhere, all the post-war river gauging stations were destroyed during the years of civil strife. SWALIM has managed to rehabilitate most of these stations, and at present six are operational, three in Juba (Luuq, Bardere and Buale) and four in Shabelle (Belet Weyne, Bulo Burti, Jowhar and Mahaday Weyne).

In the re-establishment of the gauging stations, the datum used was different from the pre-war, either because it was not possible to identify the previous datum, or the river bed has changed over time. As a result, the readings in the post-war era are different from those of pre-war. To compare the two datasets, an adjustment has to be made. The adjustments from HYDATA for each station, which also compared well to this analysis, are shown in Table 2.4.

Table 2.4: Data Adjustments for Selected Stations in Juba and Shabelle

Station	Adjustment from Pre-War to Post-War
Juba River	
Luuq	No adjustments
Bardere	+ 1.160m up to 26 th Feb 2008; + 2.620m from 26 th Feb 2008 onwards
Buale	New gauge, no adjustments
Shabelle River	
Belet Weyne	+ 1.738m
Bulo Burti	-1.000m
Jowhar	New gauge, no adjustment

For the purpose of this study, it is the pre-war data which was adjusted to post-war so that forecasted river levels could be compared to the real time observed levels. Further analysis was done on each of the six stations to identify whether there are data shifts, other than the above changes as a result of change of datum during station reinstatement. The data shifts were done for the four pre-war stations in Table 2.4 using a double mass curve analysis after the above mentioned data adjustments. Data used was for the period 1963 to 2008. The resulting mass curve graphs are presented in Figures 2.11 and 2.12.

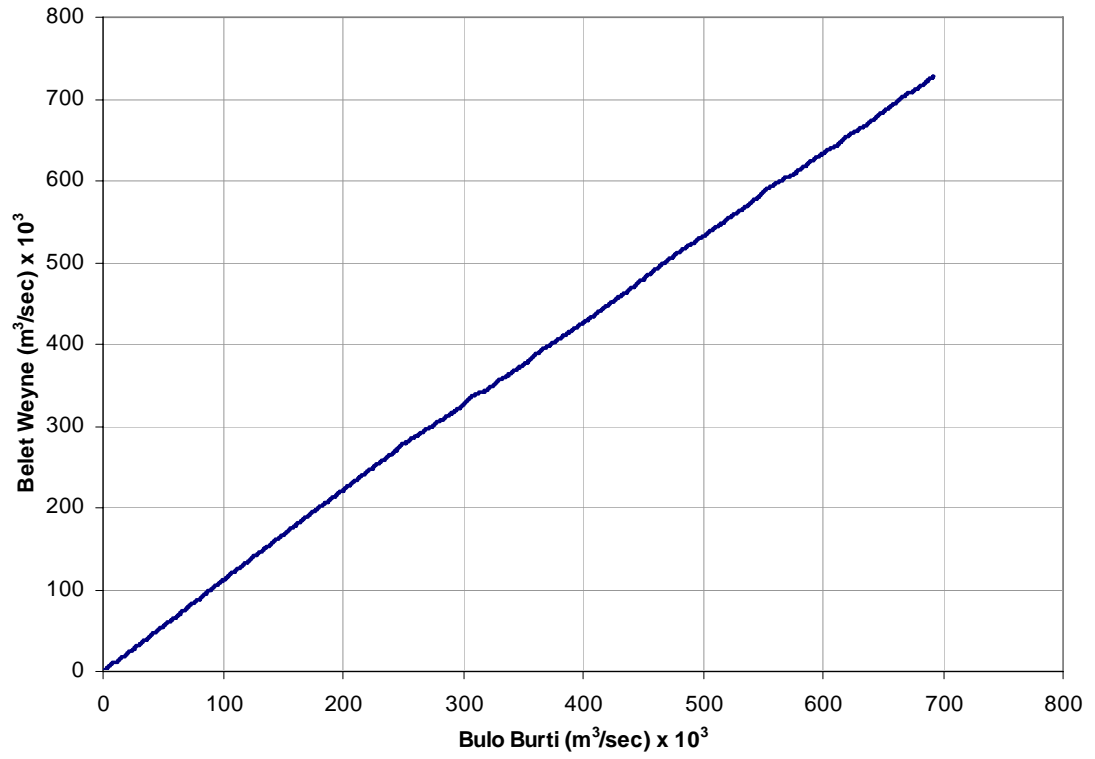


Figure 2.11: Double Mass Curve for Belet Weyne and Bulo Burti Flows

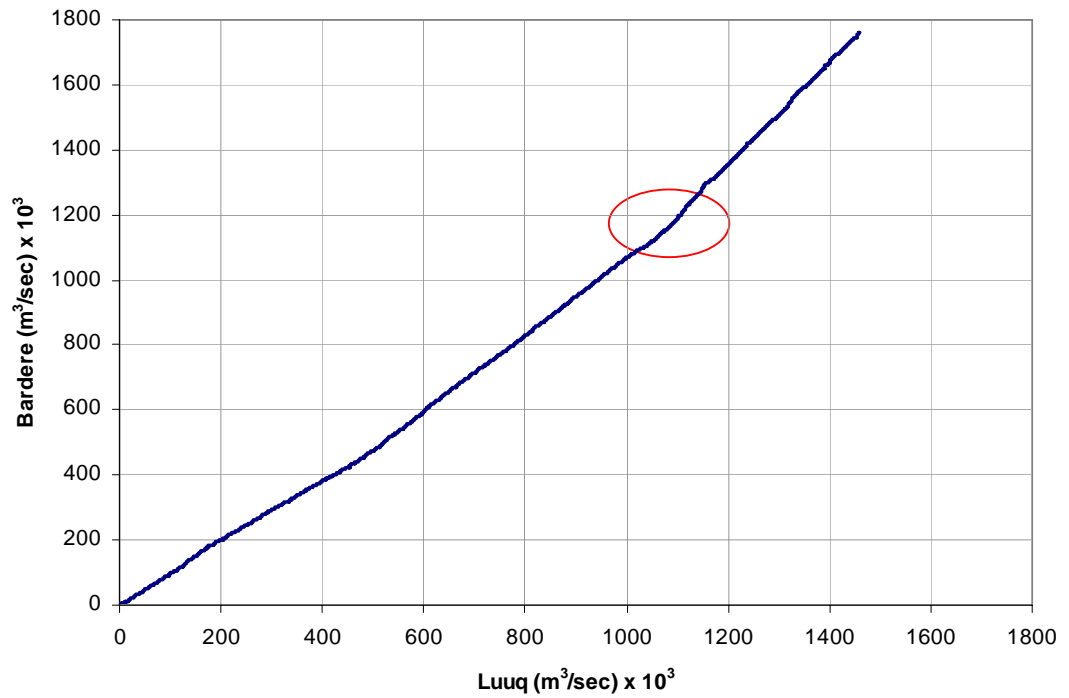


Figure 2.12: Double Mass Curve for Luuq and Bardere Flows

The relationship between the flows in Belet Weyne and Bulo Burti remained the same from pre-war to post-war, but that between Luuq and Bardere changed at some point. Further analyses were done on the data series for Luuq and Bardere to identify which data set had changed over time. The Bardere gauge has been reinstated twice, and this could have resulted into some changes in the flows.

The long term mean flow for Luuq and Bardere were taken for the pre-war and post-war datasets. The results obtained are presented in Figures 2.13 and 2.14.

From the two graphs, it is clear that the station with shift in flow is Bardere. The long term mean flow for Luuq during pre-war remained very close to that of post-war, but for Bardere there were noticeable differences for both data series (Figure 2.14). From the figure, the minimum flow for post-war data series seem to be increasing with time, which could be responsible for the increased mean flow. From literature, such discrepancies can be corrected using the mass curve approach where a factor is applied to correct the slope of the line to the original gradient. The correction factor applied is obtained by:

$$Q_{cor} = Q_{obs} \frac{Slope_{cor}}{Slope_{obs}} \quad (2.1)$$

Where Q_{cor} is the corrected discharge; Q_{obs} is observed discharge; $Slope_{cor}$ is the slope of corrected data; and $Slope_{obs}$ is slope of observed data.

The double mass curve resulting from the corrected data is shown in Figure 2.15, while the resulting mean flow is presented in Figure 2.16.

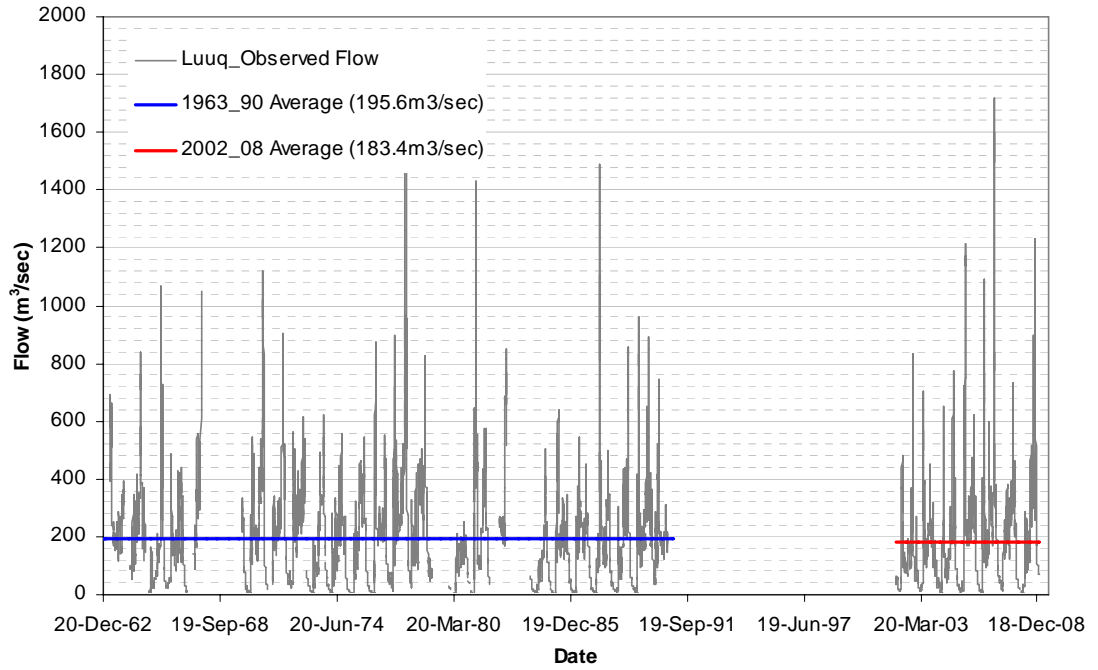


Figure 2.13: Long Term Mean Flow at Luuq

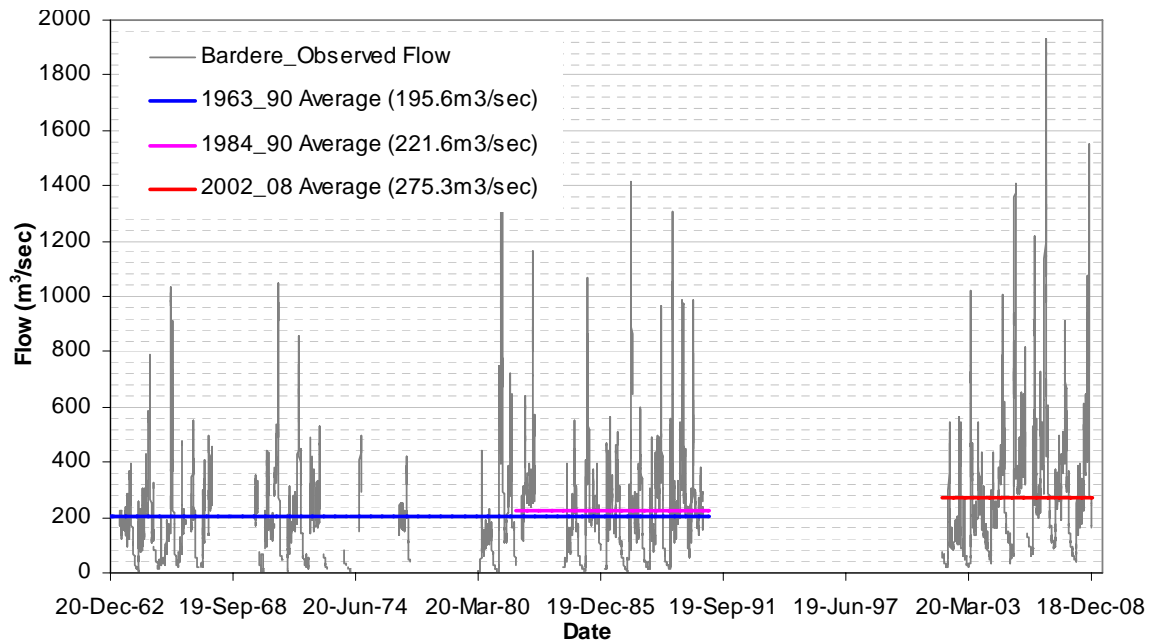


Figure 2.14: Long Term Mean Flow at Bardere

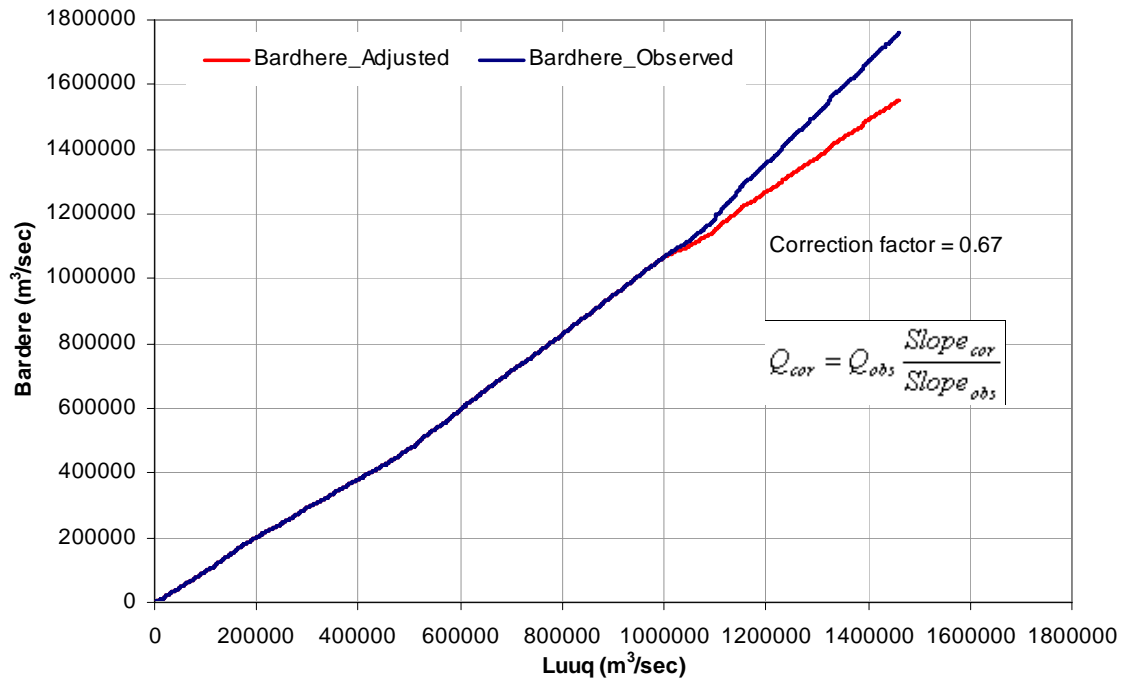


Figure 2.15: Double Mass Curve for Luuq and Corrected Bardere Flows

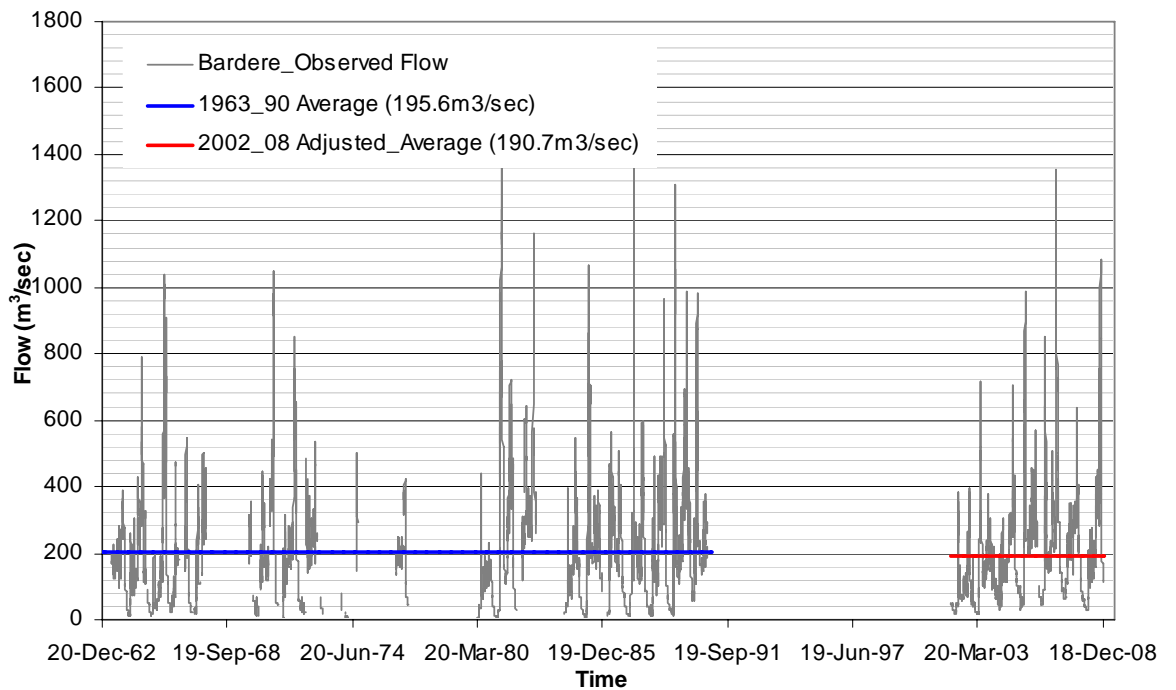


Figure 2.16: Long Term Mean Flow at Bardere after Data Correction

2.2.1.3 Preliminary Routing Analysis

Regression analysis was performed along the Juba and Shabelle Rivers between different stations for the pre-war and post-war daily data series to establish the relationship between the datasets. The analysis was done by lagging the flow at the upstream stations by certain time and regressing on the flow at the downstream stations. The regression coefficient at each time step was noted and the best lag time established from the highest coefficient value.

Figures 2.17 to 2.20 show the scatter graphs for observed flow at no lag time and two day's lag time between Luuq and Bardere along Juba, and Belet Weyne and Bulo Burti along Shabelle.

A summary of the lag times between the upstream stations, Belet Weyne in Shabelle and Luuq in Juba and downstream stations is given Table 2.5.

Table 2.5: Lag Times between Upstream and Downstream Stations along Juba and Shabelle Rivers

SHABELLE										
	Correlation Between Belet Weyne and Downstream Stations									
Lag Days From Belet Weyne	0	1	2	3	4	5	6	7	8	9
Bulo Burti	0.900	0.924	0.933	0.920						
Mahaday Weyne	0.738	0.757	0.773	0.786	0.791	0.789	0.779	0.764		
Jowhar	0.570	0.580	0.600	0.620	0.623	0.622	0.610	0.590		
Afgoi	0.580	0.600	0.618	0.635	0.651	0.665	0.676	0.680	0.678	0.669
JUBA										
Lag Days From Luuq	0	1	2	3	4	5	6	7	8	9
Bardere	0.830	0.870	0.885	0.860	0.815	0.765				
Buale	0.770	0.810	0.850	0.880	0.900	0.920	0.910	0.900		
Mareere	0.620	0.652	0.652	0.683	0.714	0.744	0.769	0.783	0.787	0.782

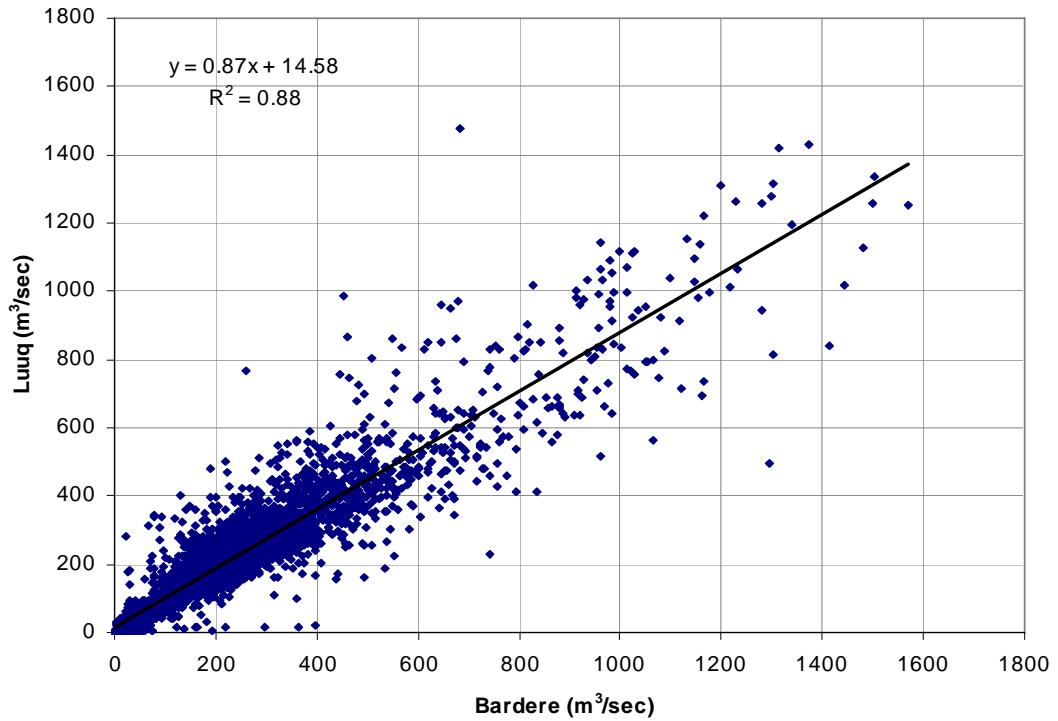


Figure 2.17: Correlation between Luuq and Bardere Flow at no Lag-time

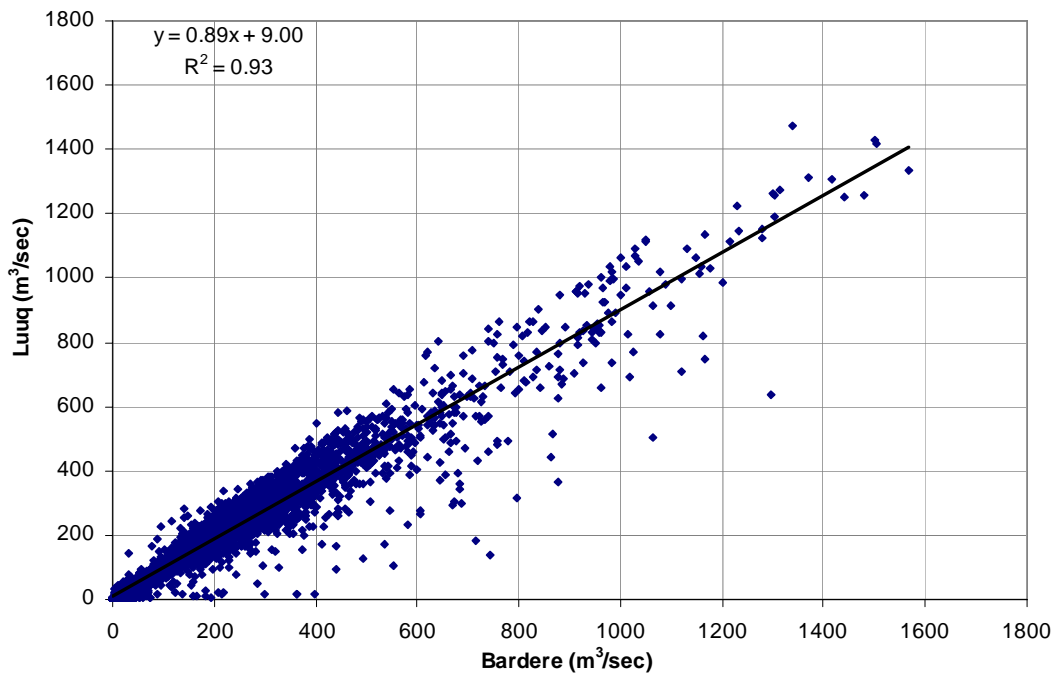


Figure 2.18: Correlation between Luuq and Bardere Flows at 2-Days Lag-time

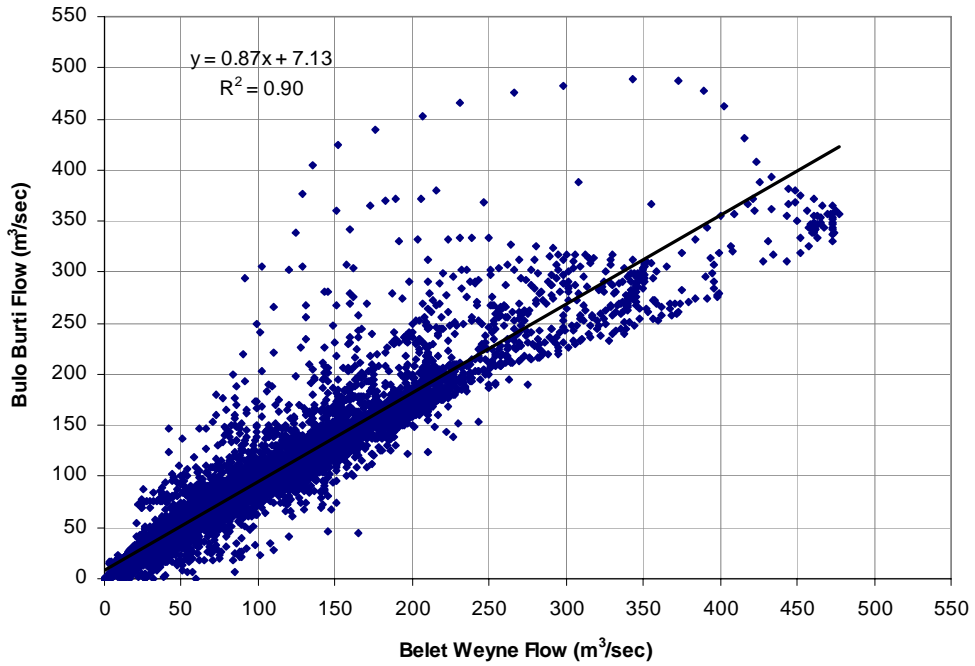


Figure 2.19: Correlation between Belet Weyne and Bulo Burti Flows at Lag zero

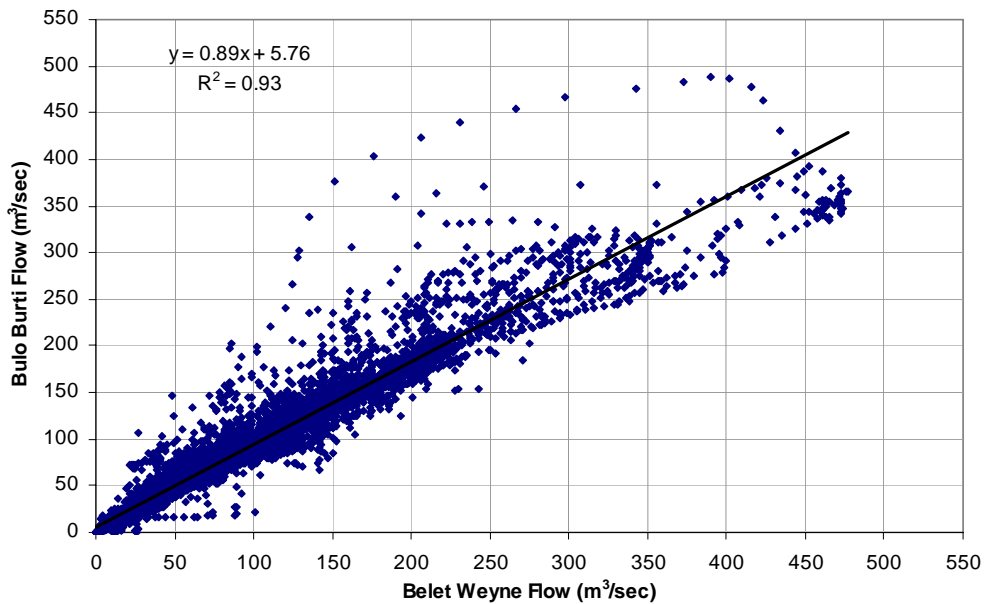


Figure 2.20: Correlation between Belet Weyne and Bulo Burti Flows at 2-Days Lag-time

The relationship between Belet Weyne and Bulo Burti with both zero and two days lag time was hysteretic, indicating that the single valued rating curve currently used for the rising and falling river levels is not be accurate. This necessitated further separation of data into rising and falling phases to see their behaviour. The resulting scatter graphs are presented in Figures 2.21 and 2.22 and a summary is given in Table 2.6.

Table 2.6: Lag Times at Rising and Falling Hydrograph Phases for Belet Weyne and Bulo Burti

Lag Days (Belet Weyne to Bulo Burti)	0	1	2	3	4
Rising	0.94	0.95	0.96	0.86	0.68
Falling	0.89	0.90	0.91	0.88	0.82

Figures 2.21 and 2.22 clearly shows that at high flows the relationship between Belet Weyne and Bulo Burti is not as linear as during low flows, even though the best correction is attained at two days lag in both rising and falling phases of the hydrograph. It is expected that the ongoing discharge measurements will be useful in updating the rating curves for the six gauging stations along Juba and Shabelle Rivers.

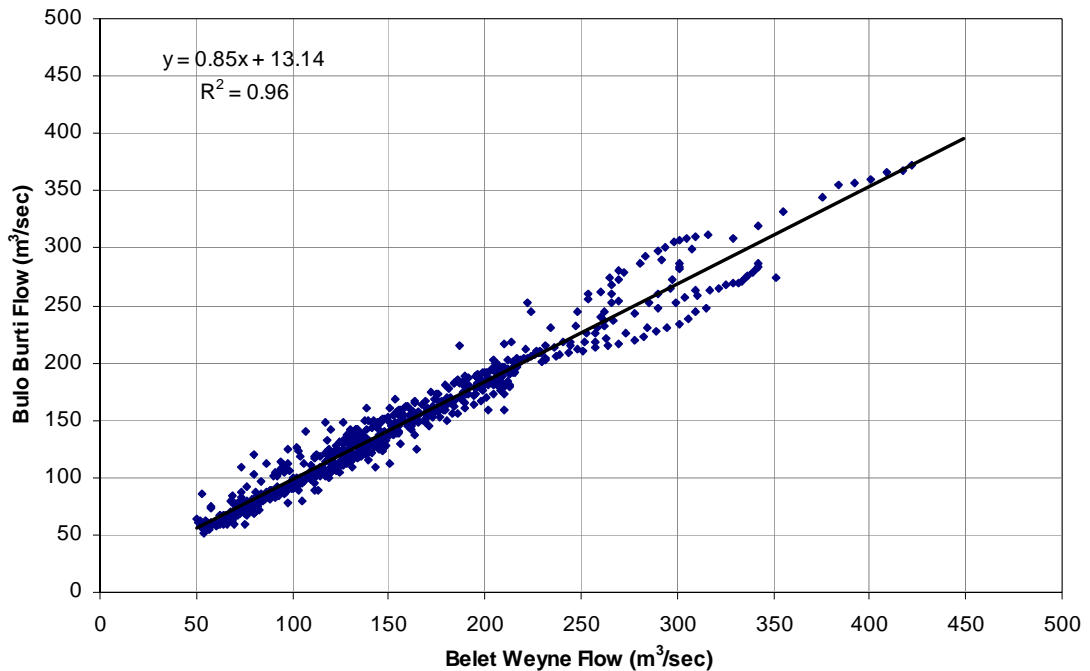


Figure 2.21: Scatter Plot of Rising Hydrograph Phase for Belet Weyne and Bulo Burti Flows with 2 Day Lag

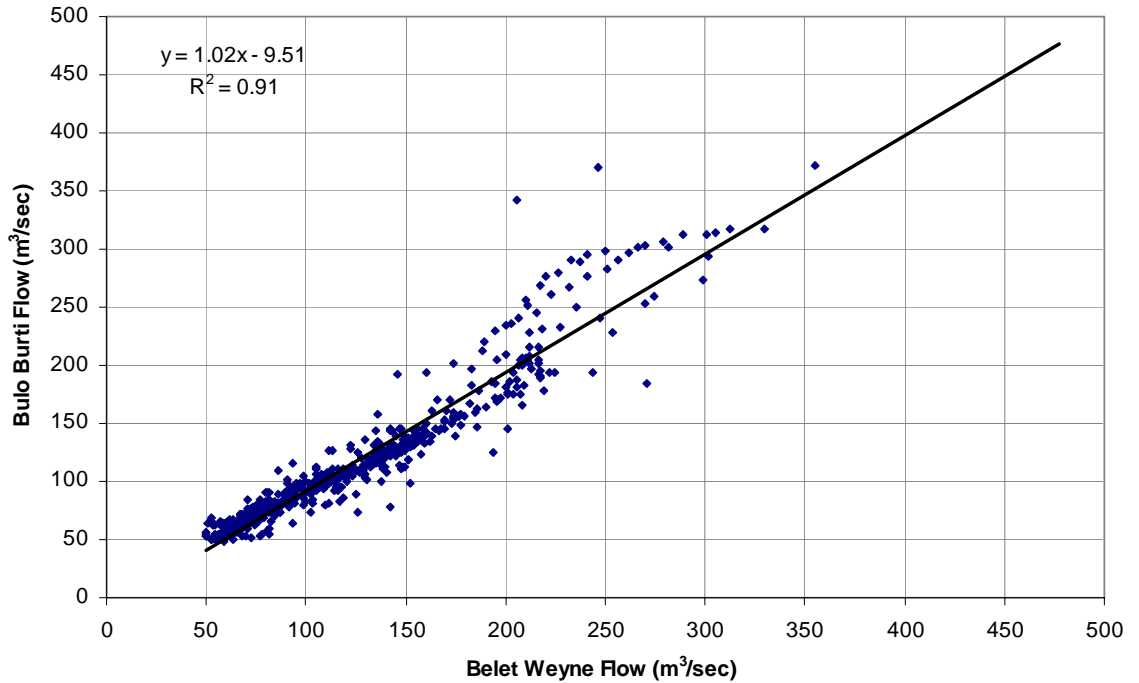


Figure 2.22: Scatter Plot of Falling Hydrograph Phase for Belet Weyne and Bulo Burti Flows with 2 Day Lag

2.2.2 Rainfall Data

Due to the limitation of access to rainfall data within the upper catchments of Juba and Shabelle, within Ethiopia, and the assumed minimal contribution of the Somalia catchments, no observed rainfall data were used in the study. The results of rainfall runoff models presented elsewhere in this report were from satellite based rainfall estimates. However, during the study it became clear that during high storms, the contribution of the Somalia catchments is significant enough to affect river levels downstream.

A detailed analysis of rainfall data within Somalia is available in SWALIM's report on the Climate of Somalia.

Chapter 3

Description of Hydrological Models

3.0 Introduction

This section of the report provides a general introduction to the hydrological models tested for flood forecasting in the Juba and Shabelle basins and their theoretical background, including conceptual representation and parameters of the models. The models are categorised as rainfall-runoff models and routing models. Summary and analysis of available data used for their calibration and validation are presented in the previous section while the results of models' application are presented in section four.

3.1 General Overview

Hydrological models are important tools for determination and prediction of rainfall-runoff relationships as well as routing of runoff. Some of these models lump or average the physical parameters over the watershed and are called lumped models. Other models distribute these parameters spatially over the watershed. Lumped models do not account for spatial variability of some aspects like topography, soil types, patterns and changes in vegetation types. Models that are based on physical relationship are called physically based models and can in principle overcome limitations through their use of parameters which have a physical interpretation and through their representation of spatial variability in the parameter values.

Traditionally hydrological modelling systems are classified into three main groups, namely, (1) empirical black box, (2) lumped conceptual and, (3) physically based distributed systems. Empirical black-box models are those forms of models which depend solely on the assumption of a very general but a flexible relationship thought to exist between the input and the output in which no attempt is made to simulate individual hydrological processes and mechanisms such as evaporation, interception, infiltration, generation of surface runoff, subsurface flow etc. Traditional methods of *curve-fitting*, *multiple regression* and *unit hydrographs* are examples widely used in empirical hydrological modelling. "*Systems model*" and "*System theoretic model*" are terms also used to refer to an empirical black-box model.

The great majority of the modelling systems used in practice today belong to the simple types (1) or (2), and require a modest number of parameters to be calibrated for their operation. Despite their simplicity, many models have proven quite successful in representing measured stream flow hydrographs. However, a severe drawback of these traditional modelling systems is that, their parameters are not directly related to the physical conditions of the catchment. Accordingly, it may be expected that their applicability is limited to areas where runoff has been measured for some years and where no significant change in catchment conditions have occurred.

3.1 Rainfall Runoff Models

Rainfall-Runoff models in the context of hydrological sciences, are intended to describe the nature and the behaviour of hydrological variables with the help of assumptions, equations and procedures, and with a view to provide an effective system for the solution of problems arising in the planning, design and management of water resource projects. Forecasting of flows in rivers is usually associated with either a reliable flood warning issuance system required for evacuating downstream habitation threatened by rising water level, or with efficient reservoir management system, or with study of various aspects of planning and design of water resources structures, etc. Below is a description of the models utilised in developing the flood forecasting model for the Juba and Shabelle Rivers in Somalia.

3.1.1 LISFLOOD Model

LISFLOOD is a distributed, hydrological rainfall-runoff model that has been developed by the Land Management and Natural Hazard Unit of the Joint Research Centre of the European Union (EU) for the simulation of hydrological processes in large river basins. It is a hybrid between a conceptual and a physical rainfall-runoff model (type 2 and 3 above) that is capable of simulating the hydrological processes that occur in large river catchments, taking into account the influences of topography, precipitation (amount and intensities), antecedent soil moisture content, soil type and land use type. The model works in a GIS environment, which has the great advantage of a flexible and easy adaptable model structure.

The model has been designed, tested and set-up for mid-latitude regions in Europe. Outside of Europe it has been applied once for the Lushi basin in China. LISFLOOD consists of three modules: a water balance mode, a flood mode and a mode to calculate the inundated areas. The water balance mode is used to estimate the initial conditions required for the flood mode.

Figure 3.1 gives a schematic overview of the LISFLOOD internal model structure. The major processes as they are depicted in Figure 3.1 are shortly described below based on the user manual published in 2008. For a detailed description of the processes including the evaluation of (sub) equations, the reader is referred to the LISFLOOD user manual.

1. Interception (Int): interception due to storage by vegetation is calculated using a storage formula based on the leaf area index derived using vegetation and land cover data and rainfall intensity. Leaf drainage (D_{int}) is modelled using a linear reservoir whole intercepted water evaporates (EW_{int}) as potential rate from open water surfaces but is limited by the amount of water stored in the leaf.

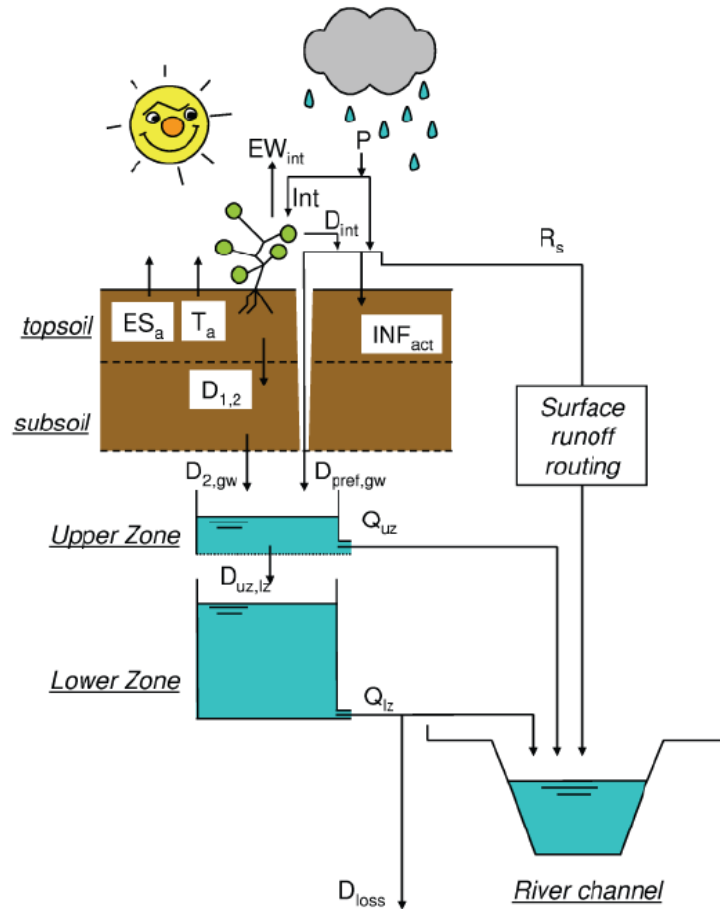


Figure 3.1: Overview of the LISFLOOD Model Internal Structure

2. *Soil Evaporation (ES_a) and Plant Transpiration (T_a):* actual evaporation from the soil is limited by the available amount of water in the soil, the maximum evaporation from bare soil (ES_{max}) decreases to the actual amount with increasing number of days since the last rain event and is estimated as the minimum value of the potential evaporation or the difference between the amount of soil moisture in the upper zone and residual amount of water in the upper zone. The actual transpiration by plants is calculated based on the approach developed by Supit and Van de Goot (2003). In case of limited soil moisture the actual transpiration decreases due to the closing of the plant's stomata.

Infiltration (INF_{act}): The actual infiltration is calculated as the smallest value out of the results of the potential infiltration INF_{pot} and the difference between the amount of water that is available for infiltration W_{av} and the preferential bypass flow ($D_{pref,gw}$). The preferential bypass flow corresponds to the water that drains directly to the groundwater without entering the soil matrix.

Surface runoff (R_s): Surface runoff is generated as a function of the available amount of water that is available for infiltration W_{av} , the preferential bypass flow $D_{pref,gw}$ and the actual infiltration INF_{act} .

Soil moisture redistribution: The vertical flow within and out of the soil is assumed to be entirely gravity-driven. The soil moisture redistribution is simulated applying a complex iterative procedure including, inter alia, Darcy's Law and Van Genuchten equation. However the evaluation of the whole approach is beyond the scope of this work, but can be found in the LISFLOOD user manual.

Groundwater: The groundwater system is described using two parallel interconnected linear reservoirs (Figure 3.1). The first reservoir is the upper zone which represents a mix of subsurface flow and fast flowing groundwater; while the second reservoir represents the lower zone which reacts much slower generating base flow.

Channel Routing: Water can be routed through the channel using the kinematics or dynamic wave approach. The kinematics wave is the default approach used in LISFLOOD.

A list of the LISFLOOD model parameters is given in Table A.2 in Annex A. Most of these parameters can be estimated from literature values or existing soil and land cover data sets or other sources. The remaining parameters need to be estimated by calibrating the model against observed discharge records.

3.1.2 Geospatial Stream flow Model – GeoSFM

This model has been developed by the National Centre for Earth Observation and Science (EROS) of the U. S. Geological Survey to support the USAID funded activity, Famine Early Warning System Network (FEWS NET) in flood monitoring in Africa after the famous Mozambique floods and assess their impact on food security. The modelling platform was later expanded to cover Southeast Asia and was implemented in the five countries that share the Mekong River basin. It's a rainfall-runoff model and is comprised of soil water accounting module that produces surface and sub-surface runoff for each sub-basin, an upland headwater basins routing module, and a major river routing module. The model consists of a GIS-based Graphic User Interface (GUI) module used for model input and data preparation. The GUI of the model is user friendly to prepare the necessary input data as well as routing of the flow and display of the outputs using the special analysis functions of the Arc View GIS software.

The runoff prediction module conceptualises the soil as composed of two main zones as shown in Figure (3.2): (i) an active soil layer where most of the soil-vegetation-atmosphere interactions take place and, (ii) a groundwater zone. The active soil layer is divided into an upper thin soil layer where evaporation, transpiration, and percolation take place and a lower soil layer where only transpiration and percolation occur. The runoff producing mechanisms considered in the model are surface runoff

due to precipitation excess (including direct runoff from impermeable areas of the basin), rapid subsurface flow (interflow), and base-flow.

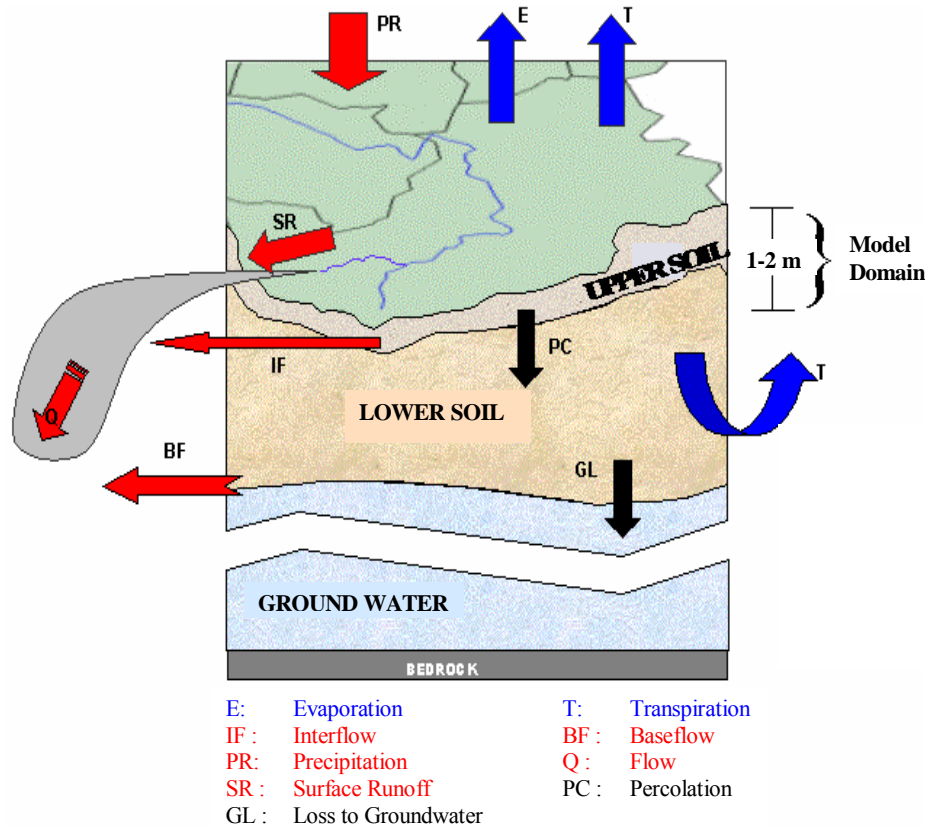


Figure 3.2: Overview of the GeoSFM Model Internal Structure

The surface upland routing module is a physically-based unit hydrograph method that relies on cell-based landscape attributes such as drainage area, slope, flow direction, and flow length derived from a digital elevation model. The interflow and base-flow components of the runoff are routed with a set of theoretical linear reservoirs. In the main river reaches water is routed using a non-linear formulation of the Muskingum-Cunge routing scheme. Most of the model parameters have a physical meaning and are determined by the spatial distribution of basin characteristics. Parameterisation of the basins' hydrological properties is accomplished through the use of three data types describing the Earth's surface: topography, land cover, and soils.

Table 3.1 lists the model parameters. Characteristics describing the physical nature of the watershed are derived from soil; terrain and land use data and are included in input files. Additional characteristics are derived from this information and used by the model to simulate stream flow and soil-water conditions.

Table 3.1: GeoSFM Model Parameters

Parameter	Description
WHC (mm)	Soil water holding capacity
TSD (cm)	Total soil depth
USD (%)	Upper soil layer depth, percent of the active soil layer from the TSD
K_s (m/hr)	Saturated hydraulic conductivity
CN	Basin runoff or SCS curve number
K_c	Pan coefficient
N	Manning's roughness coefficient for river flow
GWL	Basin loss or groundwater recharge

3.2 Inflow and Flood Routing Models

In rivers, the stage and discharge hydrographs represent the passage of waves of river depth and discharge respectively. As this wave moves down the river, the shape of the wave gets modified due to various factors, such as channel storage, resistance, lateral addition or withdrawal of flows, etc. Flood waves passing through a river have their peaks attenuated due to friction if there is no lateral inflow. The addition of lateral inflows can cause a reduction of attenuation or even amplification of a flood wave. The study of the basic aspects of these changes in a flood wave passing through a channel system is known as flood routing. The computation of these changes to the inflow hydrograph is the subject of channel and flood routing methods.

Flood routing is the technique of determining the flood hydrograph at a section of a river by utilizing the data of flood flow at one or more upstream sections. The hydrological analysis of problems such as flood forecasting, flood protection, reservoir design and spillway design invariably include flood routing. Different routing methods that show varying degrees of complexity and data needs were developed for flood routing. They generally fall into two groups. These are the hydrological, or lumped, routing methods; where the change in the hydrograph along a channel reach is computed without considering what happens to it at intermediate points, and the hydraulic, or the distributed routing methods; where outflow hydrographs are computed at a mesh of points along the channel.

Distributed models apply the physics of the flow more accurately than their lumped counterparts. However, they need detailed information that is not available especially for rural catchments. The treatment of such methods is beyond the scope of the present work. An excellent example of hydrological routing methods is the Muskingum method. This method assumes that the water temporarily stored in the channel reach is given by a linear relationship between the input and output both scaled by a factor depending upon the channel characteristics.

3.2.1 Hydrodynamic Routing Models

In hydraulic routing, flow is described by a set of hydrodynamic differential equations of unsteady-state. The simultaneous solutions of those equations lead to determination of the outflow hydrograph. These models employ the continuity equation together with the equation of motion of unsteady flow. The basic equations used in the hydrodynamic routing models, known as St. Venant equations, afford a better description of unsteady flow than hydrologic methods. Routing in this case is essentially a solution of these equations. Only for highly simplified cases can one obtain the analytical solution of these equations. Simplifications include diffusion analogy routing, kinematics wave routing, and dynamic wave routing models.

3.2.1.1 HEC River Analysis System (RAS) Model

The U. S. Army Corps of Engineers' Hydrologic Engineering Centre, River Analysis System (HEC-RAS) is developed as an integrated system of software, designed for interactive use in a multi-tasking environment. The HEC-RAS system will ultimately contain three one-dimensional hydraulic components for: (1) steady flow water surface profile computations; (2) unsteady flow simulation; and movable boundary sediment transport computations. The system is comprised of a graphical user interface (GUI), separate hydraulic analysis components, data storage and management capabilities, graphics and reporting facilities (US Army Corps of Engineers, 2002).

The model performs one dimensional hydraulic calculation for a network of river channels under steady or unsteady conditions. The steady-flow version of the model solves one-dimensional step-backwater calculations as shown in Figure 3.3 and equation 1; however, the following assumptions are necessary when using this approach for natural channels: (1) flow is comparatively steady along the whole reach because time-dependent variables are not included in the energy equation; (2) flow varies gradually between cross-sections due to the energy equation having a postulated hydrostatic pressure distribution at each cross-section; (3) flow is one-dimensional, and therefore the calculation is based on the premise that the total energy head is the same at every point in a cross section; (4) the bed-slope of the channel is less than 10% because the pressure head is represented by water depth, which is measured vertically in the energy equation; and (5) the energy slope is constant over the cross-section.

The basic computational procedure in HEC-RAS model is based on the solution of the one-dimensional energy equation. Energy losses are evaluated by friction (Manning's equation) and contraction/expansion (coefficient multiplied by change in velocity head). The momentum equation is utilised in situations where water surface profile is rapidly varied. These situations include mixed flow regime calculations (i.e. hydraulic jumps), hydraulics of bridges, and evaluating profiles at river confluences (stream junctions). The effects of various obstructions such as bridges, culverts, weirs, and structures in the flood plain may be considered in the computations. The steady flow system is designed for application in flood plain

management and flood insurance studies to evaluate floodway encroachments. Water surface profiles are computed from one cross section to the next by solving the energy equation with an interactive procedure called the standard step method. The energy equation is written as follows:

$$y_2 + z_2 + \frac{a_2 v_2^2}{2g} = y_1 + z_1 + \frac{a_1 v_1^2}{2g} + h_e \quad (3.1)$$

Where: y_1, y_2 = Depth of water at cross-sections

z_1, z_2 = Elevation of the main channel inverts

v_1, v_2 = Average velocities (total discharge/total flow area)

a_1, a_2 = Velocity weighting coefficients

g = Gravitational acceleration

h_e = Energy head loss

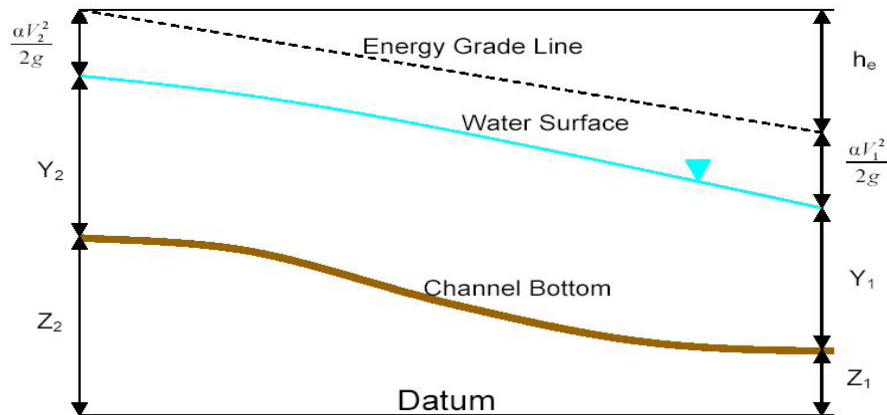


Figure 3.3: Representation of Terms in the Energy Equation for HEC-RAS

The data requirements for HECRAS include river transects, observed river stages, flow hydrographs and rating curves, hydraulic structures along the river network, storages and water diversion points along the river network; and channel and overland Manning's coefficients. Most of the hydraulic data is obtained through field surveys or extracted from digital terrain models (DTM).

3.2.2 Galway Flow Modelling and Forecasting System (GFMFS)

This software package is developed at the Department of Engineering Hydrology of the National University of Ireland at Galway as part of its international postgraduate programme and research in hydrology. The models used in the GFMFS package for simulation of flow, and also as substantive models for use in updating applications

are all mathematical, and they seek to simulate the process of transformation of the input(s) to a physical system to the output from the system by simplifying the associated complexities. *Empirical black-box models* and *lumped conceptual physically-inspired modes* are two broad categories of models used in the GFMFS. The models of this category included in the GFMFS package are:

- the Non-Parametric form of the Simple Linear Model (NP-SLM)
- the Parametric form of the Simple Linear Model (P-SLM)
- the Non-Parametric form of the Linear Perturbation Model (NP-LPM)
- the Parametric form of the Linear Perturbation Model (P-LPM)
- the Variable Gain Factor Linear Model (LVGFM) and
- the Artificial Neural Network Model (ANN)

Due to its good performance as routing model in the Juba and Shabelle catchments, only the parametric form of the Linear Perturbation Model (P-LPM) was implemented in this study. For more details about the rest of the models the reader is referred to the user manual of the software. The Schematic representation of the Linear Perturbation Model (LPM) is given in Figure 3.4.

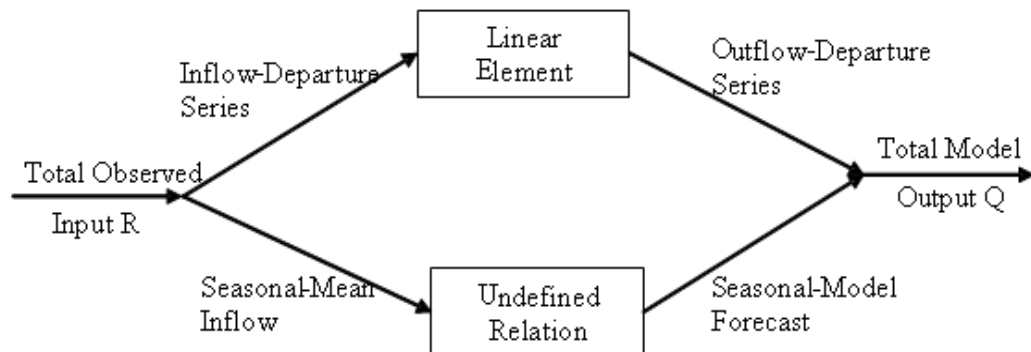


Figure 3.4: Schematic Diagram of Linear Perturbation Model (LPM)

This model uses the seasonal information of the observed rainfall and discharge series. In the LPM, it is presumed that, during a year, in which the rainfall is identical to its seasonal expectation the corresponding discharge hydrograph is also identical to its seasonal expectation. However, in all other years, when the rainfall and the discharge values depart from their respective seasonal expectations, these departures are assumed to be related by a linear time invariant system. Undeniably, the LPM structure reduces the reliance on the linearity assumption and increases the reliance on the observed seasonal behaviour of the catchment. For the discrete system with recorded data sampled at one day interval or averaged over one day interval, the discrete LPM may be described by the following assumptions:

1. If the inflow (or rainfall) on each date d in a particular year is exactly the inflow (or rainfall) seasonal mean for that date, R_d , the corresponding outflow would likewise be the outflow seasonal mean Q_d . Denoting by notations, $R_d \rightarrow Q_d$.
2. In any actual record the series of departures of the inflow (or rainfall) and the outflow from their seasonal means are linearly related

$$(R - R_d) \rightarrow (Q - Q_d), \text{ or } R' \rightarrow Q', \text{ where } R' = R - R_d \text{ and } Q' = Q - Q_d.$$

The relationship between the input departure series, the output departure series and the discrete pulse response relating to the departure series can then be expressed as:

$$Q'_i = \sum_{j=1}^m R'_{i-j+1} h'_j + e_i \quad (3.2)$$

where R' and Q' are the input (or rainfall) departures and the corresponding discharge departures from their seasonal expectations at the i^{th} instant, respectively, h'_j is the j^{th} ordinate of the discrete pulse response relating to the departure series of input and the output, e_i is the error term and m is the memory length. The multiple regression Ordinary Least Squares (OLS) method can be used to give estimates of the pulse response ordinates of the LPM, provided that the values of these departures are known.

3.2.3 Regression Models

Regression models are widely used in inflow forecasting. A simple regression model was developed for the Juba and Shabelle based on correlation between upstream and downstream flows. The relationship established between the stations is used to predict river levels / flow in the downstream station taking into account the lag times between the two stations. Both the Juba and Shabelle are slow rivers, with a lag time of up to 7 – 8 days from the entry points at the border with Ethiopia and the flood plains near the Indian Ocean.

The regression equation used to relate the upstream and downstream stations of both rivers is of the nature:

$$Q_{t+\varepsilon}^{n+1} = Q_t^{n+1} + a_0 + a_1 \Delta Q_{t,t-\tau+\varepsilon}^n \quad (3.3)$$

where Q is the discharge in m^3/s , or river level in m; n and $n+1$ are the upstream and downstream stations respectively; t is the date; τ is the lag between the upstream and downstream stations; ε denotes the number of days when the change in flow is considered.

3.3 Real-Time Flow Forecasting

Efficient forecasting of river flows is beneficial in many aspects for the prosperity of those societies living in riparian habitations. These forecasts are necessary to provide warnings against floods in order to prevent loss of life and to minimise damages to properties and livestock. Forecasting of river flows is also essential for operation of various hydraulic structures which, in some way or other, depend on the magnitude of river flow. In general, forecasting of river flows is necessary for proper management of water resources. Therefore, in order to issue flood warnings confidently, and to manage water resources optimally, it is desirable that the best possible realistic real time forecasts be made.

Simulation models on their own utilise the input (e.g. rainfall with or without evaporation data, upstream flow values for routing type models, etc.) and possibly the present and the previous model outputs to estimate the discharge values, without taking into consideration the recorded discharge values at the time of making the forecast, whereas the updating procedure is used to provide feedback information. The response of real-time forecasting models to the feedback information is a unique characteristic of the real-time forecasting models. The two parts of the real time forecasting model (i.e. the simulation model and the updating procedure) are complementary and the definition of any real-time hydrological forecasting model is generally incomplete without specification of the updating procedure.

The enhancement of the accuracy of the forecasts may generally be achieved through the improvement of the substantive model (i.e. input to output simulation) structures, updating techniques, the optimum specification or representation of the input data and by improved specification of measures of forecast uncertainty (Moore, 1986). The use of updating procedures generally has a major impact on the forecasting accuracy for short lead-times. However, undoubtedly, the improvement in forecasting accuracy for longer lead-times can be achieved only through the improvement of the forecasting accuracy of the simulation model.

In practice, the application of the real-time forecasting models requires the specification or forecasts of the model input variables (e.g. rainfall, evaporation etc.) over the lead-time of the forecast. However, in the cases where such input variable forecasts are not available, or in the case of perceived failure of the telemetry network, resort may generally be made to a number of hypothetical input scenarios which are constructed by retrospection of historical events (Grijnsen et al., 1992; Cunge et al., 1992; Fleming, 1977, p. 293). These input scenarios normally contain assumptions such as the occurrence of no further rainfall, or of maximum rainfall, or of seasonal expectations of the input variables occurring over the lead-times, or of values based on persistence in the observed input data series exploited by an Auto-Regressive (AR) procedure, etc. Normally, one input scenario is selected for the purpose of making the forecasts.

3.4 Model Calibration and Verification

Calibration means to adjust the model parameters in the way that the model output fits to the observation. A measure of the fit between the two series is called a calibration criterion which is expressed in form of an Objective Function (OF). The goal of the calibration is to find the optimal values for the model parameters that maximizes (or minimizes) the specific objective function.

Models with a large number of calibration parameters and the number of catchments are usually calibrated using an automatic calibration routine. The key to automated model calibration is a search method for adjusting parameters to minimize the objective function value and find optimal parameter values. There are many search optimisation methods used for calibration algorithms. To mention a few, e.g. in system models the: Simplex, Genetic Algorithm and Rosenbrock methods are used. The Shuffled Complex Evolution Method has been identified as being the best calibration algorithm in terms of robustness, effectiveness and efficiency for the identification of multi-parameters in a rainfall-runoff model such as LISFLOOD.

Although most hydrological processes that are incorporated in LISFLOOD and GeoSFM are physically based, some are only represented in a lumped conceptual way. Hence, these two models hold a number of parameters that lack the physical basis which means that these are neither directly measurable nor derivable from literature and must therefore be estimated through model calibration.

The consistency of the model performance is checked by split sampling i.e. breaking the record into two distinct periods, one in which the model is calibrated as explained above, and the other in which it is tested using calibrated parameters (verification period). No parameter adjustment is needed during model verification.

Chapter 4

Models Application and Results

4.0 Model Evaluation Criteria

Different researchers have suggested different criteria for evaluating model performance. The model performance is judged based on the extent to which it satisfies its objective of simulating the real life phenomenon (observed values). The evaluation can also be done on the extent to which the model can sustain a certain level of accuracy when subjected to diverse applications and tests other than those used for calibrating the model.

The criterion used to determine the model accuracy in this study was the coefficient of determination (r^2). For each time step, the model's simulated values were compared to the observed values to determine the accuracy of the model, and adjustments made to improve on the correlation. The coefficient of determination (r^2) is given by

$$r^2 = 1 - \left[\frac{\sum_{i=1}^N [(Q_o)_i - \bar{Q}_o] [(Q_e)_i - \bar{Q}_e]}{\left\{ \sum_{i=1}^N [(Q_o)_i - \bar{Q}_o]^2 \right\}^{0.5} \left\{ \sum_{i=1}^N [(Q_e)_i - \bar{Q}_e]^2 \right\}^{0.5}} \right]^2 \quad (4.1)$$

Where \bar{Q}_o and \bar{Q}_e are the mean of the observed and the estimated discharge / stage data series over the data period considered; and 'N' is the total number of data points in the period.

Visual comparisons were also done on the simulated and observed hydrographs to identify the lag and magnitude of peaks.

4.1 Application of LISFLOOD Model

4.1.1 Data Used to Configure LISFLOOD Model

Meteorological observations available for Juba and Shabelle are sparse, and time series data are often interrupted by missing records. Application of LISFLOOD was based on four re-analysis data sets, ERA-40, CHARM, ERA-interim and RFE. Observed flow data from Luuq and Belet Weyne stations was used to calibrate the model.

4.1.2 Model Calibration

LISFLOOD model was calibrated for the years 1976 – 1981 using ERA-40 and CHARM data, and 2002 – 2007 using ERA interim and RFE data. The calibration was done in two stages, manually and through an automated algorithm.

In the manual (trial and error method), only parameters which are not incorporated in the automatic calibration, and which are expected to affect runoff generation, were considered. These include:

- Soil depth
- Depth of top soil
- Leaf area index
- Crop coefficient
- Thetas and Lambda

The influence of each parameter adjustment on the model outcome was determined before proceeding to automatic calibration.

Automatic calibration was done using SCE-UA algorithm. The calibration was done using different meteorological data sets: ERA-40, ERA interim, CHARM and RFE.

The automatic calibration focused more on the adjustments of soil related parameters and other predefined model parameters. For each gauging station, eight distinctive calibration processes were carried out; twice with each of the four datasets. The first calibration was done with a simple objective function, and the second with a weighted objective function (Thiemig, 2009). The calibration process was set to be executed with 600 iterations. Values of the final calibration parameters obtained are presented in Table A.2 in Annex A.

4.1.3 Calibration Results

Results obtained from the model runs indicated a significant overestimation of discharge, which was initially associated with uncertainties in the input data, and model errors. However, it was later discovered that the problem was with the calibration routine of the model. The routine could not find the optimum parameter sets for the ground water and water loss. The results presented here are those of the initial calibration, as the new calibration results have not been received from JRC. Figures 4.1 and 4.2 show the correlation between observed and simulated flows at Belet Weyne and Luuq from LISFLOOD model. Flow hydrographs for Belet Weyne and Luuq are presented in Figures B.1 and B.2 respectively.

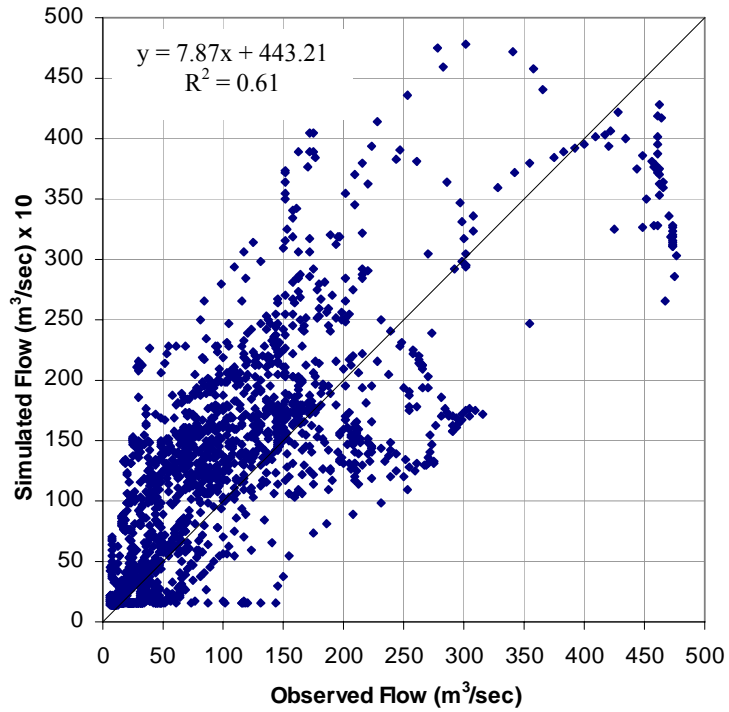


Figure 4.1: Observed and Simulated Flow at Belet Weyne using LISFLOOD

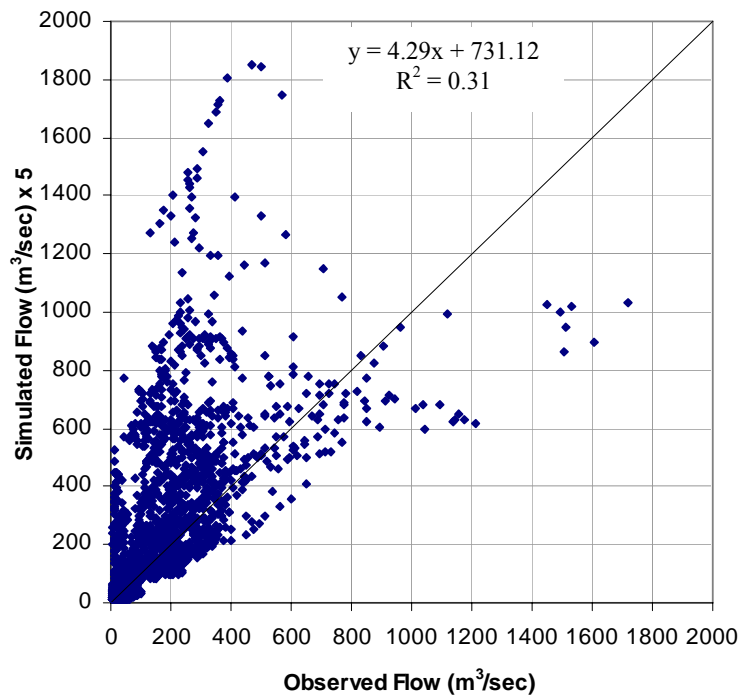


Figure 4.2: Observed and Simulated Flow at Luuq using LISFLOOD

LISFLOOD has produced good results for the European catchments. However for the Juba and Shabelle basins, there was a great overestimation of discharge. In Luuq, simulated discharge exceeded the observed values by about ten times, while in Shabelle the simulated values were about six times more than the observed.

Despite the extremely high magnitude in simulated discharge, the general dynamic of the simulated hydrograph was similar to the observed, with fair timing of the peaks in most cases. This can be explained as the reason for the relatively high correlation coefficient (r^2) especially for Shabelle (0.61) despite the big differences in generated and observed flows.

Comparing the different rainfall datasets indicated that generally the amplitude of discharge overestimation was lower for the RFEs than ERA dataset (Figure B.3).

4.2 Application of the USGS Model

The USGS stream flow model was run on the Juba River basin within Ethiopia to compare the different data sets used to run the LISFLOOD model. The rainfall runoff model has been widely used in the Horn of Africa river basins for flood forecasting at regional scale.

The application of the model for this study was limited to comparing the RFE and ECMWF data sets. The use of the model was necessitated by the extremely high discharge values generated by LISFLOOD model as discussed under section 4.1. It was not clear whether the high flows were as a result of data or model errors, hence the need for a second model.

4.2.1 Data Used to Configure the USGS Model

The data sets used to run the USGS Stream flow model were:

- Rainfall :- RFE and ECMWF
- Evaporation data
- 90m DEM
- Soil data
- Land use / land cover
- Flow data

The sources of these datasets have been described in chapter 2 of this report.

4.2.2 Model Calibration

Calibration of the USGS Stream flow model requires long data series for rainfall and evaporation for the basin under study. For the upper catchments of Juba and Shabelle, these two series were not available, and the model was run on satellite based data for the purpose of comparing different datasets (RFE and ECMWF) as mentioned above. No calibration was done on the model.

4.2.3 Model Results

Results of the un-calibrated USGS model are presented below. The model was run using both the RFE and ECMWF datasets. The resulting scatter graphs for the observed and simulated flows for the two datasets are presented in Figures 4.3 and 4.4. A flow hydrograph comparing the observed flow against simulated flow for RFE and ECMWF is presented in Figure B.4 in the Annex.

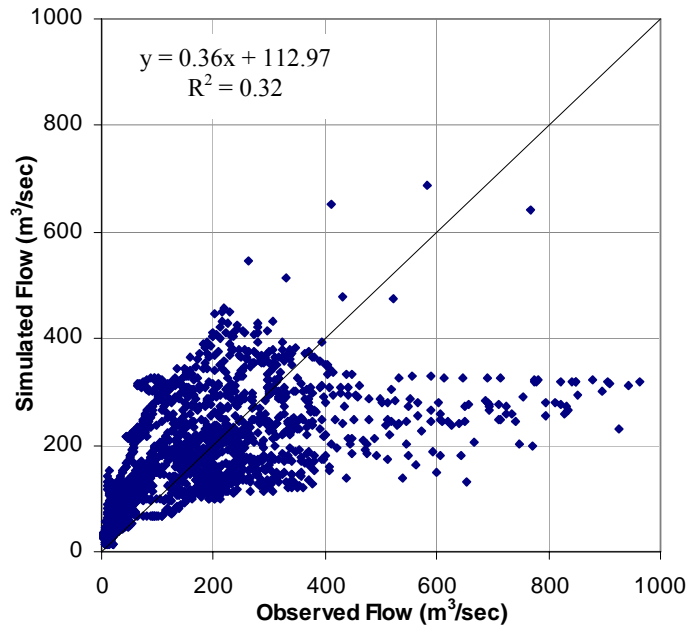


Figure 4.3: Simulated and Observed Flow at Luuq using ECMWF Data

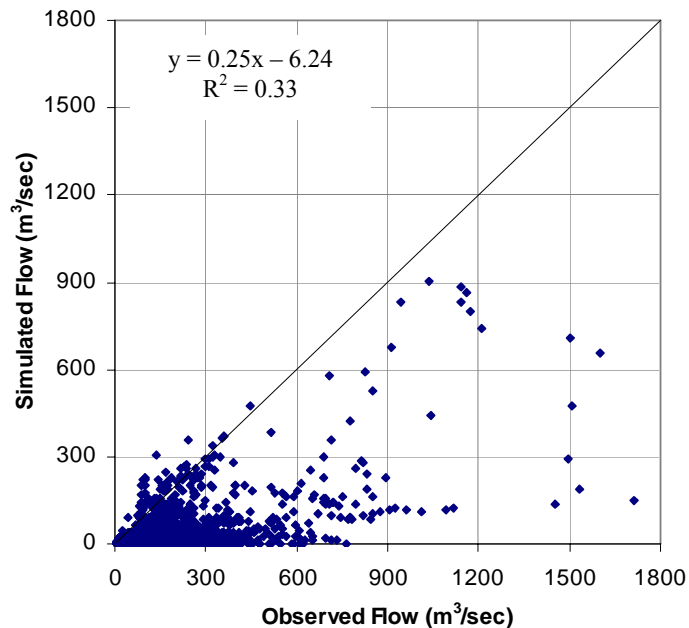


Figure 4.4: Simulated and Observed Flow at Luuq using RFE Data

The correlation between the observed and simulated flow in both datasets was poor, 0.32 and 0.33 for ECMWF and RFE datasets respectively. However, the model was not calibrated, which could be responsible for the poor correlation.

Comparing the two datasets, ECMWF gave good results especially for the low flows, though in some cases like in 2003 (Figure B.4) simulated flow overshoot the observed flow by quite a big margin. The RFE gave better results in high flows, but the simulated low flows were below the observed.

It was clear from the results that the overestimation of flow in LISFLOOD model was more of a model problem than data. Despite the fact that the USGS model was not calibrated, the difference in the simulated and observed discharge was much less than the ten times difference consistently generated by LISFLOOD. There are only few occasions where the USGS model generated extremely high or low flows in both datasets.

4.3 Application of HECRAS Model

4.3.1 HECRAS Data Requirements

HEC-RAS requires the input of geometric data to represent river networks, channel cross-section data, and hydraulic structure data such as bridges, culverts and weirs data. The data can be prepared within HEC-RAS, or prepared in Arc GIS using HEC GeoRAS extension, which was the case for this study. Flow data is required to represent hydrologic events.

(i) River Networks

River networks, Figure 4.5, define the connectivity of the river system from upstream to downstream. A river system consists of a collection of reaches, all oriented downstream. A reach is defined in HEC-RAS as starting or ending at junctions - locations where two or more streams join together or split apart. Hence, a river may be composed of one or more reaches.

(ii) Cross-Section Data

Channel cross-section data are used in HEC-RAS to characterize the flow carrying capacity of the river and adjacent floodplain. The cross section data defines the river bank lines, which separate the main channel from the over bank as shown in Figure 4.6. The downstream reach of the channel is also calculated from one cross section to the next cross section, and parameters such as roughness coefficients, contraction and expansion coefficients determined for that reach length.

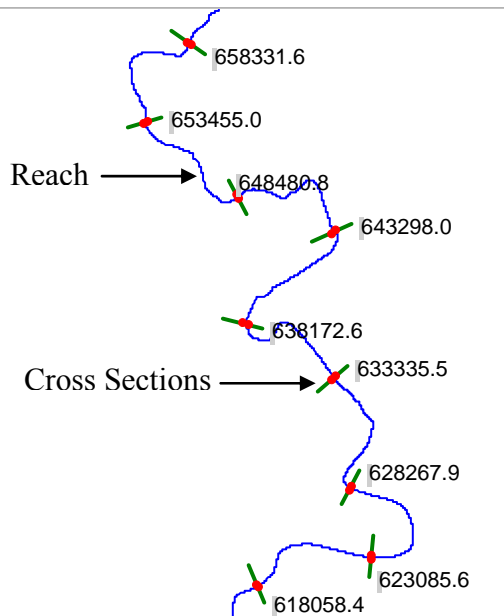


Figure 4.5: HECRAS River Network

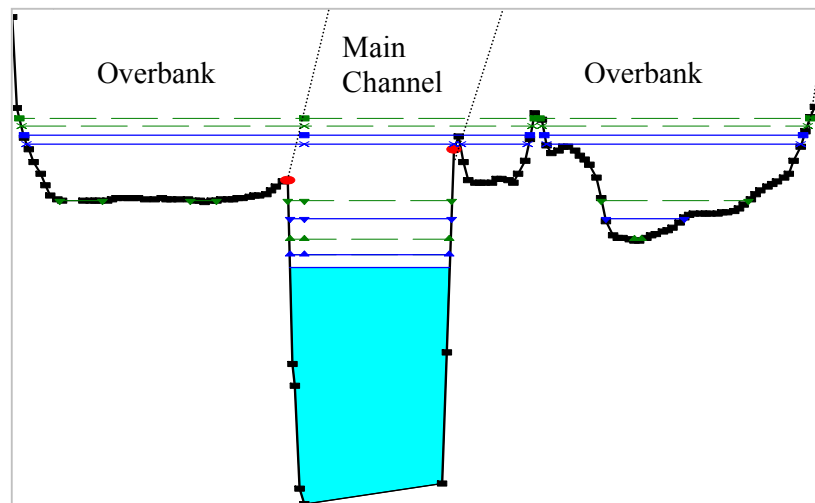


Figure 4.6: HECRAS Channel Geometry

The distance between cross sections is known as reach lengths and is used for energy loss calculations in HEC-RAS. Reach lengths are considered for the main channel, left and right over banks and indicate the path of flow between cross sections. The cross sections for the general stretch of the two rivers were done at 5km interval. In places where there exists hydraulic structures, transects were taken at closer intervals both upstream and downstream of the structure.

Roughness coefficients are an indication of the relative channel roughness. Channel roughness is considered for calculating frictional energy loss between cross sections. Typically, channel roughness is indicated by Manning's n-values. Contraction and expansion coefficients are flow dependent and characteristic of abrupt changes in flow direction. The roughness coefficients were estimated from literature, with the aim of improving them to reflect the ground condition from the aerial photography results on land use along the riverine areas.

(iii) Hydraulic Structure Data

Hydraulic structure data include data such as bridges, culverts, barrages and weirs. The structures cause some abrupt change in flow, hence affecting the contraction and expansion coefficients. The hydraulic structure data for Juba and Shabelle was obtained from the aerial photography datasets.

(iv) Flow Data

In HEC-RAS, hydrologic events are represented by flow data. Flow data includes both the flow magnitude (which may vary on a cross section to cross section basis) and boundary conditions, which are dependent on the flow regime. The model was run on both the pre-war and post-war flow data.

4.3.2 Model Calibration

The HECRAS model was run in unsteady conditions, where flow at a particular location varies with time. The input data were observed flow at Belet Weyne and Luuq, which was routed down the two river channels. The main parameter for HECRAS calibration is the Manning's coefficient of the main river channel and over bank. Values of the coefficient are determined by the nature of the channel, and over bank. When the channel is rough due to obstacles such as rocks, vegetation, etc, then there is increased resistance of flow. The Manning's value is high under such conditions and low when the channel is smooth without many obstacles.

For this study, the assumed Manning's values for the main channel and over bank were estimated from literature, and varied from 0.025 to 0.035. Further calibration is expected with more realistic values from the aerial photography results on land use and land cover along the riparian areas of the two rivers.

The simulated discharge was compared to the observed values at key stations along the two rivers. The selected stations were those that are currently operational: Luuq, Bardere and Buale along Juba River, and Belet Weyne, Bulu Burti and Jowhar along Shabelle River. Results from Bardere and Bulu Burti are presented in section 4.3.3.

4.3.3 Model Results

Scatter graphs for the observed and simulated flow at Bulo Burti and Bardere are presented in Figure 4.7. Flow hydrographs for the calibration of the two stations are presented in Figures B.5 and B.6 in the Annexes.

A fairly good correlation was obtained for both stations, but from the flow hydrograph the peaks, both in magnitude and timing, were not very accurately captured. It is however expected that with more calibrations the model would better capture the peak flows.

The refined calibration of the HECRAS model would also involve improved input data on the channel characteristics and hydraulic structures. There is a lot of river bank cutting along the Juba and Shabelle Rivers which divert water from the channel to irrigation fields. These cuts need to be incorporated into the model, as well as tributaries which contribute to flow into the rivers to further improve the results.

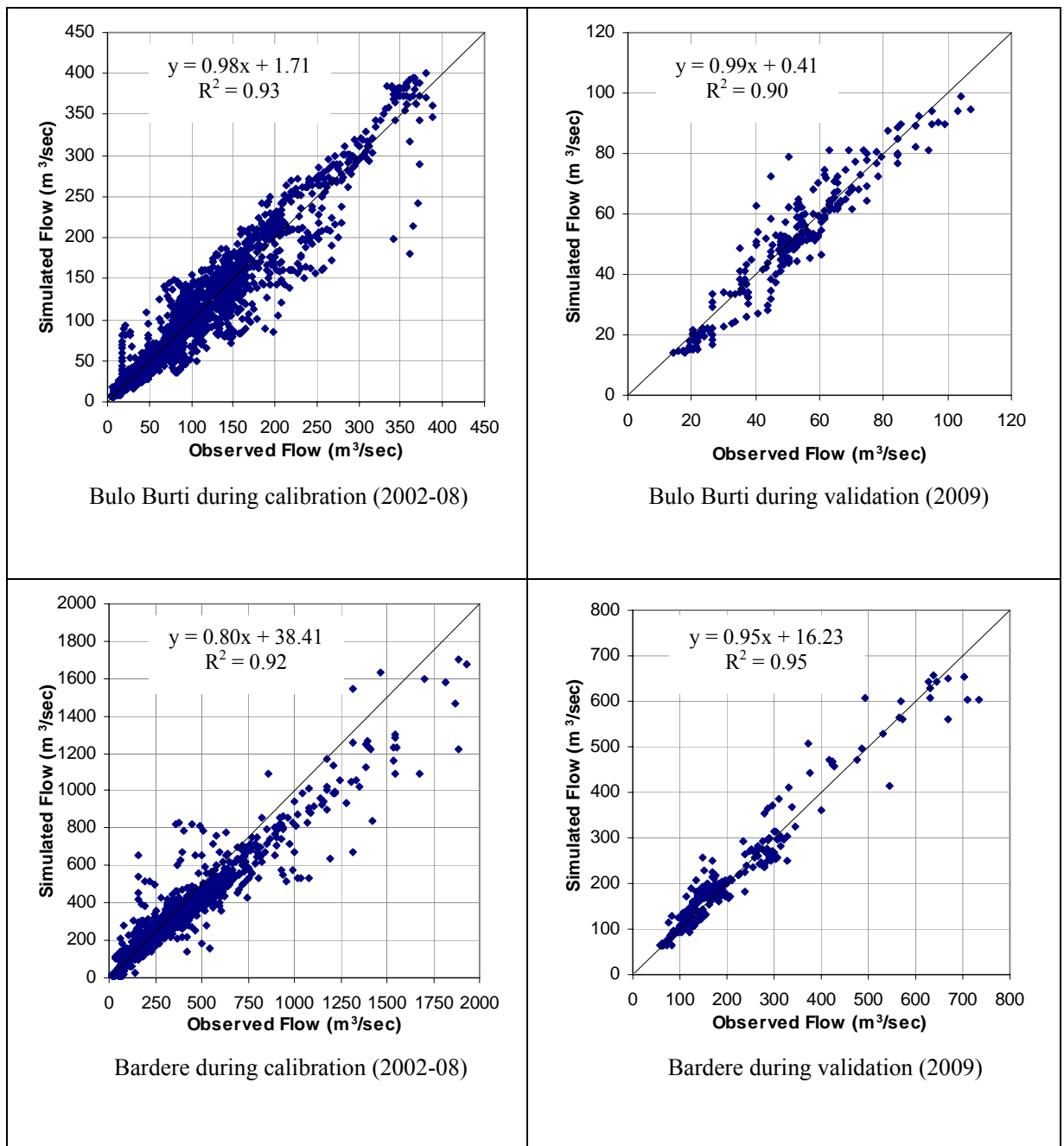


Figure 4.7: Scatter Graphs for Observed and Simulated Flow at Bulu Burti and Bardere using HECRAS

The calibrated model, which gave the correlations presented in Figure 4.7 was run in order to estimate (forecast) flow in the downstream stations. Figures 4.8 and 4.9 show the hydrographs of the forecast flow against the observed values in 2009 for Bulu Burti and Bardere.

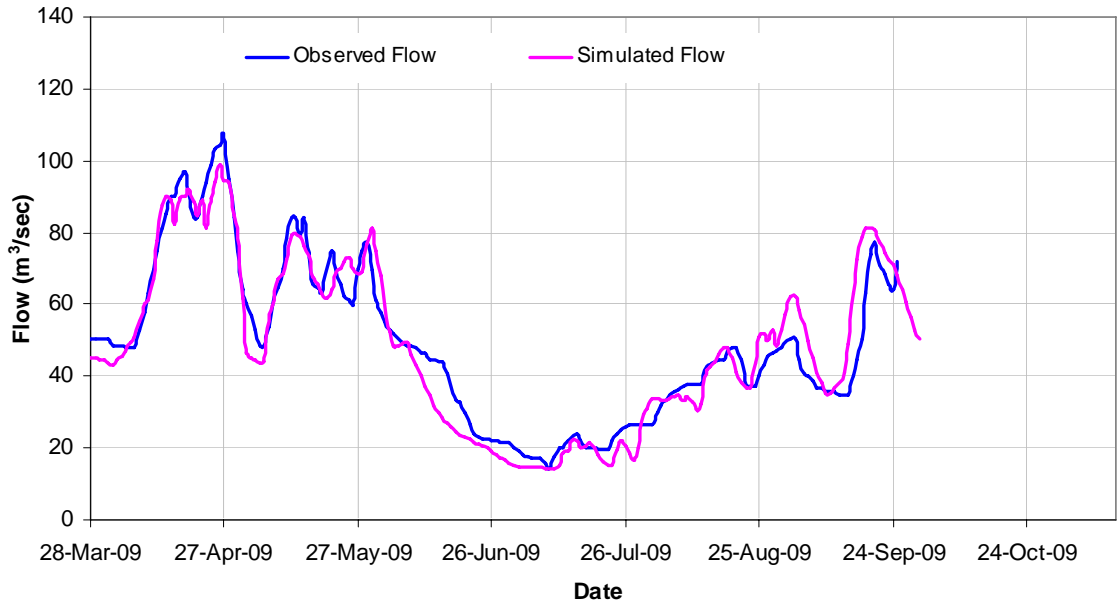


Figure 4.8: Observed and Forecast Flow at Bulu Burti using HECRAS

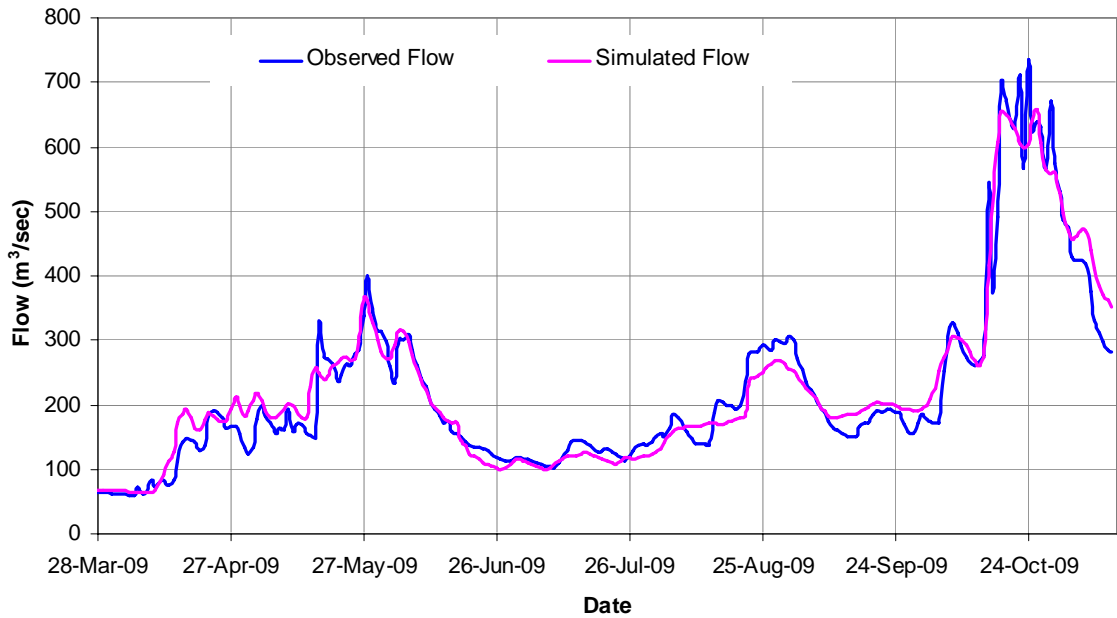


Figure 4.9: Observed and Forecast Flow at Bardere using HECRAS

4.4 Application of GFMFS

The GFMFS consists of various mathematical models used in simulation of flow, as well as substantive models used in updating applications. The models seek to simulate the process of transformation of the input(s) to a physical system to the output from the system by simplifying the associated complexities.

The model used to simulate flow was the parametric form of the linear perturbation model (P-LPM). The model prescribes the general nature of the relationship between upstream and downstream hydrographs and then fit the model to the system using historical records of data.

4.4.1 GFMFS Data Requirements

The data used to run the GFMFS models was river flow data and rainfall from the few stations within the catchment. However, the rainfall stations available in the Somali catchments of the two rivers are sparsely located, and lack long term data series. Emphasis was therefore put on discharge data.

4.4.2 Model Calibration

GFMFS models allow for calibration through varying of the system memory length and lag times between the upstream and downstream stations. The datasets were divided into two; 2003 to 2008 for calibration, and 2009 for validation. The change in memory lengths and lag times was through trial and error, though the range of the lag times was guided by the previous analysis done on data series between the gauging stations. Input data were from the two upstream stations, Luuq in juba and Belet Weyne in Shabelle.

4.4.3 Model Results

Scatter graphs between the observed and simulated flow at Bardere and Bulo Burti stations are presented in Figure 4.10. The resulting calibration hydrographs are presented in Figures B.7 and B.8 in the Annexes of this report.

High correlation values were obtained during calibration, 0.99 for both Bardere and Bulo Burti. The correlations during validation were 0.95 and 0.97 for the two stations respectively, which is equally good.

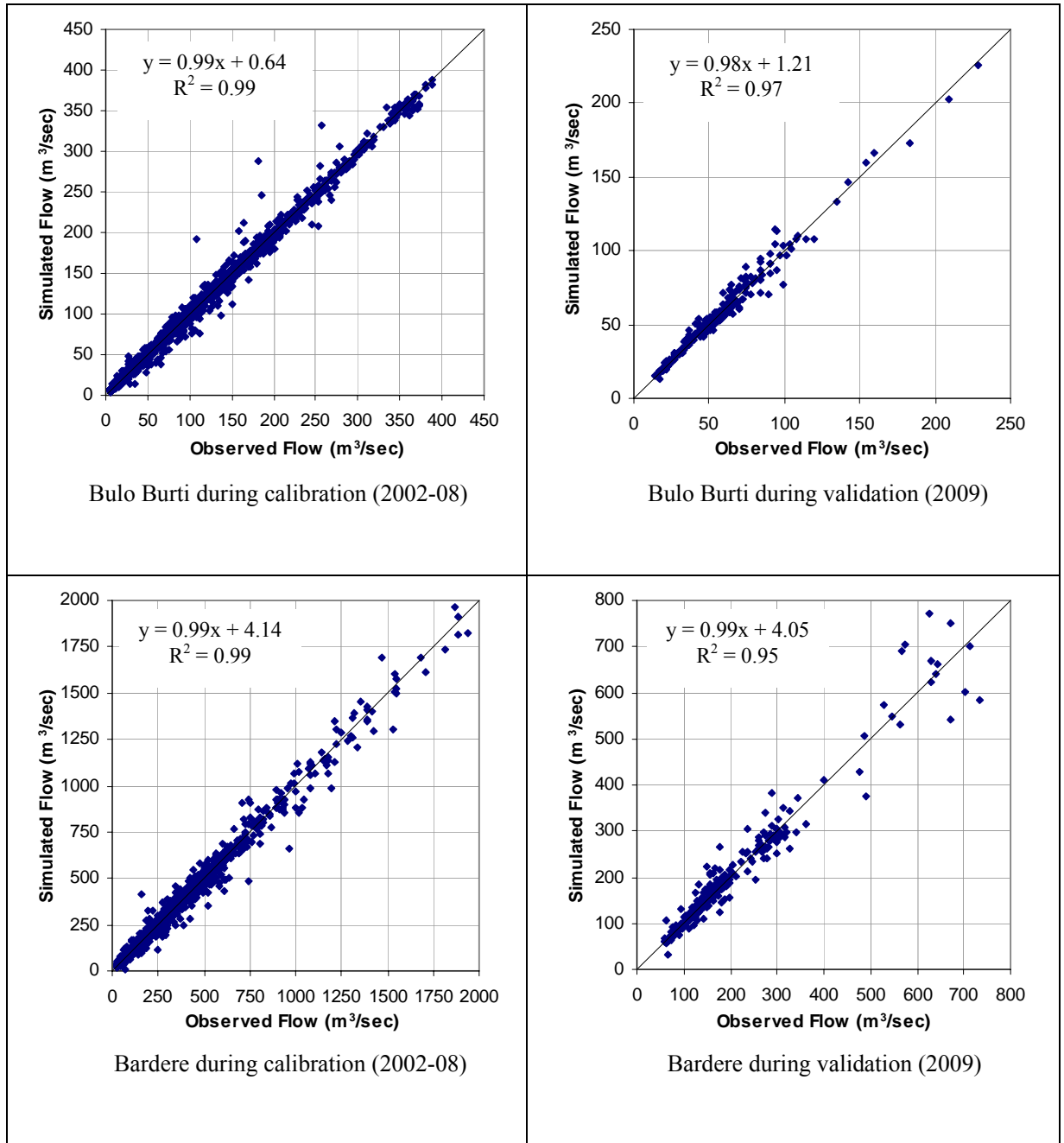


Figure 4.10: Scatter Graphs for Observed and Simulated Flows at Bulu Burti and Bardere using GFMFS

When the calibrated model was used to forecast flow at downstream stations, the following hydrographs were obtained for Bulu Burti and Bardere. From the hydrographs (Figures 4.11 and 4.12), the timings of the peaks and magnitude was fairly good.

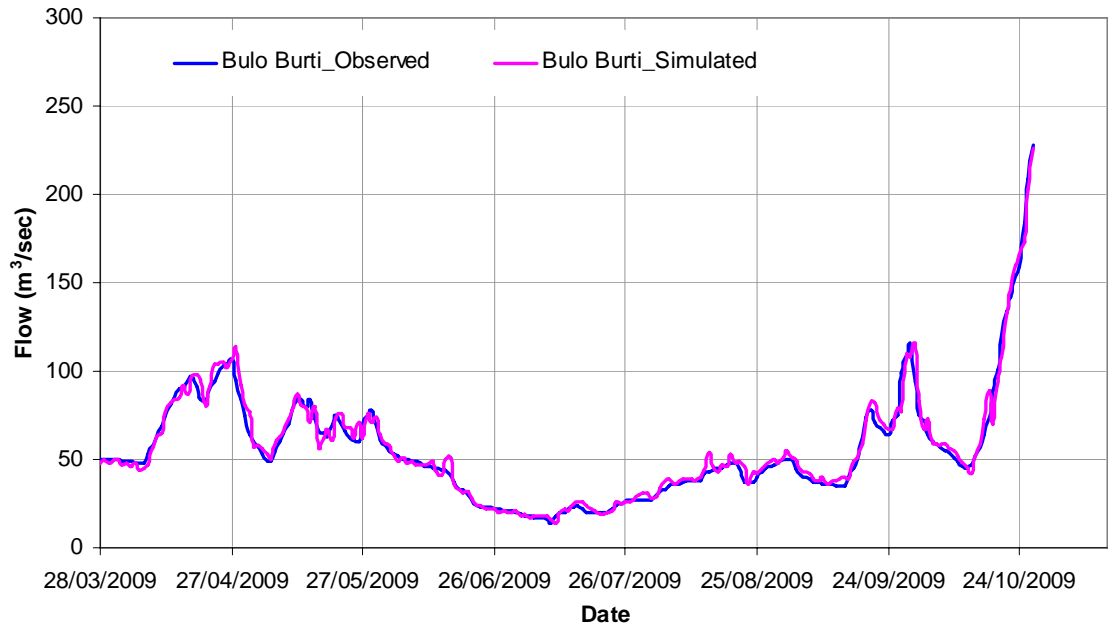


Figure 4.11: Hydrograph of Observed and GFMFS Forecast Flows at Bulo Burti

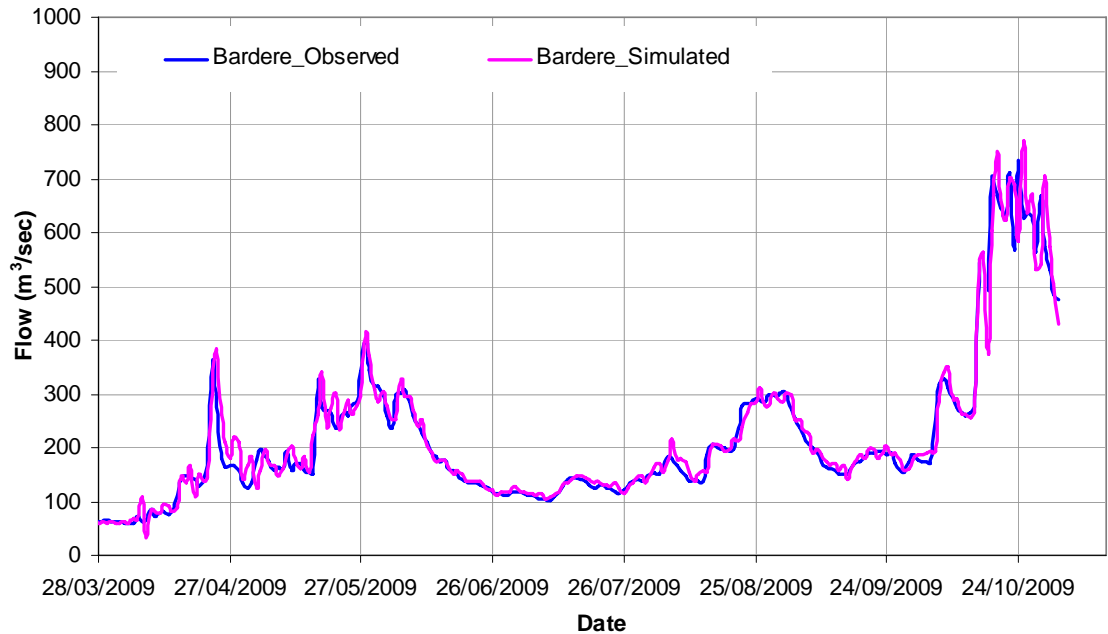


Figure 4.12: Hydrograph of Observed and GFMFS Forecast Flows at Bardere

4.5 Regression Models

Regression models were used in this study to establish relationships between the upstream and downstream discharges / river levels. The established relationships

were used to predict the discharge / river levels depending on the current conditions in the upstream and downstream stations.

Various approaches were undertaken with the regression models. The initial regression analysis done was on the data series to establish the lag times between upstream and downstream stations. The results of the lag time analysis are presented under data availability and analysis chapter of this report.

Another approach used under regression analysis was that defined by equation 3 under section 3.2.3. In this approach, the forecast river level for a downstream station is a function of the current river level at the upstream and downstream stations, and the change in flow in the upstream station over a period of time equal to the lag time between the upstream and downstream stations.

The next analysis done was to establish the relationships between change in flow in upstream stations and corresponding change in flow in a downstream station. With such a relationship, it was possible to forecast the river rise in a downstream station by establishing the rise upstream.

The other regression analysis done was on the peak flows. Looking at the long term flow hydrographs for the upstream and downstream stations, it was clear that an upstream peak resulted to a peak in the downstream station, irrespective of the time difference between the two peaks. In this approach, comparisons were done on the peak flows for the upstream and downstream stations to develop a relationship between the two peaks.

4.5.1 Data Used

The regression models were run on either river flow or river level data. The analysis were done by trying to find a relationship between the upstream and downstream stations, which can be used to forecast downstream flow / river level depending on the observed values upstream.

4.5.2 Model Results

It has been mentioned that there were different approaches to regression modelling. The following sections briefly describe results obtained for each approach.

4.5.2.1 Lag Time between Upstream and Downstream Stations

Juba and Shabelle Rivers have long stretches, extending to over 1,000km inside Somalia. The slope in both rivers is generally gentle, which leads to low flow rates. The lag times between the upstream and downstream stations extends to over a week. The different lag times between river gauging stations in Juba and Shabelle were established through regression analysis. Results for the lag times between stations are presented in Chapter 2 of this report.

4.5.2.2 General Relationship between Upstream and Downstream Stations

A general relationship between the upstream and downstream stations was established based on equation 3, where flow in a downstream station is established based on the current levels at upstream and down stream stations, and the flow conditions in the upstream station in the recent days. The resulting relationships are presented in Figures 4.13 and 4.14. Stage hydrographs associated with these scatter graphs are presented in Figures 4.15 and 4.16.

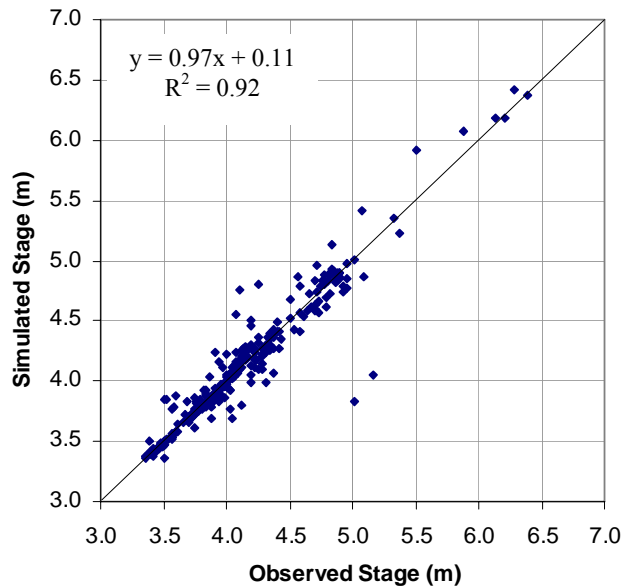


Figure 4.13: Bardere, 2 Day Forecast Based on Observed Levels at Luuq

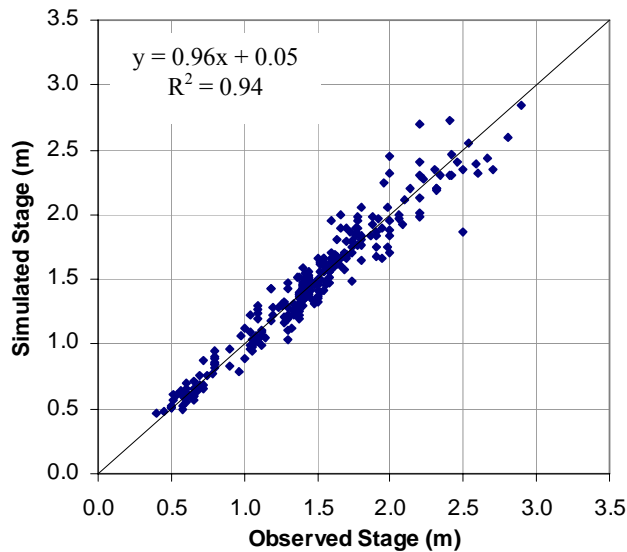


Figure 4.14: Bulu Burti, 2 Day Forecast Based on Observed Levels at Belet Weyne

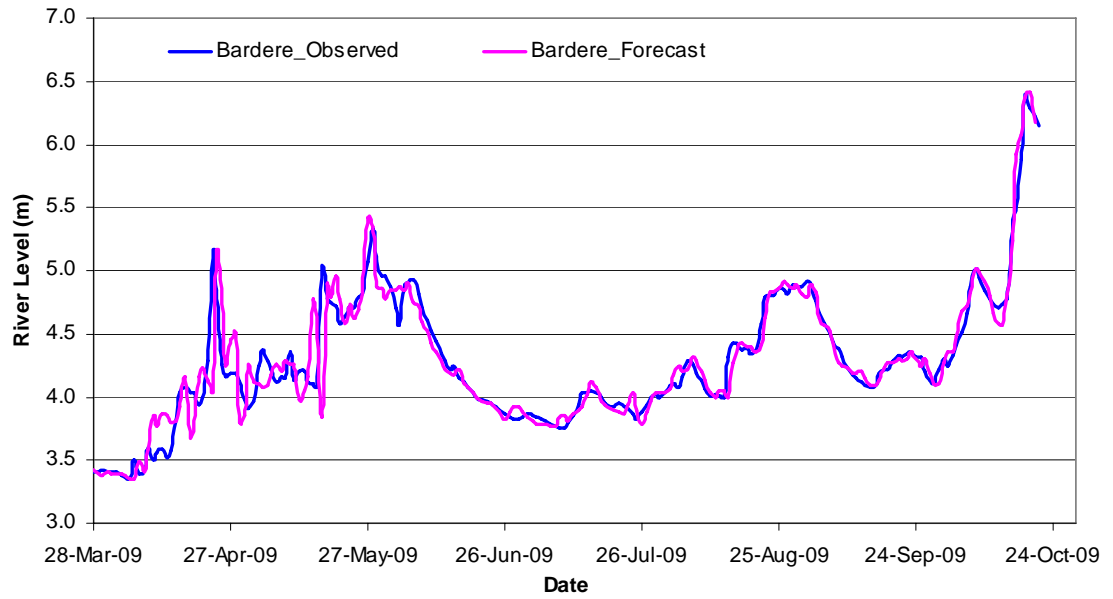


Figure 4.15: Observed and Forecast River Levels at Bardere Based on Observed Levels at Luuq

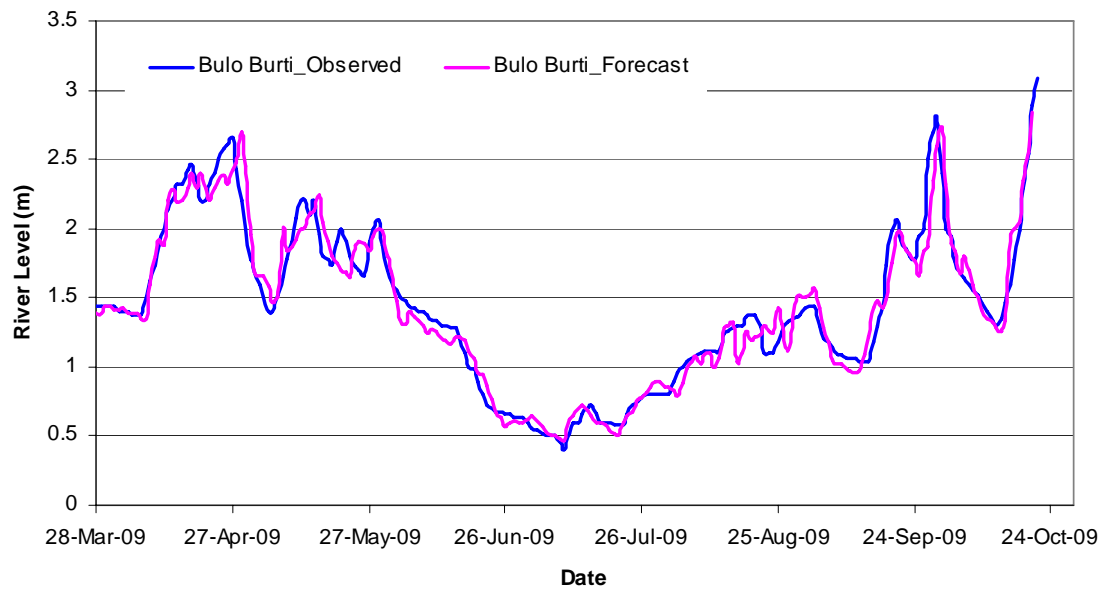


Figure 4.16: Observed and Forecast River Levels at Bulu Burti Based on Observed Levels at Belet Weyne

4.5.2.3 Change in Flow between Upstream and Downstream Stations

An increase in flow in an upstream station is expected to cause an equivalent rise in flow in a downstream station, if no water is added or lost. Under normal circumstances though, the perfect relationship between the stations is not possible, due to losses and inflow between the stations.

The relation between rise in river level in the upper and lower stations was established for the high flows. The best relationship between Belet Weyne and Bulo Burti, and Luuq and Bardere are given in Figures 4.17 and 4.18.

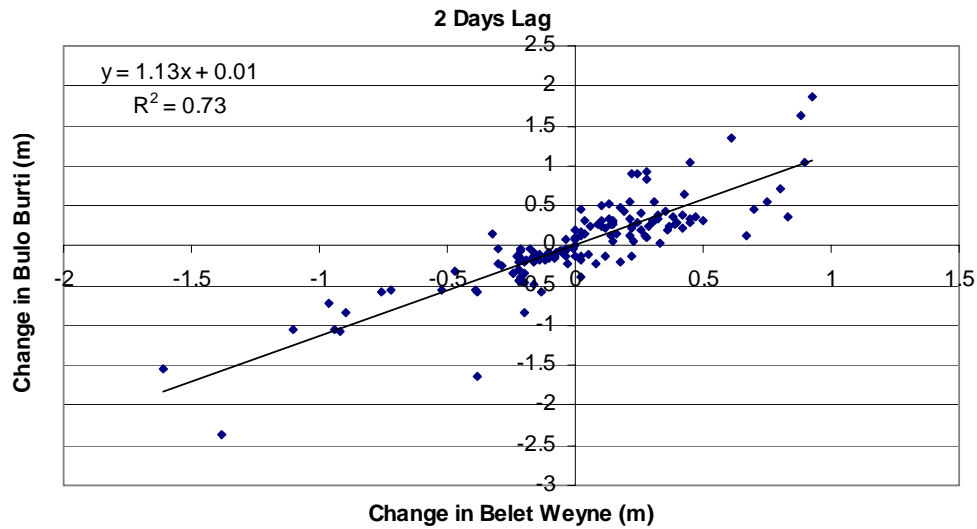


Figure 4.17: Belet Weyne - Bulo Burti with a 2 Day Lag during High Flows

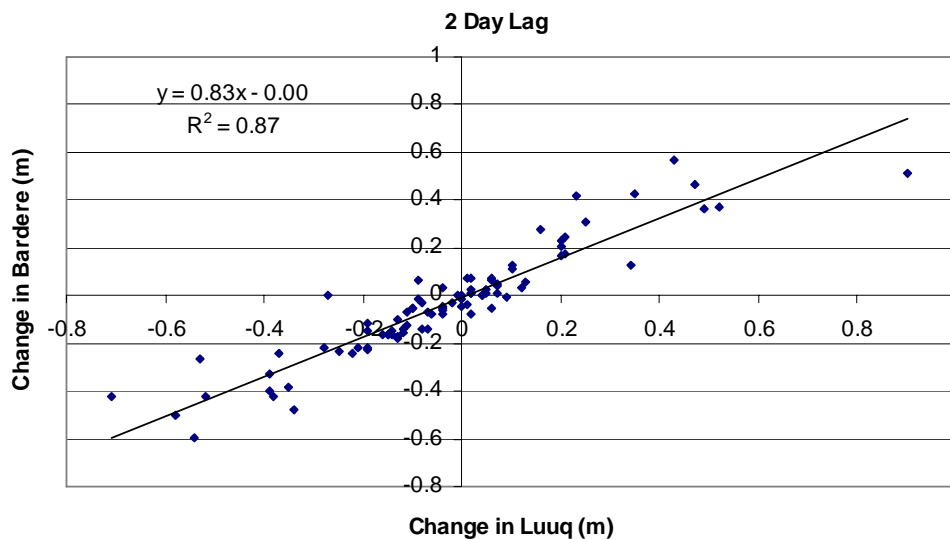


Figure 4.18: Luuq - Bardere with a 2 Day Lag During High Flows

The relationships established were used to forecast river levels at Bulo Burti and Bardera. The resulting stage hydrographs for Bulo Burti and Bardere are presented in Figures 4.19 and 4.20.

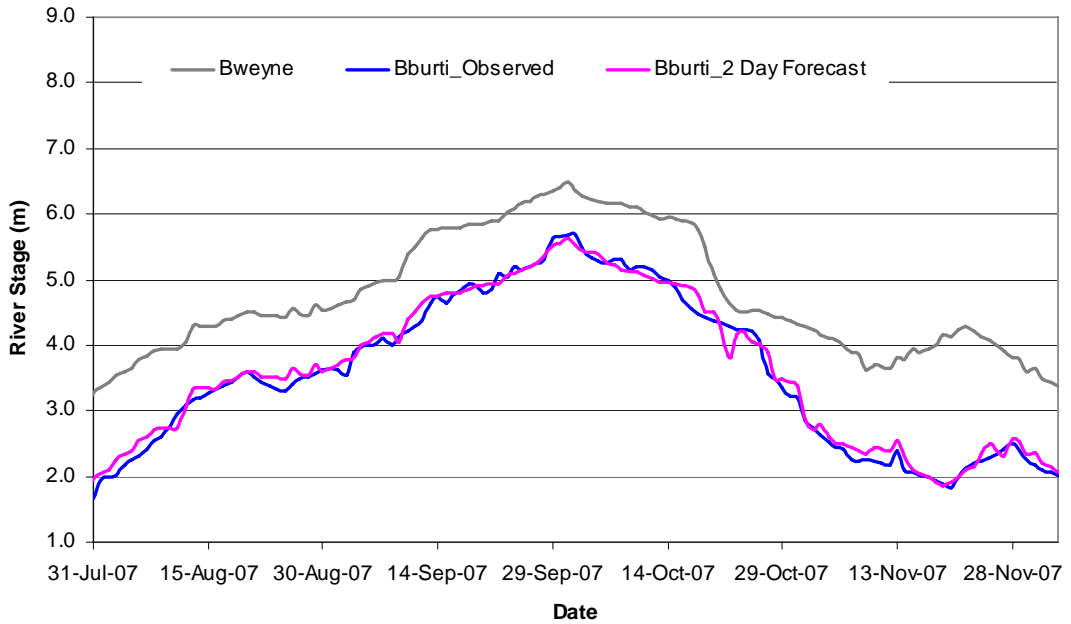


Figure 4.19: Observed and Forecast Flows at Bulo Burti

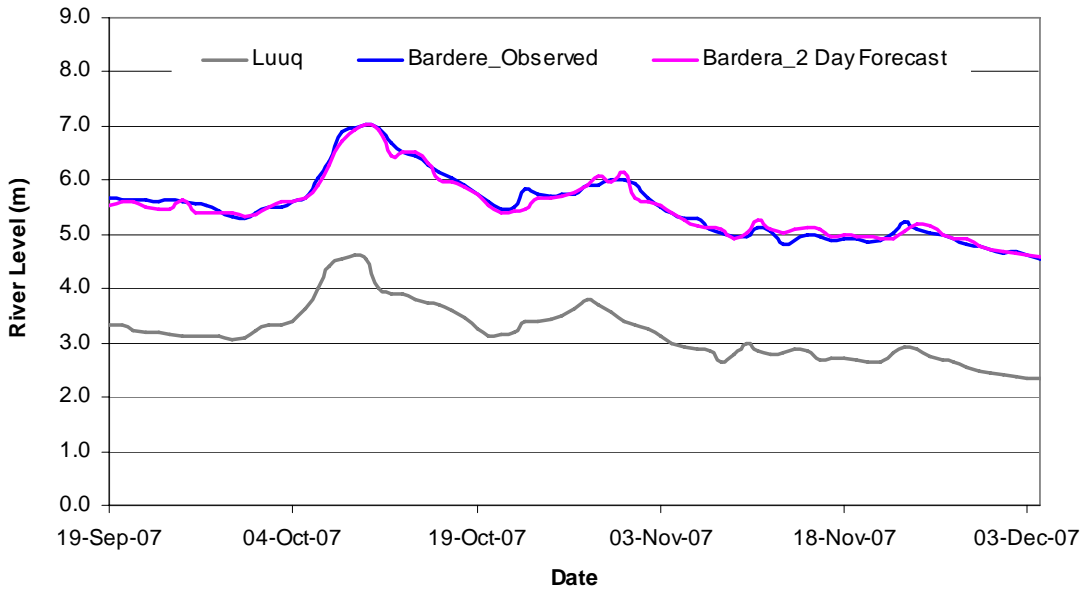


Figure 4.20: Observed and Forecast Flows at Bardera

4.5.2.4 Peak Flows between Upstream and Downstream Stations

The next analysis done was on peak flows, where the relationship between the peak values of an upstream station was correlated to the corresponding peak of a downstream station.

After establishing the scatter between the peaks in Luuq and Bardere, further categorization was done based on levels at Bardere. The two established categories were 4.5 – 6.5m, and >6.5m. The scatter between the two peaks is presented in Figure 4.21

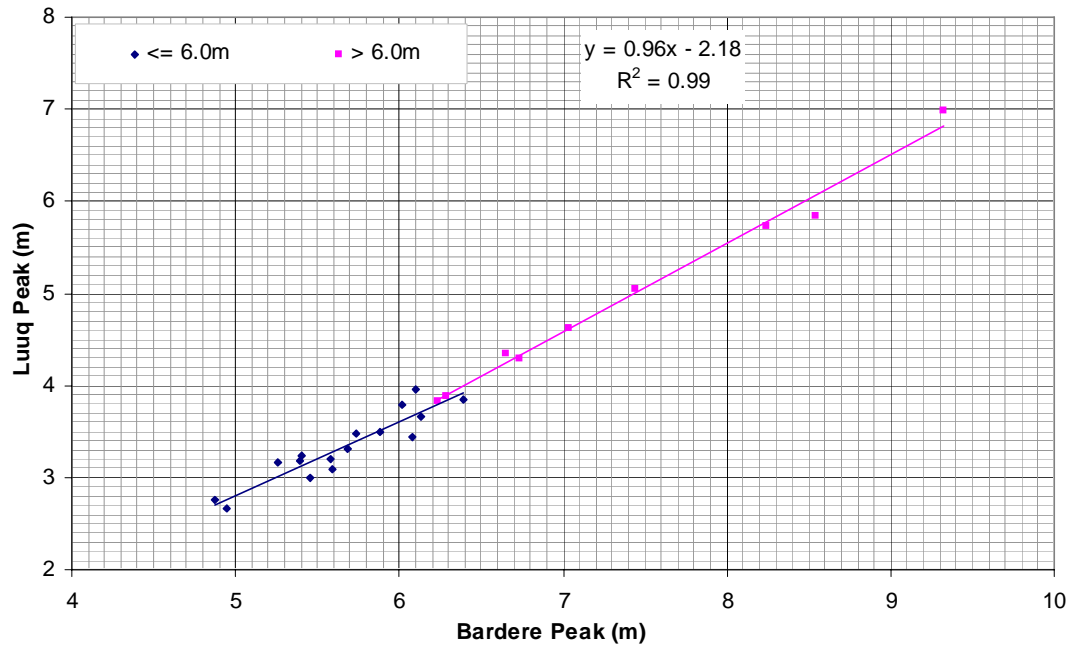


Figure 4.21: Luuq - Bardera Peaks

Based on this relationship, peak levels were forecast at Bardere for the period of 2006 to 2009. Comparing the observed and forecast peaks for this period, the magnitudes were well captured in almost all the peaks for this period. Figure 4.22 shows the results obtained for Deyr 2007.

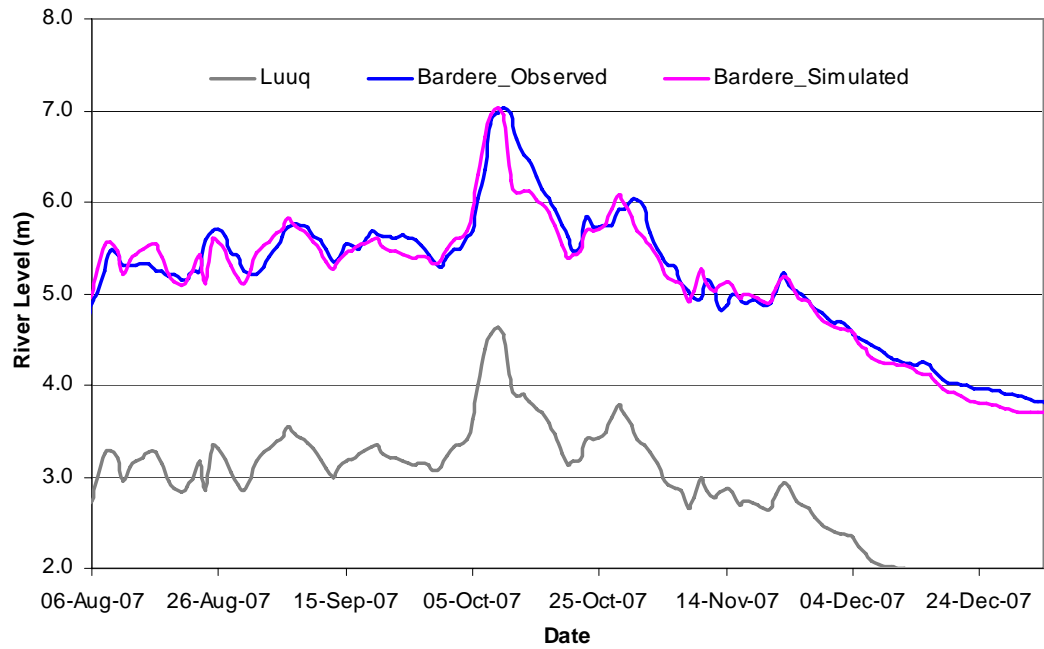


Figure 4.22: Forecast Peaks at Bardera

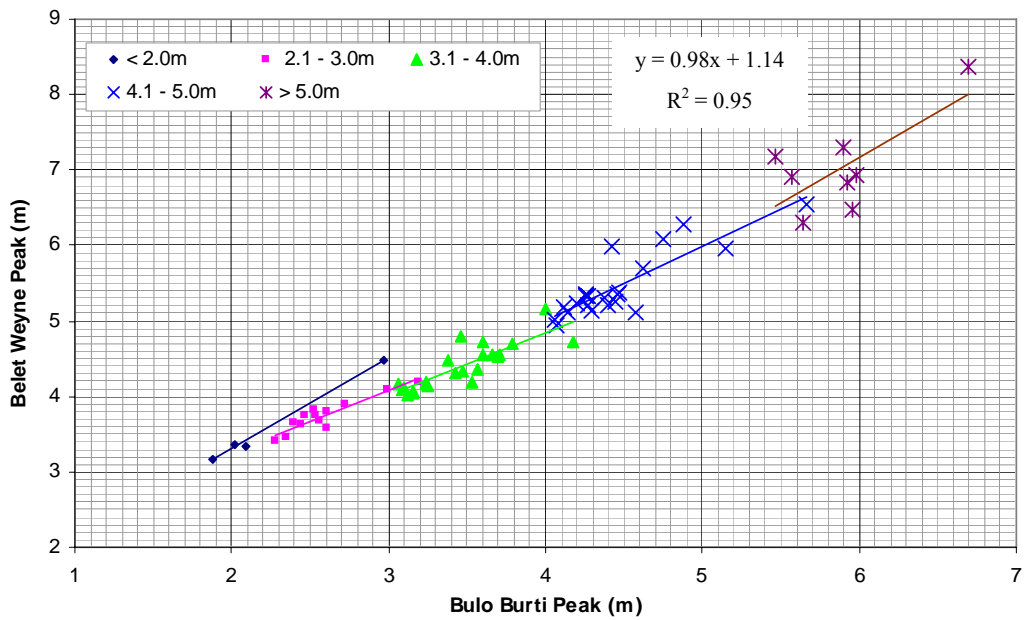


Figure 4.23: Belet Weyne - Bulo Burti Peaks

Between Belet Weyne and Bulo Burti, the third parameter introduced into the correlations between the peak values had more categories: <2m, 2.1-3m, 3.1-4m, 4.1-5m and >5m. Figure 4.23 shows the resulting scatter between the peaks of Belet Weyne and Bulo Burti.

From the established relationships, peak levels at Bulo Burti were forecasted based on the peaks at Belet Weyne for the period 2006 to 2009. Results for Deyr 2007 are presented in Figure 4.24.

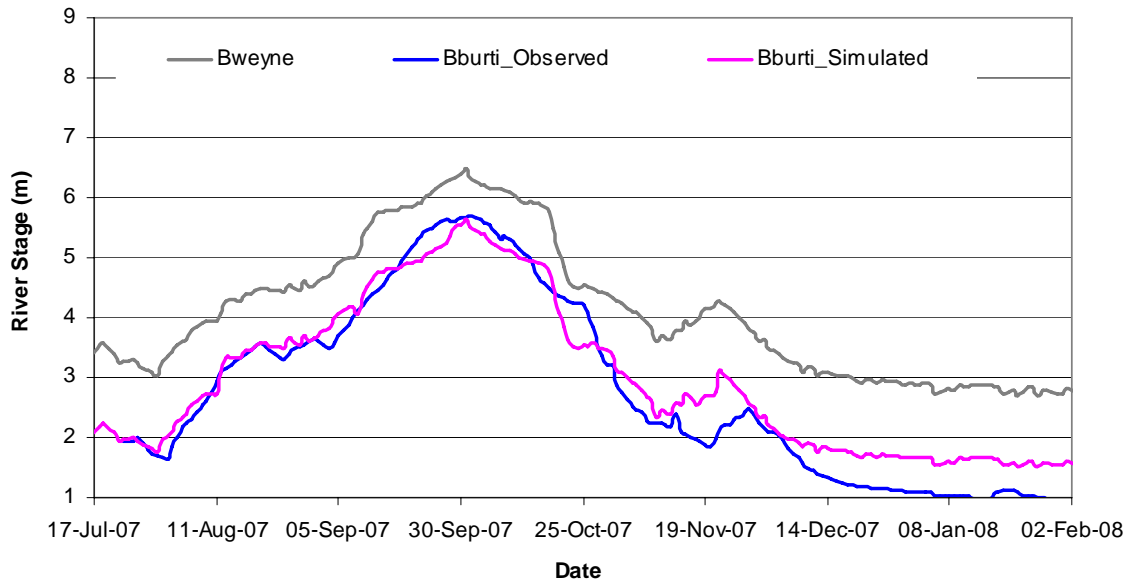


Figure 4.24: Forecast Peaks at Bulo Burti

The peak forecasts for Bulo Burti were quite good, especially the medium peaks. The relationship also worked fairly well in forecasting the other levels (other than the peaks), as seen in Figures 4.22 and 4.24. Generally, the results were better in Bardere (Juba) than Bulo Burti (Shabelle) for the peak analysis.

4.6 Models Summary Results

For the different models used in the study, the simulated flow was plotted against the observed values to determine how well the datasets compare. The coefficient of determination (R^2) described in section 4.0 was used to evaluate the models. Table 4.1 gives correlation coefficients obtained for the different models.

Table 4.1: Correlation Coefficients for Different Models used in the Study

Model	Shabelle		Juba	
	Calibration (R ²)	Validation (R ²)	Calibration (R ²)	Validation (R ²)
LISFLOOD	0.31	-	0.61	-
USGS GeoSFM*				
ECMWF Dataset	-	-	0.32	-
RFE Dataset	-	-	0.33	-
HECRAS	0.93	0.90	0.92	0.95
GFMFS	0.99	0.97	0.99	0.95
REGRESSION				
Lag Times	0.94	-	0.92	-
Rising River Levels	0.73	-	0.87	-
Peaks	0.95	-	0.99	-

* The model was not calibrated, but run on default model parameters to compare the two datasets, ECMWF and RFEs.

Chapter 5

Challenges and Limitations

The success of a flood forecasting system depends on many factors. The selection of the best model under the prevailing conditions; timely availability of reliable data; efficient communication channels for information dissemination and many others are some of the challenges which may hinder the effectiveness of a flood forecasting system.

Some of the challenges encountered during the development of the flood forecasting system for the Juba and Shabelle Rivers are discussed below.

5.1 Data Limitations

Somalia used to have a good data collection network for rainfall and river flow until late 1980s. With the collapse of the government, all the data collection stations were damaged either intentionally or due to lack of maintenance for long periods. SWALIM has since 2002 been trying to re-establish the data collection networks, and even expand to new sites. The exercise is however time and resource consuming. Up to now, majority of the pre-war stations have been re-established, and new stations including telemetric automatic weather stations established.

The period between 1990 and 2002 provides more than a decade of missing hydrometeorology data for all stations. Data collected during pre-war was fairly good, but with some missing values for few days, weeks and occasionally months. The missing values can only be estimated through statistical methods, and cannot be as correct as the observed data. A lot of collected data was also lost during the civil strife. Out of the more than 60 rainfall stations across the country, daily rainfall data was recovered for only 13 stations. The available data for all the other stations is monthly.

In the postwar rainfall data collection, SWALIM has partnered with NGO's for data collection. Some of the gauge readers are employed directly by SWALIM, while other stations are managed by NGO's who read the gauge and send data to SWALIM. Data collected is of good quality, but still there are challenges mainly associated with security, where the gauge readers cannot access the gauge, or an NGO is refused to operate in an area where the gauge is installed.

For the river gauges, SWALIM has re-established data collection in seven locations. After re-establishment, initial data collection in all the seven stations was river level, until 2008. In 2009, SWALIM trained the gauge readers and acquired equipment for discharge measurement in six locations along the Juba and Shabelle Rivers. The rating curves currently being used are the ones developed during pre-war periods, and have not been updated since late 1980's, and could give wrong discharges if the river characteristics at that station have changed.

Data on the upper catchments of both rivers, inside Ethiopia is not available at SWALIM. Efforts to access the data have not yielded results so far. Since majority of runoff is generated from the Ethiopian catchments, the system would benefit a lot from these data if available. The rainfall runoff models are currently run on satellite based rainfall data, which adds to the errors of simulated flows.

5.2 Model Limitations

The prevailing basin conditions and capabilities of a particular model determine the suitability of the model in that basin. Models are known to perform very well in some basins and poorly in others due to differences in climate, soils, land use and other datasets used in the model setup. To come up with the best model(s) for flood forecasting in the Juba and Shabelle Rivers, different models were tried. The data limitations discussed under section 5.1 were a major limitation to all the models applied in the study. Other major limitations for each of the models are summarized below:

LISFLOOD model generated extremely high flows compared to the observed values. The model was developed under European conditions, and may need modifications to suit the Horn of Africa. However, as mentioned elsewhere in this report, JRC, the developers of the model reported that the problem was in the automatic calibration routine. The model needs to be tested with the corrected routine.

The USGS Stream flow Model (GeoSFM) gave poor results, even though no much effort was done to calibrate the model. The model was mainly used to compare the different satellite based rainfall data, and from the poor preliminary results obtained the model may not work well with such datasets. Since the observed rainfall data for the upper catchments are currently not available, the applicability of the model in the two basins is limited.

GFMFS model gave relatively good results. The models are however black box, and cannot be manipulated to suit specific conditions. The model has a rainfall component, but could not be used due to lack of rainfall data to represent the catchment.

Regression models also gave relatively good results, and are promising to be useful in flood forecasting for the two rivers. Better data collection networks, both for rainfall and stream flow in the streams feeding to the Juba and Shabelle channels within Somalia would improve further the usefulness of such models in flood forecasting.

HECRAS model gave fair results, even though it was not fully calibrated. The problems encountered in using this model in Somalia rivers is the lack of sufficient data on channel characteristics such as over bank cuttings, canals, reservoirs, etc, all of which contribute to lateral flows. Though, there is a chance to improve on this from aerial photography data.

Chapter 6

Conclusions and Recommendations

6.1 Conclusions

Different models were applied in the Juba and Shabelle Rivers with the aim of establishing the best performing model to be adopted in the development of a flood forecasting system. The tested models were LISFLOOD and USGS GeoSpatial Streamflow Model both of which are rainfall runoff models; HECRAS, GFMFS and Regression models for flow routing down the river channels.

The models were calibrated for the Somali river conditions using both the prewar and postwar river and rainfall data, depending on the data requirements for individual models. The calibration period was up to 2008, while 2009 was used to validate the models. The model results varied from one model type to another.

GFMFS and regression models produced the best results, judged by the correlation coefficients between simulated and observed flows, and timing and magnitude of the peaks. It is expected that HECRAS results would improve with further calibrations. LISFLOOD model results were poor in terms of the magnitude of simulated discharge. The GeoSFM was used mainly in comparison of different satellite based rainfall data sets, and the preliminary results were poor.

Majority of the flow in Juba and Shabelle Rivers originate from the Ethiopian highlands. A good setup of a rainfall-runoff model should capture the rainfall, evaporation and flow data in the upper parts of the catchment. There exists some rainfall and river gauge stations in the Ethiopian catchments, but SWALIM does not have access to this data, which limits the application of such models in the catchment.

Due to the minimal contribution of the Somalia catchment to the flow in Juba and Shabelle Rivers, observing flow at the entry points at Belet Weyne and Juba and routing it downstream would be achieved with high accuracy. Lessons learned from the Deyr 2009 rains however show that during heavy storms the contribution of the Somali catchments is significant. Some heavy storms received in the area between Belet Weyne and Bulo Burti for example caused more than half a meter rise at Bulo Burti station, whereas the river level in Belet Weyne remained relatively stable.

6.2 Recommendations

The success of a flood forecasting system depends more than anything else on the availability of quality data in good time to allow running of the model and dissemination of information before actual flooding occurs to save life and property. SWALIM has done a lot to improve on the data collection network in Somalia. It would however be recommended that more rain gauges be installed in the upper and

middle catchments. The additional rain gauge data would allow the use of rainfall-runoff models within Somalia to monitor local contribution.

There is considerable amount of water extracted for irrigation especially in the middle and lower reaches of both the Juba and Shabelle Rivers. Currently, there are no estimates available for the amount of water extracted and at what location along the rivers. To better understand the water balance in the two basins, further investigations needs to be done on irrigation water withdrawal.

Further calibration of the LISFLOOD model with the modified calibration routine is recommended before a decision is made on whether the model can be used under the Somali conditions or not. If the performance is found to be satisfactory, then the routing component of the model can be tested as well since it was not done in this phase.

HECRAS model can be used to generate flooded areas from simulated flow through the HEC GeoRAS extension, something which other models tested are not capable of. The model therefore provides an opportunity to combine flow routing and inundation mapping in one application. It is recommended that the model be further refined using data from aerial photography to better capture flows in magnitude and timing.

After the calibration and setup of the flood forecasting system, it is recommended that a Graphical User Interface (GUI) be developed for the system. The GUI would connect different components of the flood forecasting system and automate processes such as data retrieval and initializing running of the model after receiving new data.

A more active role by SWALIM's partners in the field is recommended to make the system a success. It is the partners on the ground that would provide new information for model updates especially towards the start of the rainy season. Information such as new river bank breakages, embankment conditions etc would be crucial in model setup.

Bibliography and Literature Consulted

Artan G., Asante K., Smith J., Pervez S., Entenmann D., Verdin J., and Rowland J. (2007) Users Manual for the Geospatial Stream Flow Model (GeoSFM), U.S Geological Survey, Reston, Virginia.

Cunge, J.A., Erlich, M., Negre J.L, and Rahuel, J-L. (1992) Construction and assessment of flood forecasting scenarios in the hydrological forecasting system HFS/SPH. In: A.J. Saul (Editor), Floods and Flood Management. Kluwer Academic Publishers, pp. 291-312.

Fleming, G. (1977) Computer simulation techniques in hydrology. Elsevier, North-Holland.

Grijssen, J.G., Snoeker, X.C., El-Amin M., and Mohamed, Y.A. (1992) An information system for flood early warning. In A.J. Saul (Editor): Floods and Flood Management. Kluwer Academic Publishers, pp. 263-289.

Johan K. and Ad de Roo (2008) LISFlood Revised User Manual, European Commission's Joint Research Centre, Scientific and Technical Reports.

Monomoy G. (2005) Galway Flow Forecasting and Modelling System User's Manual, Department of Engineering Hydrology, National University of Ireland, Galway, Ireland.

Moore, R.J. (1986) Advances in real-time forecasting practice. Invited paper, Symposium on Flood Warning Systems, Winter Meeting of the River Engineering Section, The Institution of Water Engineers and Scientists 23 p.

Muchiri P.W. (2007) Climate of Somalia. Technical Report No W-01, FAO-SWALIM, Nairobi, Kenya.

Supit I., and Van Der Goot E. (Eds.), (2003) Updated System Description of the WOFOST 6.0 Crop Simulation Model Implemented in the Crop Growth Monitoring System Applied by the European Commission Treemail, Heelsum, the Netherlands, 120pp.

Thiemig V. (2009) Masters Thesis on Early Flood Warning in Africa, Juba-Shabelle River Basin Feasibility Study, Faculty of Science, Radboud University, Nijmegen, the Netherlands.

US Army Corps of Engineers (2002) HEC-RAS Hydraulic Reference Manual Version 3.1, Institute for Water resources, Hydrologic Engineering Centre.

Annexes

Annex A: List of Rainfall Monitoring Stations

Annex A-1: List of Operational Post-War Rainfall Monitoring Station

Rainfall Station	Longitude	Latitude	Date Installed	Region	District	AGENCY RESPONSIBLE	OBSERVING AGENCY
Waajid ACF	43.24000	3.80000	Jul-06	Bakool	Wajid	ACF	ACF
Garowe ADRA	48.48024	8.40620	Apr-06	Nugal	Garowe	ADRA	ADRA
Huddur ADRA	43.09365	4.11836	Apr-06	bakool	Huddur	ADRA	ADRA
Bardheere	42.30000	2.35000	Apr-06	Gedo	Bardera	CARE	SADO
Luuq	42.45000	3.58333	Apr-06	Gedo	Luuq	CARE	ACA
Jowhar	45.50000	2.76667	Jan-99	M. Juba	Jowhar	CEFA	CEFA
Bananey	45.02685	2.01064	Oct-06	Lower Shabelle	Afgoi	CONCERN	CONCERN
Barrire	44.89766	2.04842	Oct-06	Lower Shabelle	Afgoi	CONCERN	CONCERN
Mubarak	44.77730	1.92045	Oct-06	Lower Shabelle	Awdhegle	CONCERN	CONCERN
Mukidumis	44.43000	1.59850	Oct-06	Lower Shabelle	Kurtwareey	CONCERN	CONCERN
Wanle Weyne	44.89360	2.61945	Oct-06	Lr. Shabelle	Wanle Weyne	CONCERN	CONCERN
Boroma coopi	43.00000	10.00000	Apr-06	Awdal	Boroma	COOPI	COOPI
Hargeisa coopi	44.03651	9.55886	Apr-06	W. Galbeed	Hargeisa	COOPI	COOPI
Baidoa	43.66667	3.13333	Apr-05			FEWSNET	FEWSNET
Afgooye	45.13333	2.13333	Apr-05	Shabelle	Afgooye	FSAU	FEWSNET
Bardaale	43.19809	3.21460	Apr-05	Bay	Dinsor	FSAU	FEWSNET
Ceel Berde	43.65993	4.82821	Apr-05	Bakool	Ceel Berde	FSAU	FEWSNET
Diinsor	42.98333	2.41667	Apr-05	Bay	Bardale	FSAU	FEWSNET
Garowe FEWS	48.48270	8.40710	Apr-05	Nugaal	Garowe	FSAU	FEWSNET
Genale	44.75000	1.83333	Apr-05	L. Shabelle	Marka	FSAU	FEWSNET
Halgan	45.56596	3.85357	Apr-05	Hiran	Bulo Burti	FSAU	FEWSNET
Huduur FEWS	43.90000	4.16667	Apr-05	Bakool	Hudur	FSAU	FEWSNET
Jalalaqsi	45.59941	3.37951	Apr-05	Hiran	Jalalaqsi	FSAU	FEWSNET
Jamame	42.73333	0.05000	Apr-05	L. Juba	Jamame	FSAU	FEWSNET
Sakow	42.45217	1.63938	Apr-05	Middle Juba	sakow	FSAU	FEWSNET
Xasbahale	48.61611	8.57917	Apr-05	Nugaal	Garowe	FSAU	FEWSNET

Annex A

Rainfall Station	Longitude	Latitude	Date Installed	Region	District	AGENCY RESPONSIBLE	OBSERVING AGENCY
Adad	43.25308	10.14475	Apr-04	Awdal	Boroma	GAA	GAA
Baki	43.36222	10.01733	Apr-02	Awdal	Baki	GAA	GAA
Bonn		10.19411	Apr-04	Awdal	Boroma	GAA	GAA
Boroma GAA	43.18333	9.93333	Apr-02	Awdal	Boroma	GAA	GAA
Dilla GAA	43.36583	9.77889	Apr-02	Awdal	Baki	GAA	GAA
Garba raho	43.63499	10.23733	Apr-02	Awdal		GAA	GAA
Gargara	43.80567	10.31228	Apr-04	Awdal	Boroma	GAA	GAA
Harmata	43.35719	10.10944	Apr-04	Awdal	Baki	GAA	GAA
Heego	43.25944	10.08194	Apr-04	Awdal	Boroma	GAA	GAA
Horey	43.37806	10.17992	Apr-04	Awdal	Baki	GAA	GAA
Badhan HR	48.33917	10.71467	Mar-06	Sool	Badhan	Horn Relief	Horn Relief
Agsibiri	44.86975	4.74880	Oct-06	Hiraan	Belet Weyne	SCF	SCF
Belet weyne	45.18450	4.73386	Jan-97	Hiran	Belet Weyne	SCF	SCF
Kerialo	45.39156	4.40555	Oct-06	Hiraan	Belet Weyne	SCF	SCF
Mataban	45.52284	5.19937	Oct-06	Hiraan	Mataban	SCF	SCF
Yibir Suge	45.68286	4.98484	Oct-06	Hiraan	Mataban	SCF	SCF
Abrin	43.80575	9.51743	Apr-07	Galbeed	Hargeisa	SWALIM	SCF
Baran	48.33042	10.71430	Apr-07	Sanag	Baran	SWALIM	MOLAE
Berbera	45.03333	10.43333	Apr-07	Galbeed	Berbera	SWALIM	MOA
Borama	43.17916	9.94007	Nov-06	Awdal	Borama	SWALIM	MOA
Bossasso	49.17605	11.28265	Apr-07	Bari	Bossasso	SWALIM	MOLAE
Bulo burti	45.56667	3.25000	Jan-97	Hiran	Bulo Burti	SWALIM	MOA
Burao	45.56667	9.51667	Apr-07	Togdheer	Burao	SWALIM	MOA
Dilla	43.35675	9.74188	Nov-06	Galbeed	Dilla	SWALIM	MOA
Eerigavo	47.36667	10.61667	Apr-07	Sanaag	Eerigavo	SWALIM	MOA

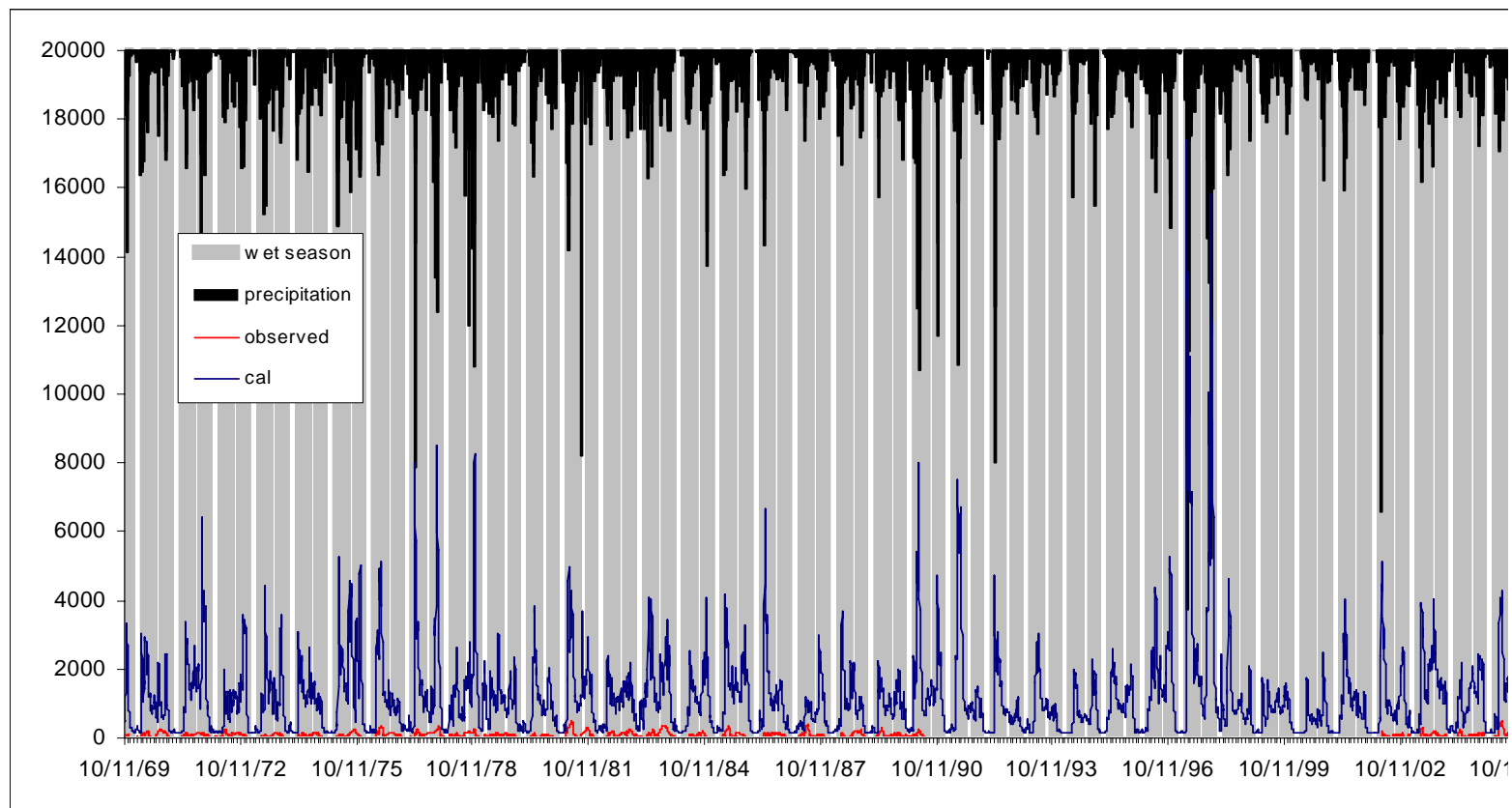
Annex A

Rainfall Station	Longitude	Latitude	Date Installed	Region	District	AGENCY RESPONSIBLE	OBSERVING AGENCY
Elfweyne	47.21680	9.93027	Apr-07	Sanaag	Elfweyne	SWALIM	MOA
Galkayo	47.42272	6.77719	Apr-07	Mudug	Galkayo	SWALIM	MOLAE
Garowe	48.47754	8.40458	Apr-07	Nugal	Garowe	SWALIM	MOLAE
Gebilley	43.28333	9.61667	Jan-05	Galbeed	Gebilley	SWALIM	MOA
Hargeisa	44.06680	9.55975	Jan-05	Galbeed	Hargeisa	SWALIM	MOA
Las Anod	47.35301	8.47927	Apr-07	Sool	Las Anod	SWALIM	MOLAE
Odweyne	45.06170	9.40858	Apr-07	Togdheer	Odweyne	SWALIM	MOA
Qardo	49.08678	9.50690	Apr-07	Bari	Qardo	SWALIM	MOLAE
Quljeed	43.00190	10.09167	Apr-07	Awdal	zeylac	SWALIM	MOA
Sheikh	45.18333	9.91667	Apr-07	Togdheer	Sheikh	SWALIM	MOA
Bualle	42.57317	1.24477	Jan-02	Bay	Bualle	WVI	WVI
Hargeisa_WV	44.08000	9.50000		W. Galbeed	Hargeisa	WVI	WVI
Sakoow_WV	42.45217	1.63938		Bay	Dinsor	WVI	WVI
Salagle	42.29569	1.81187		L.Juba	jilib	WVI	WVI
Tiaglow	44.51270	4.01820		Bay	Tieglo	WVI	WVI
Wajid_WV	43.24839	3.80948		Bakool	Wajid	WVI	WVI
Afmadow	42.1	0.5	Nov-06	Lr. Juba	afmadow	AFREC	AFREC

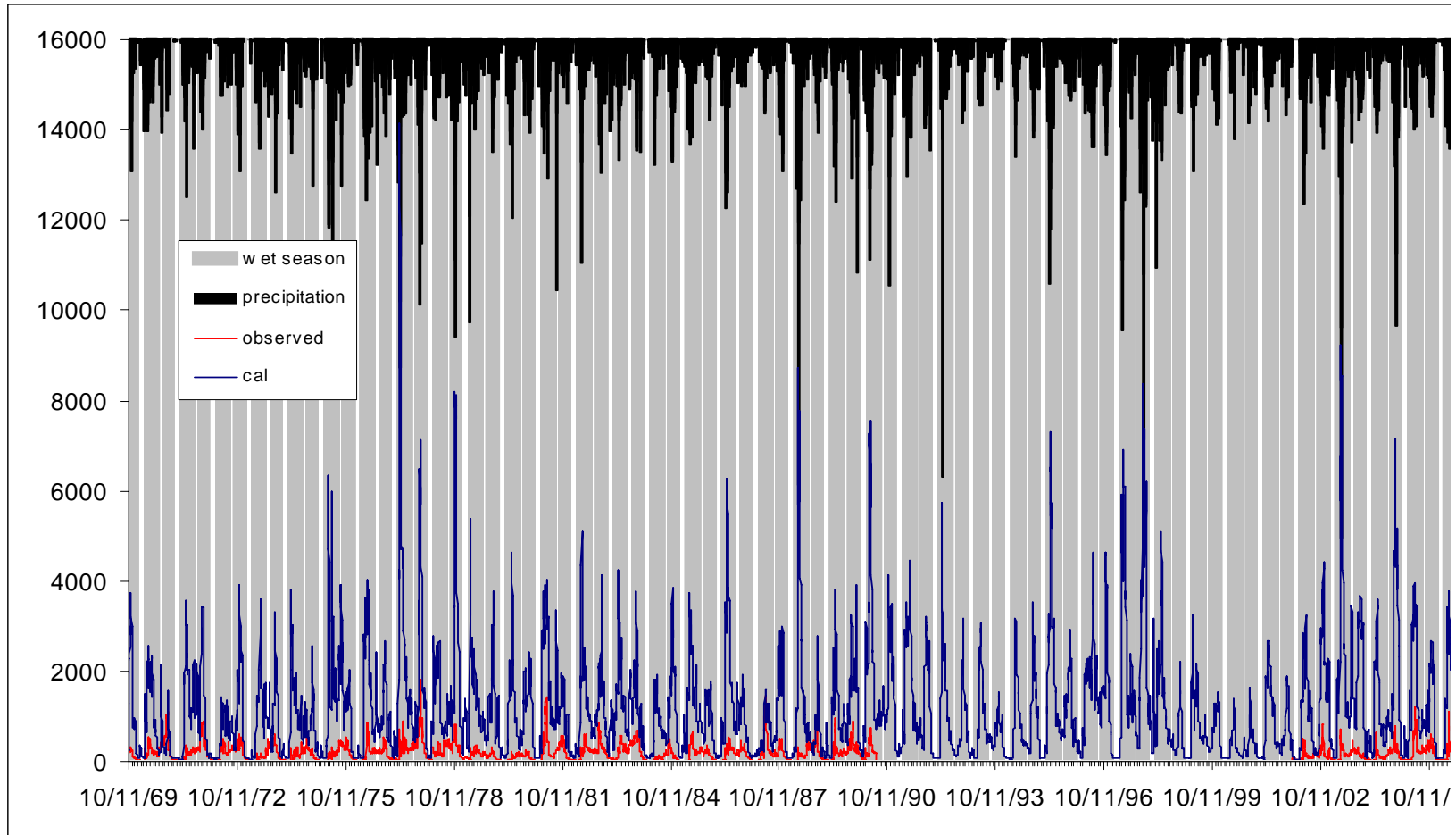
Annex A-2: Calibrated Model Parameters for LISFLOOD Model

Parameter	Description	Unit	Initial Value	Lower Bound	Upper Bound
<i>UPZTC</i>	Time constant for the upper groundwater zone	Days	10	1	50
<i>LZTC</i>	Time constant for the lower groundwater zone	Days	1000	50	2500
<i>GWPV</i>	Maximum rate of percolation going from the upper to the lower groundwater zone	mm/day	0.5	0.01	1.5
<i>GWLF</i>	Rate of flow out of the lower groundwater zone, expressed as a fraction of the total outflow	-	0.0	0.0	0.7
<i>bxinj</i>	Power in the infiltration equation	-	0.1	0.0001	1
<i>PWPF</i>	Power in the preferential flow equation	-	3	0.5	10
<i>CCM</i>	Multiplier that is applied to the Manning's roughness maps of the channel system	-	1	0.1	15
<i>CalEvap</i>	Multiplier that is applied to the potential evapo(transpi)ration input	-	1	1	1.5

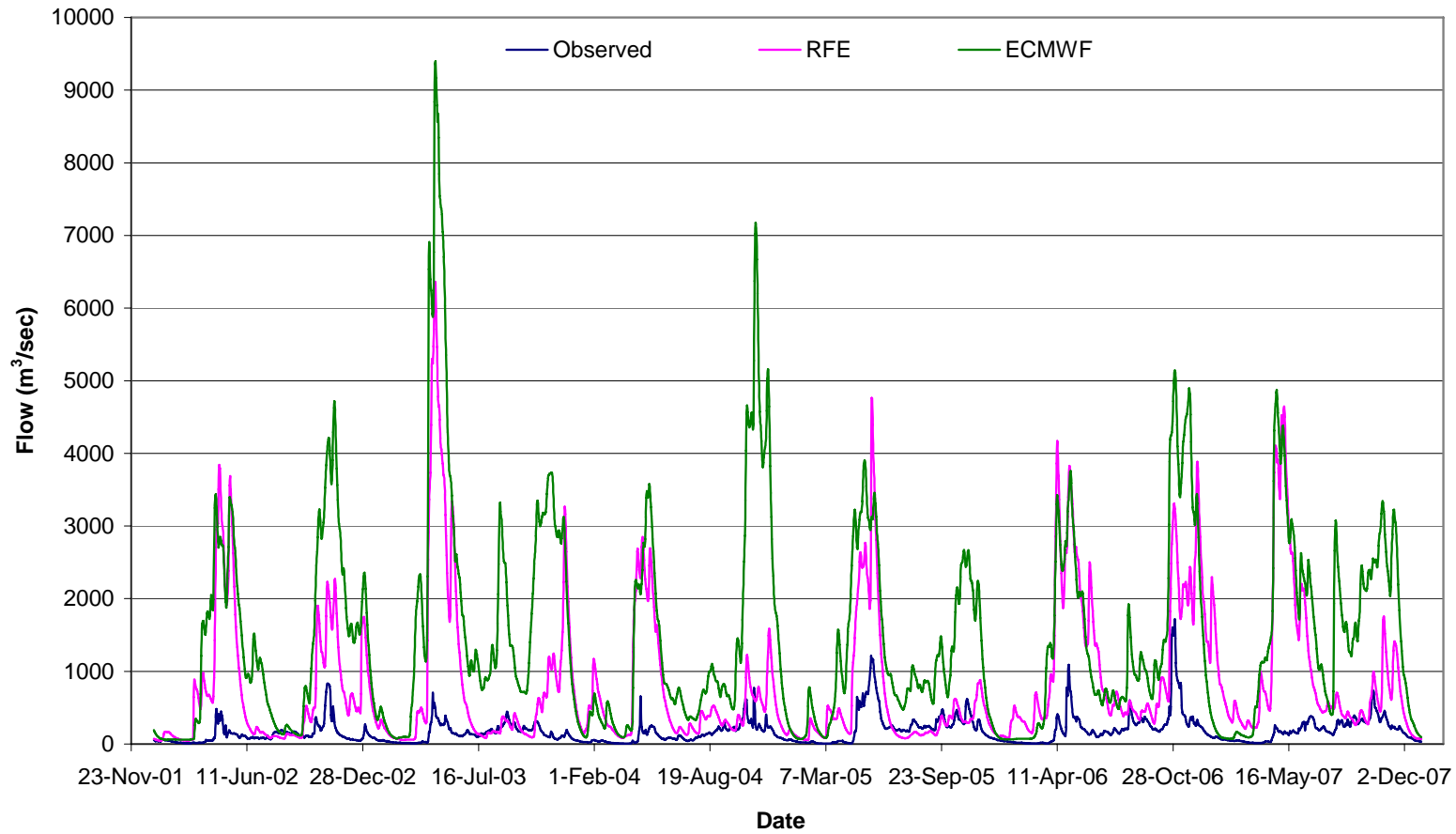
Annex B: Results of Models Calibration



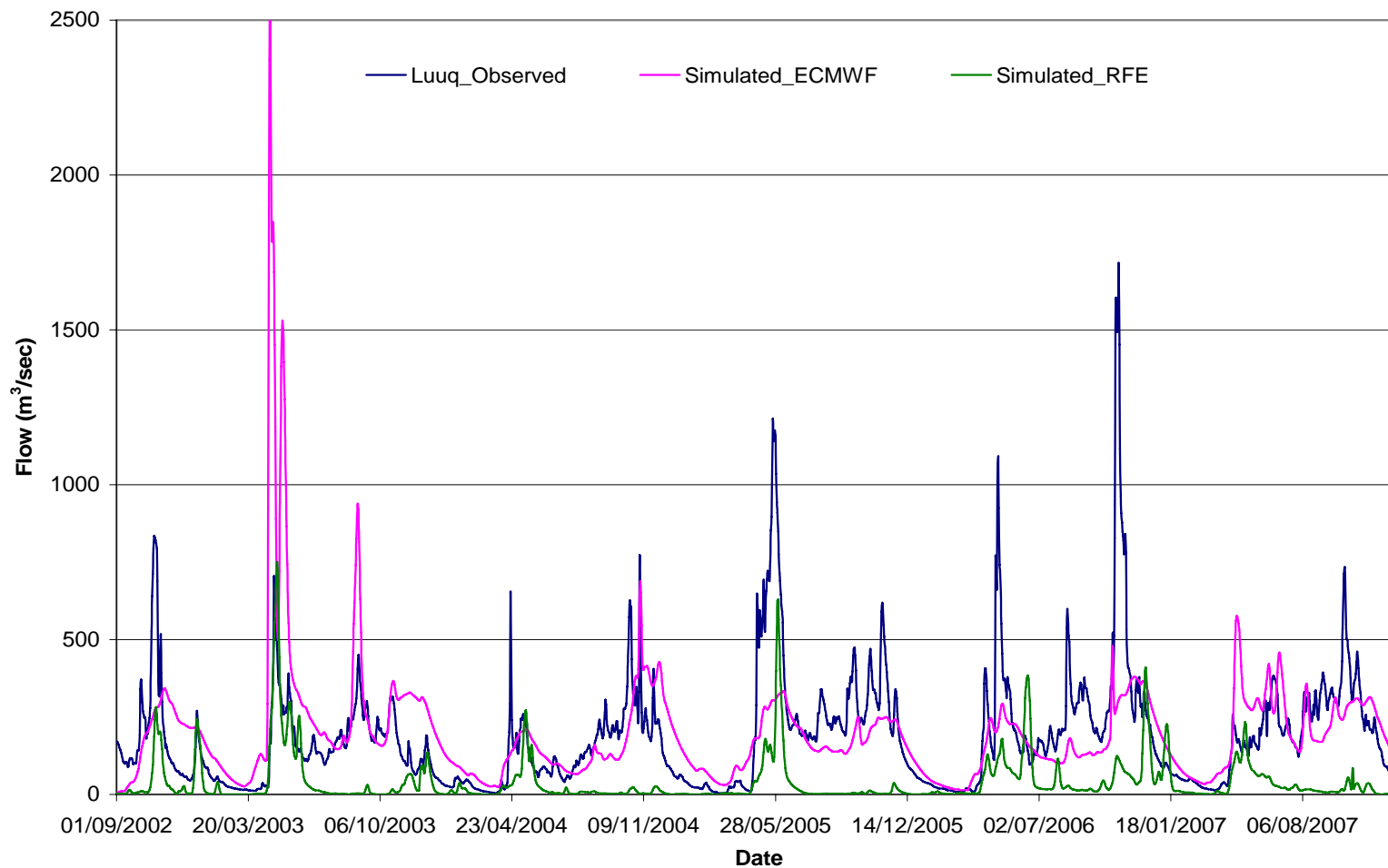
Annex B-1: Calibration Results for LISFLOOD Model at Belet Weyne



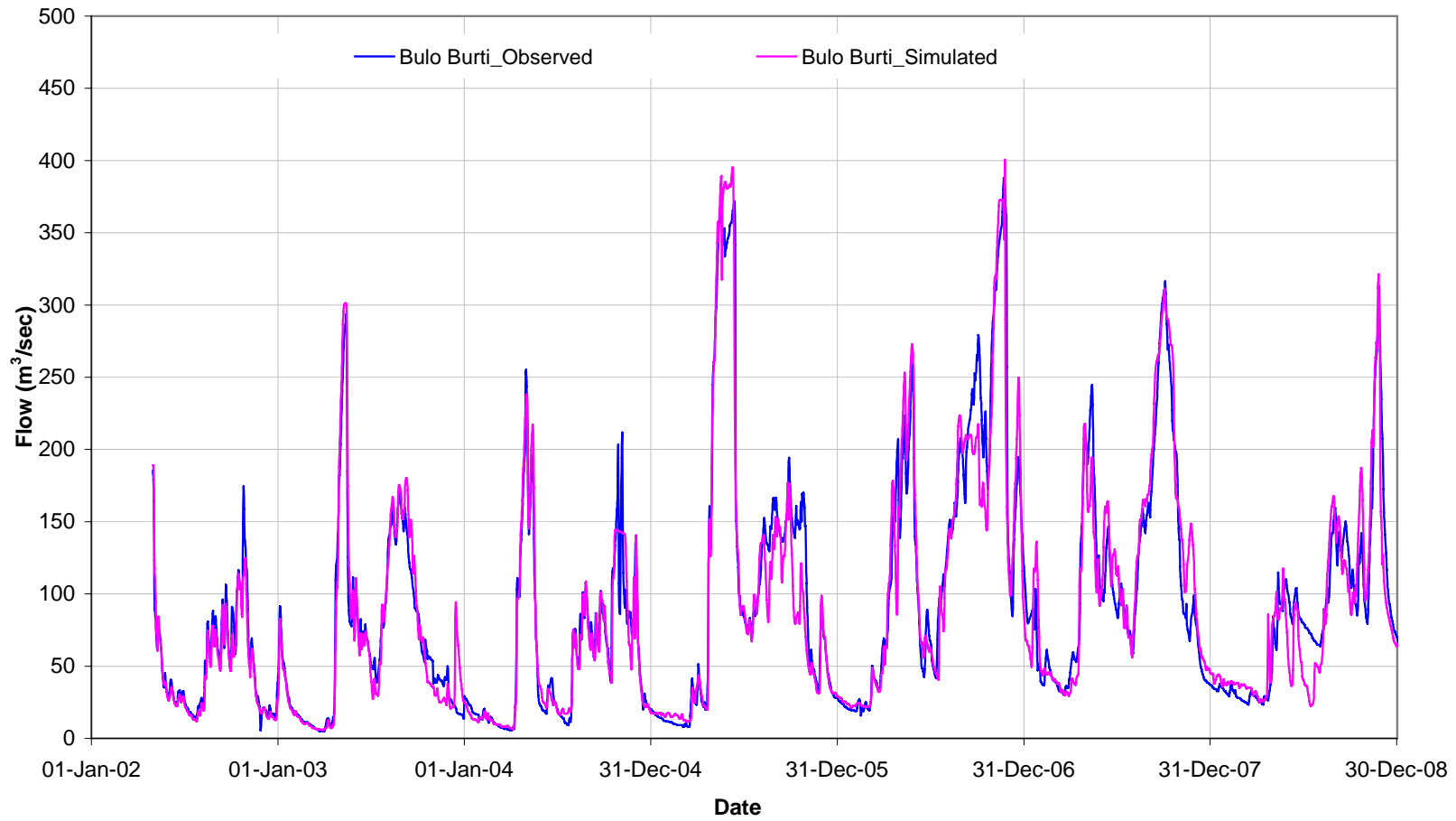
Annex B-2: Calibration Results for LISFLOOD Model at Luuq



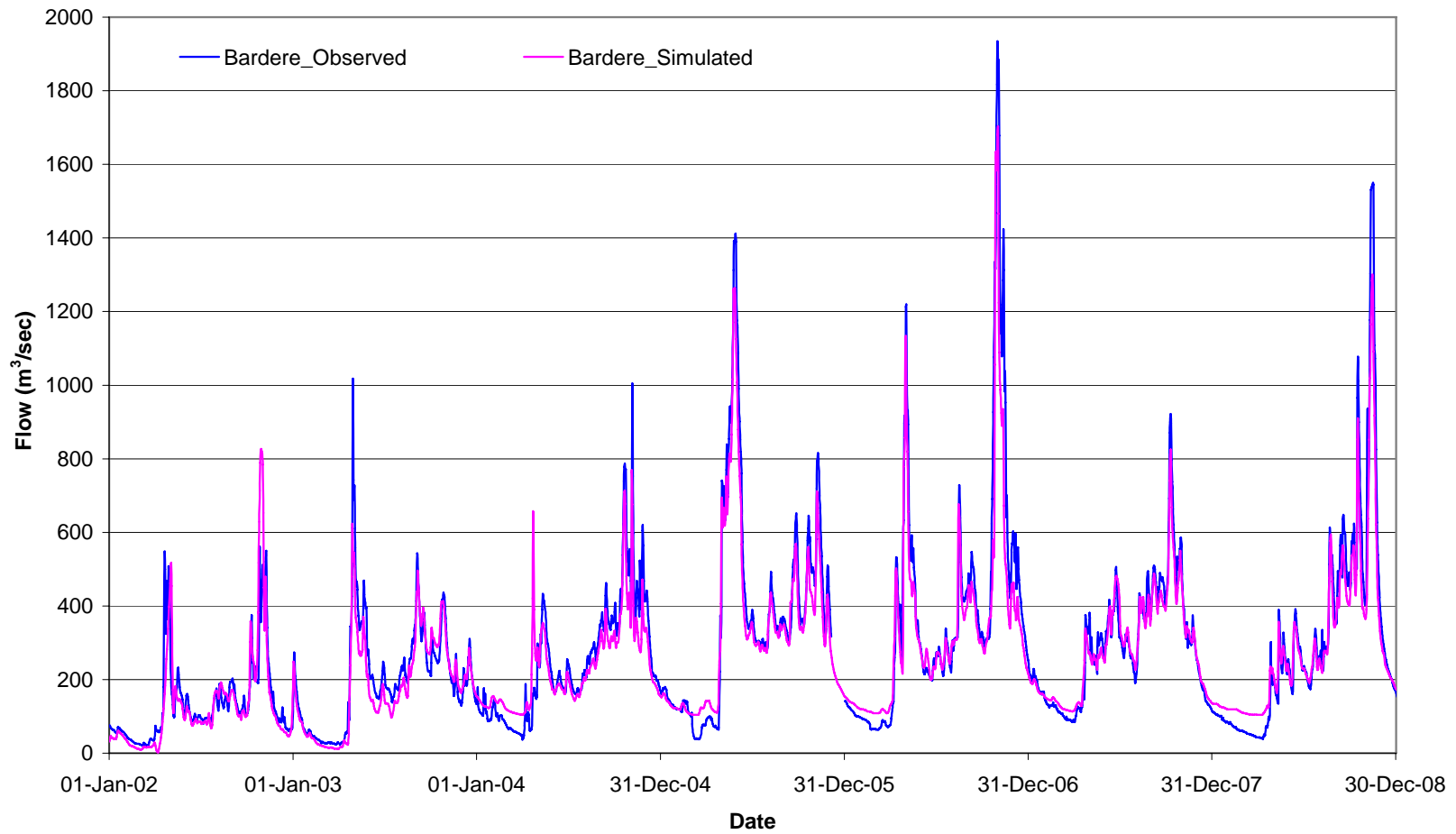
Annex B-3: LISFLOOD Calibration Results at Luuq, Based on Different Rainfall Datasets



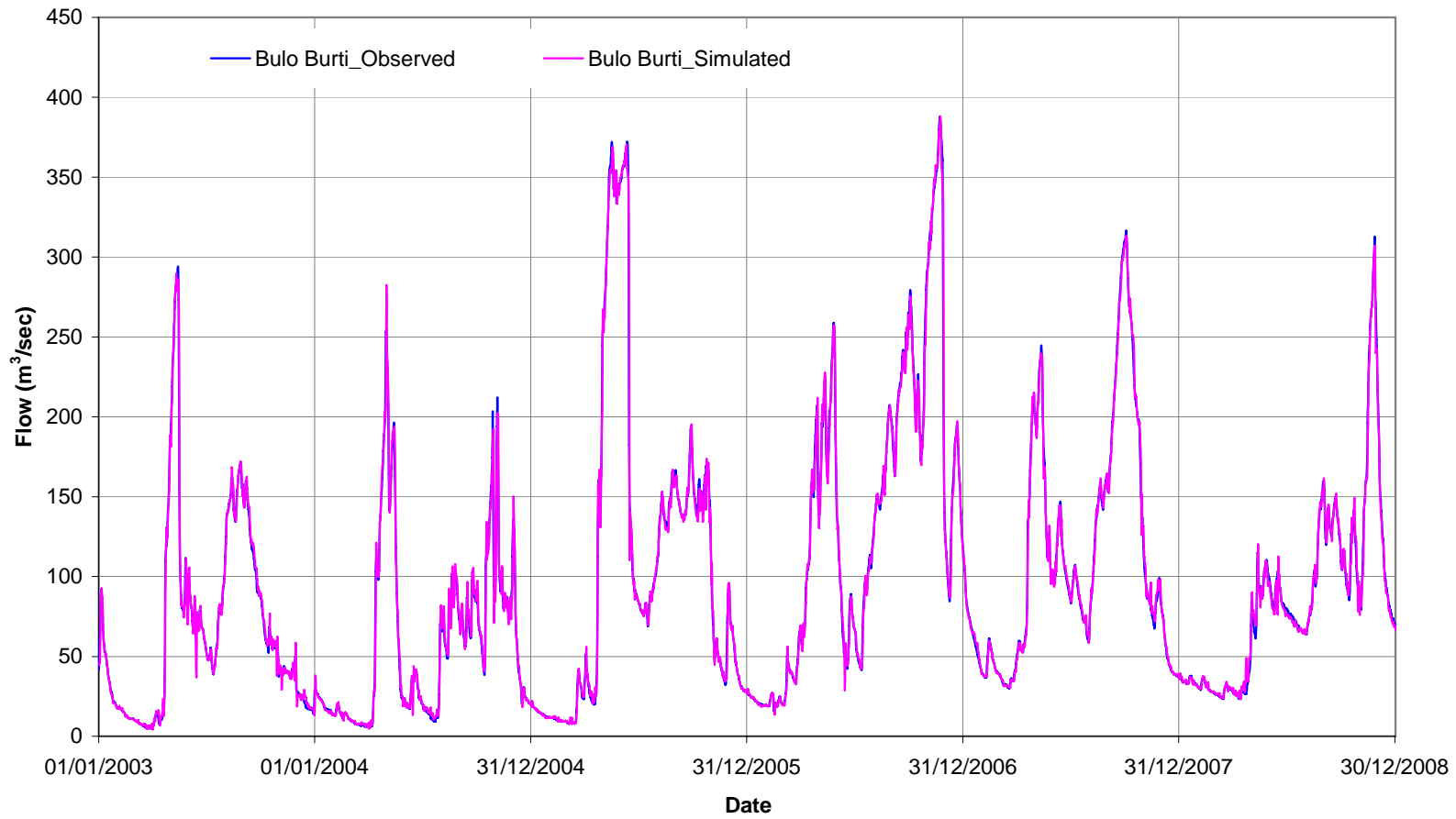
Annex B-4: GeoSFM Results at Luuq, Based on Different Rainfall Datasets



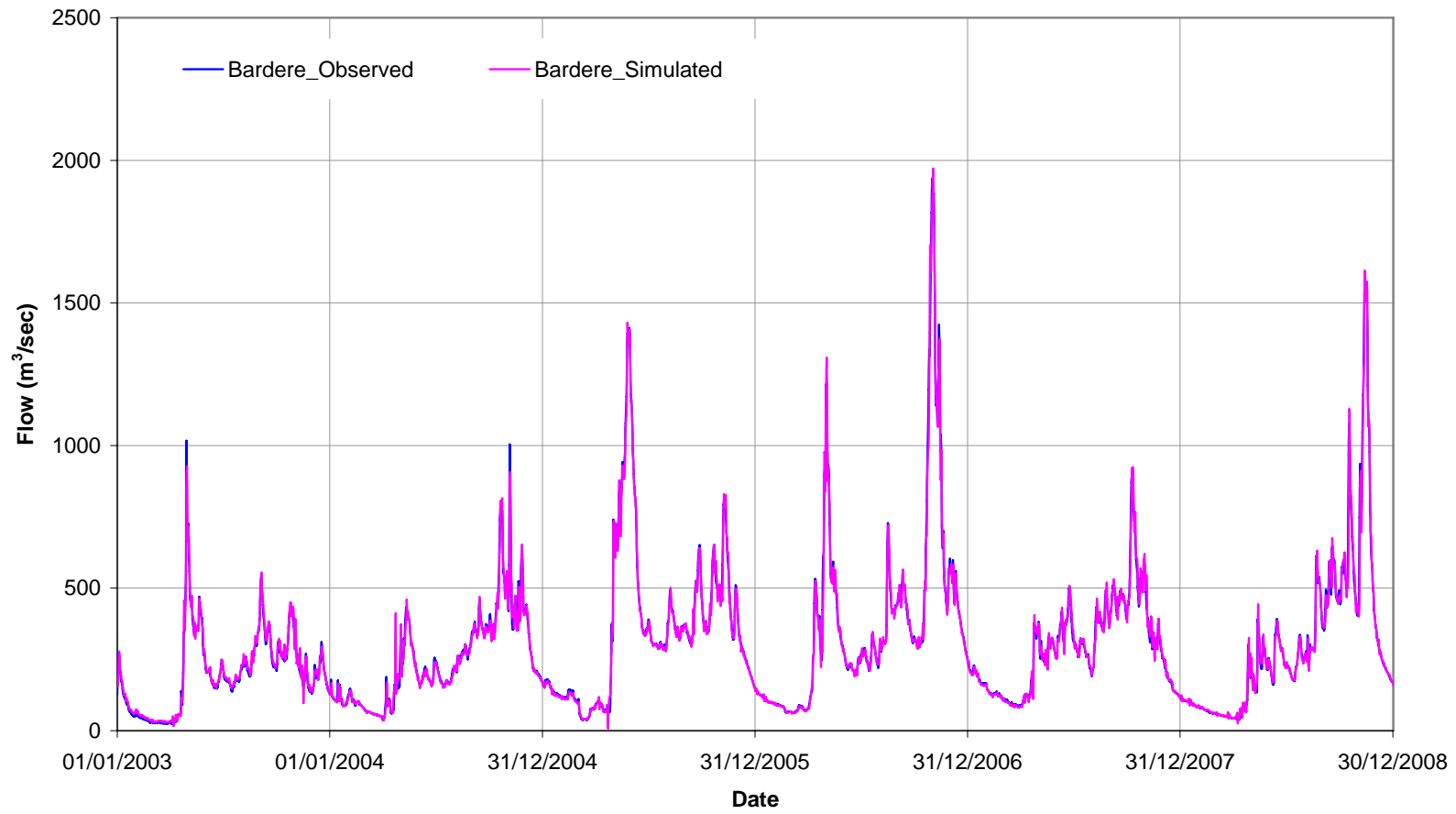
Annex B-5: Observed and Simulated Flow at Bulo Burti using HECRAS Model for calibration



Annex B-6: Observed and Simulated Flow at Bardere using HECRAS Model for Calibration



Annex B-7: Observed and Simulated Flow at Bulu Burti using GFMFS Model for calibration



Annex B-8: Observed and Simulated Flow at Bardere using GFMFS Model for calibration